AD-A192 328 INTERACTIONS BETWEEN SYNOPTIC AND PLANETARY SCALES OF MOTION(U) NAVAL POSTGRADUATE SCHOOL MONTEREY CA M D MCATEE DEC 87 1/2

UNCLASSIFIED F/G 4/2 NL

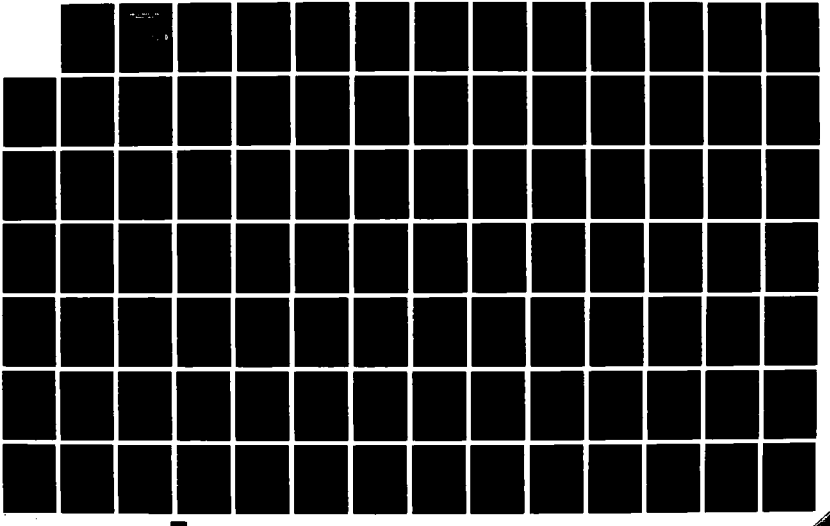

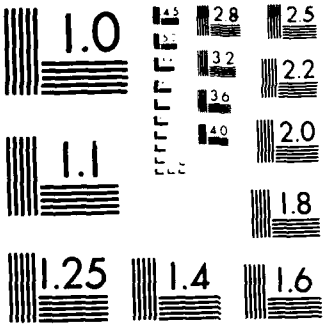

NAVAL POSTGRADUATE SCHOOL
Monterey, California

DISSERTATION

INTERACTIONS BETWEEN SYNOPTIC AND PLANETARY SCALES OF MOTION

by

Michael D. McAtee

December 1987

Thesis Advisor R. T. Williams

SECURITY CLASSIFICATION OF THIS PAGE A102 228

REPORT DOCUMENTATION PAGE

1a. REPORT SECURITY CLASSIFICATION UNCLASSIFIED	1b. RESTRICTIVE MARKINGS
2a. SECURITY CLASSIFICATION AUTHORITY	3. DISTRIBUTION / AVAILABILITY OF REPORT Approved for public release; distribution is unlimited.
2b. DECLASSIFICATION / DOWNGRADING SCHEDULE	
4. PERFORMING ORGANIZATION REPORT NUMBER(S)	5. MONITORING ORGANIZATION REPORT NUMBER(S)
6a. NAME OF PERFORMING ORGANIZATION Naval Postgraduate School 6b. OFFICE SYMBOL (If applicable) 63	7a. NAME OF MONITORING ORGANIZATION Naval Postgraduate School
6c. ADDRESS (City, State, and ZIP Code) Monterey, California 93943-5000	7b. ADDRESS (City, State, and ZIP Code) Monterey, California 93943-5000
8a. NAME OF FUNDING / SPONSORING ORGANIZATION 8b. OFFICE SYMBOL (If applicable)	9. PROCUREMENT INSTRUMENT IDENTIFICATION NUMBER
8c. ADDRESS (City, State, and ZIP Code)	10. SOURCE OF FUNDING NUMBERS PROGRAM ELEMENT NO / PROJECT NO / TASK NO / WORK UNIT ACCESSION NO

11. TITLE (Include Security Classification)
Interactions Between Synoptic and Planetary Scales of Motion

12. PERSONAL AUTHOR(S)
McAtee, Michael D.

13a. TYPE OF REPORT	13b. TIME COVERED	14. DATE OF REPORT (Year, Month, Day)	15. PAGE COUNT
Ph. D. Thesis	FROM _____ TO _____	1987 December	123

16. SUPPLEMENTARY NOTATION

17. COSATI CODES			18. SUBJECT TERMS (Continue on reverse if necessary and identify by block number)
FIELD	GROUP	SUB-GROUP	Nonlinear interactions, Planetary waves, Planetary scale, Normal modes, Synoptic scale, Kelvin

19. ABSTRACT (Continue on reverse if necessary and identify by block number)

The effects of synoptic waves on the dynamics of planetary waves are investigated using normal mode analysis. Initialized analyses of the Navy Operational Global Atmospheric Prediction System (NOGAPS) for 19 days between January and April 1986 are projected onto the normal modes of a linearized version of the model. For each analysis, the different terms (adiabatic nonlinear, linear and diabatic) which affect the time tendency of planetary-scale modes are determined by a one-time step integration of the NOGAPS model. The effect of synoptic scales on planetary scales is determined by computing the difference between the adiabatic nonlinear term computed from the NOGAPS analyses and analyses for the same period that have been spectrally filtered to remove most of the synoptic-scale waves. The energy tendency due to the nonlinear adiabatic term and the synoptic-scale contribution to this term are also

20. DISTRIBUTION / AVAILABILITY OF ABSTRACT	21. ABSTRACT SECURITY CLASSIFICATION	
☒ UNCLASSIFIED/UNLIMITED ☐ SAME AS RPT ☐ DTIC USERS	UNCLASSIFIED	
22a. NAME OF RESPONSIBLE INDIVIDUAL R. T. Williams	22b. TELEPHONE (Include Area Code) (408)-646-2296	22c. OFFICE SYMBOL 63 Wu

DD FORM 1473, 84 MAR 83 APR edition may be used until exhausted
All other editions are obsolete

SECURITY CLASSIFICATION OF THIS PAGE

☆ U.S. Government Printing Office: 1986—606-243

19. cont.

computed. It is shown that the synoptic-scale contribution to the adiabatic nonlinear term and the time tendency of planetary-scale modes can be a very large percentage of these terms.

By eliminating momentum advections in the model and computing the adiabatic nonlinear term for the filtered and unfiltered analyses, the relative importance of interactions through mass field interactions or momentum field interactions are determined. It is shown that synoptic-scale interactions which affect the planetary-scale barotropic modes are primarily through the momentum advections, while mass and momentum interactions are possible for the baroclinic modes. The importance of mass field interactions generally increases as the vertical scale of the wave decreases.

Because of the importance of synoptic waves to the dynamics and energetics of planetary waves, errors in the forecasts of planetary waves may in part be due to the synoptic-scale forecast errors.

Approved for public release; distribution is unlimited.

Interactions Between Synoptic and Planetary Scales of Motion

by

Michael D. McAtee
Captain, United States Air Force
B.A., University of California at Berkeley, 1978
M.S., Naval Postgraduate School, 1984

Submitted in partial fulfillment of the
requirements for the degree of

DOCTOR OF PHILOSOPHY IN METEOROLOGY

from the

NAVAL POSTGRADUATE SCHOOL
December 1987

Author: Michael D. McAtee
Michael D. McAtee

Approved by:

R. T. Williams
Professor of Meteorology
Dissertation Advisor

R. L. Elsberry
Professor of Meteorology

M. A. Rennick
Adjunct Professor of Meteorology

B. Neta
Associate Professor of Mathematics

R. W. Garwood
Associate Professor of Oceanography

Approved by: R. J. Renard, Chairman,
Department of Meteorology

Approved by: Kneale T. Marshall,
Acting Academic Dean

ABSTRACT

The effects of synoptic waves on the dynamics of planetary waves are investigated using normal mode analysis. Initialized analyses of the Navy Operational Global Atmospheric Prediction System (NOGAPS) for 19 days between January and April 1986 are projected onto the normal modes of a linearized version of the model. For each analysis, the different terms (adiabatic nonlinear, linear and diabatic) which affect the time tendency of planetary-scale modes are determined by a one-time step integration of the NOGAPS model. The effect of synoptic scales on planetary scales is determined by computing the difference between the adiabatic nonlinear term computed from the NOGAPS analyses and analyses for the same period that have been spectrally filtered to remove most of the synoptic-scale waves. The energy tendency due to the nonlinear adiabatic term and the synoptic-scale contribution to this term are also computed. It is shown that the synoptic-scale contribution to the adiabatic nonlinear term and the time tendency of planetary-scale modes can be a very large percentage of these terms.

By eliminating momentum advections in the model and computing the adiabatic nonlinear term for the filtered and unfiltered analyses, the relative importance of interactions through mass field interactions or momentum field interactions are determined. It is shown that synoptic-scale interactions which affect the planetary-scale barotropic modes are primarily through the momentum advections, while mass and momentum interactions are possible for the baroclinic modes. The importance of mass field interaction generally increases as the vertical scale of the wave decreases.

Because of the importance of synoptic waves to the dynamics and energetics of planetary waves, errors in the forecasts of planetary waves may in part be due to the synoptic-scale forecast errors.

TABLE OF CONTENTS

LIST OF TABLES

LIST OF FIGURES

ACKNOWLEDGEMENTS

The completion of this work would not have been possible without support and assistance of many individuals. Unfortunately there is not enough room here to thank everyone personally, so a general thank you will have to suffice for those not mentioned below.

First and foremost, I would like to thank my advisor Prof. R. T. Williams. He always knew what I could do even when I didn't. His gentle, yet persistent guidance was key to the completion of this research. Thanks go to Prof. Russ Elsberry, for his careful and professional review of this manuscript. I would also like to thank the other members of my doctoral committee (Professors Garwood, Rennick, and Neta) for their time, patience and encouragement. My deepest thanks and gratitude to LCDR Larry Warrenfeltz, who provide me with encouragement and a place to stay during my hectic return trips to Monterey.

Special thanks go to Drs. Ed Barker and Tom Rosmond of NEPRF. Without Ed's help with the complex normal mode analysis software and Tom's many helpful suggestions, this project would have never begun or have been completed. Thanks also to Dr. Ron Errico of NCAR, who helped me understand the complex theory of normal modes and gave me many helpful suggestions that were incorporated into this work.

Computer resources for this research were provided by the Fleet Numerical Oceanography Center and the W. R. Church Computer Center of the Naval Postgraduate School.

Finally, my love and unexpressable gratitude to my family-- to Mellissa and Alexander who gave up many hours with their Dad, so he could "study"; and to my wife, Deborah, who patiently supported me and was my strength through the many long days and nights it took to complete this work. It is to Deborah, that I dedicate this work.

I. INTRODUCTION

Atmospheric predictability studies (Lorenz, 1969) indicate that each scale of motion has different predictability, e.g. small-scale motions are theoretically predictable to an hour, synoptic scales to a few days and planetary scales to a few weeks. However, a number of studies (Lambert and Merilees, 1978; Baumhefner and Downey, 1978; and Morse, 1983) have shown that synoptic-scale motions, rather than planetary-scale motions, are the most accurately forecast by numerical models. Although planetary wave errors have been reduced in current operational models (Wallace et al., 1983; Bettge and Baumhefner, 1984), planetary waves are still not forecast as accurately as cyclone scale waves. This result does not seem to be dependent on the type of model used. Baumhefner and Downey examined a number of different models and found the same error pattern. The error in forecasting planetary-scale waves might not seem to be that important given that the error in the synoptic scales is smaller and that the synoptic scales of motion produce most of the day-to-day weather changes. The importance of accurate planetary-scale predictions is clear when one considers medium- to long-range forecasts (up to 10 days). Since planetary waves often steer the smaller synoptic disturbances, an improved planetary planetary-scale forecast would presumably lead to an improvement on the synoptic scale.

There are at least two reasons why planetary waves are not forecast as well as theory suggests. One reason is that the dynamics for planetary waves are poorly understood. Planetary waves consist of a quasi-stationary component and a generally smaller transient component. The quasi-stationary component is thought to be a response to forcing by a combination of topography, differential heating due to land-sea differences and possibly scale interactions. It would seem reasonable to suspect that errors in the quasi-stationary component might be due to inadequacies in the model forcing. Another source of error for planetary waves is spurious excitation of transient planetary waves (Daley et al., 1981; Somerville, 1980; Lambert and Merilees, 1978; Roads and Somerville, 1982). These spurious waves are thought to be the result of errors in initial data or an inadequate model domain. Such waves are a major contributor to planetary wave error in the first 24 to 48 hours of a forecast (Daley et al., 1981). These transient waves have often been examined in terms of the normal

modes of the linearized set of equations describing oscillations of a stratified resting atmosphere on a spherical earth. The mode that has been most often identified as being spuriously excited is the so-called external Rossby mode. This mode has a large phase speed and a period of approximately 5 days. This fact has led some to refer to this mode as the 5-day wave. Daley et al. (1981) showed that large-scale external Rossby modes are excited when a hemispheric domain is used rather than a global domain, and when bad or poorly analyzed tropical data are used. Daley also showed that application of the nonlinear normal mode initialization procedure of Machenhauer (1977) to the large-scale external Rossby modes improved the forecast in a root mean squared sense for the cases examined. However, he properly notes that there is no evidence to show that the Machenhauer balance condition, which seems to be appropriate for the gravity modes, is applicable to the fast Rossby modes.

Very little is known about these Rossby modes in the atmosphere or in numerical prediction models. The best observational evidence for the existence of these normal modes is from the studies of Madden and Julian (1972) and Ahlquist (1982). Applying time series analysis techniques to station pressure data, Madden and Julian were able to identify westward propagating 5-day waves. The observed characteristics of these waves were shown to be not inconsistent with those of a planetary-scale Rossby wave. Ahlquist projected 1200 consecutive days of twice daily National Meteorological Center tropospheric analyses of velocity and geopotential onto three-dimensional, normal mode Rossby wave structures. Through spectral analyses of these time series, Ahlquist was able to identify 14 planetary-scale, normal mode waves. By contrast, a rather large amount of research (Dickenson and Williamson, 1972; Williamson, 1976; Machenhauer, 1977; Errico, 1984) has been done to determine the nature of the dynamic balance of the gravity modes. It is from these investigations that the nonlinear normal mode initialization procedure was developed. The dynamic balance of the gravity modes has been studied primarily by long-term model integrations.

A third and as yet unexamined reason for errors in numerical predictions of planetary waves is that these errors are due to errors in the smaller (cyclone) scales. The dynamics of planetary waves may be such that nonlinear interactions from smaller scales are important. If this is the case, then errors in cyclone scales would lead to errors in the planetary scales. The planetary scale prediction errors in numerical models cannot be fully understood or corrected until the importance of nonlinear scale interactions are determined.

It is the general hypothesis of this study that nonlinear interactions with cyclone waves are an important factor in the dynamics of planetary waves. The purpose of this study is twofold:

1. Determine the importance of these nonlinear interactions using the normal mode analysis technique of Errico (1984); and
2. Identify some of the mechanisms of these nonlinear interactions.

A number of studies have examined nonlinear interactions and their importance to the maintenance of planetary waves. One of the earliest studies to illustrate how nonlinear interactions could maintain large-scale, quasi-permanent flow was by Saltzman (1959). Using a highly simplified barotropic model with an idealized flow that crudely simulated a Northern Hemisphere winter 500 mb flow pattern, Saltzman found that there was a substantial energy transfer from the synoptic waves to the planetary waves. Saltzman and Fleisher (1960) used 500 mb data to show that in the mean there was a net kinetic energy transfer from synoptic scales to planetary scales. A more recent study by Kao and Lee (1977) showed that the primary contribution of nonlinear interactions to the energy transfer is essentially through the interactions of the slowly moving waves, the stationary long waves and zonal mean flow. Saltzman (1970) gives a review of the major studies that have used Fourier analysis to identify nonlinear interactions. Gall et al. (1979) used a simplified general circulation model to demonstrate that the initial development of the ultralong waves from a zonal mean basic state can be forced by the interaction between the cyclone waves and the basic flow. Gall argued that the ultralong waves were forced mainly by planetary scale variations in the meridional heat flux convergence of the higher wavenumber modes, which produces a positive correlation between planetary scale upward motion and temperature. The principal kinetic energy source for the planetary waves was the conversion of wave available potential energy to wave kinetic energy at a given wavenumber. A more recent study by Young and Villere (1985) confirmed in part Gall's results, but also showed that direct transfer of kinetic energy from intermediate scales to planetary scale was of equal importance. In both of these studies, the nonlinear transfer of potential energy was not computed directly. This transfer was implied by showing that the conversion of eddy available potential energy to eddy kinetic energy was much greater when nonlinear interactions were allowed.

The analysis of the scale interactions in this study are done using Errico's normal mode analysis procedure. This analysis procedure requires the use of a numerical

model and its associated normal modes. The model that will be used in this study is a version of the Navy Operational Global Atmospheric Prediction System (NOGAPS). The normal modes used in the analysis procedure are derived from this model. This analysis method is used because it has a number of advantages over previously used methods such as Fourier or spherical harmonics analysis. The most important advantage of using normal mode analysis is that the total effect of other scales (vertical, meridional and zonal) on a given mode can be determined. Another important advantage is that the nature of wave motions can be identified physically and high-frequency noise can be separated consistently from low-frequency meteorologically significant waves in both mass and velocity fields. Normal mode analysis also allows one to separate the data into different vertical, zonal and meridional scales while maintaining the physical nature of the data. The other techniques that were mentioned above do not have this advantage. While it is true that a combination of the Fourier and spherical harmonic could be used to decompose the data into different vertical, meridional and zonal scales, this representation would be artificial and it has the disadvantage of having no explicit relationship between spectral modes of mass and velocity. Finally, since divergence is significant in the motion of ultralong waves, it may be more appropriate to represent data as solutions of linearized primitive equations rather than as solutions of the non-divergent vorticity equation (i.e. spherical harmonics).

There have only been a few studies in recent years (Kasahara and Puri, 1981; Ko, 1985) that have used normal mode analysis to examine the spectral distribution of atmospheric energy. These studies were confined to examining just the spectral distribution of atmospheric energy and not the energy conversions between modes of different vertical and horizontal scales . There has been even less work in determining the energy exchange between the different vertical and horizontal modes. The little work that has been done in this area has focused on zonal mean-eddy kinetic energy exchange (Tanaka et al., 1986). Tanaka used normal mode analysis, to examine 25 days of daily First GARP (Global Atmospherics Research Program) Global Experiment (FGGE) IIIb analyses from the Goddard Laboratory for Atmospheres (GLA) and the Geophysical Fluid Dynamics Laboratory (GFDL). Tanaka examined the distribution of kinetic energy as well as the kinetic energy interactions between the barotropic mode and baroclinic modes of different zonal wavenumbers. The focus of his study was on zonal mean-eddy kinetic energy exchange. This study is unique in

that the focus of the normal mode analysis is on the interaction between synoptic scales and planetary scales and that these interactions are examined in term of the total energy exchange (potential and kinetic) between scales.

A description of the NOGAPS model used in this study is given in Chapter II. The normal modes of this model are derived in Chapter III. To assist in the interpretation of results from the NOGAPS model, a nonlinear scale analysis and the results from a simple analytic model are presented in Chapter IV. The results of the experiments conducted to determine the importance and mechanisms of nonlinear interactions are given in Chapter V. Chapter VI contains a brief summary and some conclusions of this work.

II. THE MODEL

The model used in this study to investigate the dynamics of planetary scale waves is version 2.2 of the Navy Operational Global Atmospheric Prediction System (NOGAPS). This model is a modified version of the general circulation model developed at the University of California at Los Angeles (Arakawa and Lamb, 1977). It is a global finite difference model and uses the primitive equations in sigma coordinates. The resolution of the mass variables (surface pressure and temperature) is 2.4° latitude by 3.0° longitude with nine levels from 50 mb to the surface. The model uses scheme C staggering (Arakawa and Lamb, 1977) in the horizontal, and finite differencing in the vertical according to Arakawa and Suarez (1983). The horizontal finite differencing is energy conserving and it conserves enstrophy when the motion is nondivergent. The vertical differencing conserves the global mass integral of the potential temperature under adiabatic processes and it employs a local form of the hydrostatic equation. The time differencing is a combination of five leapfrog steps for each Matsuno backward step, while the heating is computed during a single forward step that precedes the Matsuno step. However, in this study only the forward time step of the Matsuno step is used in the analysis procedure.

Physical processes include radiation, moist and dry convective adjustment and a cumulus parameterization technique (Arakawa and Schubert, 1974), which interacts with a bulk parameter boundary layer (Randall, 1976; Lord, 1978).

The objective analyses of wind and geopotential are done with a three-dimensional successive corrections method that is a form of the scheme used by Barnes (1964). The analyses of wind and mass are done independently. Since the NOGAPS initialization method is fully described by Barker (1982), only a brief description of this method will be given here. The results of the independent wind and mass analyses are combined via a calculus of variation method in which the balance equation is used as a constraint. The functional

$$F(\phi,\psi) = \int_A (\phi-\tilde{\phi})^2 + \beta(\mathbf{V}-\tilde{\mathbf{V}})^2 + 2\lambda[\nabla\cdot f\nabla\psi + 2J(u,v) - \nabla^2\phi]\,dA \tag{2.1}$$

is minimized and the associated Euler-Lagrange equations are solved over the entire earth. Here ϕ is geopotential, ψ is the stream function, A is the horizontal area over which the integral is applied, λ is a Lagrange multiplier and the symbol $\sim$ denotes analyzed values. The quantity β can be made a function of latitude if desired to force more adjustment toward either one of the analysis fields in certain areas. Thus, β would have relatively greater weight in low latitudes where the wind is a more reliable parameter for analysis and prediction than the geopotential field. The above procedure minimizes the change to the analyzed geopotential and non-divergent wind while constraining these variables toward the balance condition. The problem of generating an appropriate divergence to go with the nondivergent winds produced by this balancing procedure is solved by using the forecast first-guess divergence. The problem of vertically inconsistent corrections is minimized by vertically coupling the variables. The variables are coupled before they are initialized by projecting them onto empirical orthogonal functions. The smoothness of the four empirical orthogonal functions used insures that the inconsistent vertical variations of wind or geopotential that could be generated by the initialization procedure are eliminated.

The initialization procedure used in this version of the NOGAPS model initializes objectively analyzed correction fields for V and ϕ rather than the updated fields. This procedure has the advantage of not affecting areas without new data. The resulting initialized corrections are interpolated to the model sigma coordinates surfaces and added to the first-guess forecast. This method minimizes vertical interpolation error and preserves the model generated first guess divergence.

III. NORMAL MODES

Since the data used in this study are analyzed using the normal modes of the linearized equations from the NOGAPS model, it is important to have a fundamental understanding of these modes. This understanding may be gained by examining the derivation and structure of the modes. The normal modes for an earlier (lower resolution) version of the NOGAPS model were derived by Barker (1982). He followed the method of Temperton (1977) and Temperton and Williamson (1981). Three different sets of modes are derived for the version of the NOGAPS model used in this study. They are obtained below by separation of variables. Except where noted, their derivation closely follows that of Barker (1982). Each set of modes is examined for consistency with the model as well as for similarities to modes derived by other authors. It will be shown that modes derived with a model top at 0 mb are best suited for use in this study.

A. VERTICAL MODES

The linearized governing equations used by Temperton and Williamson (1981) are

$$\frac{\partial \mathbf{V}}{\partial t} + f\mathbf{k} \times \mathbf{V} + \nabla(R\overline{\mathbf{T}} \ln p_s + \phi) = \mathbf{Q}_v \tag{3.1}$$

$$\frac{\partial \mathbf{T}}{\partial t} + \tau(\nabla \cdot \mathbf{V}) = \mathbf{Q}_p \tag{3.2}$$

$$\frac{\partial \ln p_s}{\partial t} + \mathbf{\Pi}^T(\nabla \cdot \mathbf{V}) = \mathbf{Q}_T \tag{3.3}$$

$$\phi = \phi_s + \mathbf{G}\mathbf{T}. \tag{3.4}$$

Here the vertical discretization is taken into account by writing the equation in vector form. Thus, $\mathbf{V}$ is the vector form of the wind, $\mathbf{T}$ is the perturbation temperature, $\overline{\mathbf{T}}$ is the rest-state temperature, p_s is surface pressure, ϕ is the perturbation geopotential, $\nabla \cdot \mathbf{V}$ is divergence and ϕ_s is terrain geopotential. τ and $\mathbf{G}$ are linearized matrix operators and $\mathbf{\Pi}^T$ is a vector. $\mathbf{Q}_V$, $\mathbf{Q}_T$ and $\mathbf{Q}_p$ are the nonlinear components of their

respective equations. All of the above operators and vectors are defined in Temperton and Williamson (1981). Their exact form is not important. However, it is important to note that the entries that make up these matrices are constant and that σ is defined as p/p_s.

Barker approximated (3.1) - (3.4) using the σ system of the NOGAPS model as

$$\frac{\partial \mathbf{V}}{\partial t} + f\mathbf{k} \times \mathbf{V} + \nabla(\overline{\sigma\pi\alpha} \ln \pi + \phi) = \mathbf{Q_v} \tag{3.5}$$

$$\frac{\partial \mathbf{T}}{\partial t} + \tau(\nabla \cdot \mathbf{V}) = \mathbf{Q_T} \tag{3.6}$$

$$\frac{\partial \ln \pi}{\partial t} + \Pi^T (\nabla \cdot \mathbf{V}) = \mathbf{Q_p} \tag{3.7}$$

$$\phi = \phi_s + \overline{\mathbf{G}}\mathbf{T} \tag{3.8}$$

where

$$\sigma = \frac{p - p_t}{\pi} \tag{3.9}$$

and

$$\pi = p_s - p_t. \tag{3.10}$$

p_t is the pressure at the top of the model atmosphere and α is specific volume. τ and G are once again matrix operators that are similar to those in (3.2)-(3.4). They are consistent with the Arakawa and Suarez (1983) vertical finite difference scheme used in the NOGAPS model and are given in Appendix A. A different treatment of (3.4) will be discussed later.

Following Temperton and Williamson (1981), Barker (1982) defined a vector h whose horizontal derivative represents the pressure gradient force.

$$\mathbf{gh} = \phi + \overline{\sigma\pi\alpha} \ln \pi \tag{3.11}$$

This definition allows the determination of a single equation for mass by operating on (3.6) with G, multiplying (3.7) by $\overline{\sigma\pi\alpha}$, and then adding the resulting two equations to obtain

$$g\frac{\partial \mathbf{h}}{\partial t} + \mathbf{C}(\nabla \cdot \mathbf{V}) = \mathbf{Q_h} \tag{3.12}$$

where

$$\mathbf{C} = \overline{G}\tau + \overline{\sigma\pi\alpha}\Pi^{T} \tag{3.13}$$

and

$$\mathbf{Q_h} = \overline{\mathbf{G}}\mathbf{Q_T} + \mathbf{Q_p}R\overline{\mathbf{T}}. \tag{3.14}$$

Although equation set (3.12) is vertically coupled, it can be transformed by separation of variables into a set that is not coupled. This is done through the diagonalization of the matrix **C** by:

$$\mathbf{E}^{-1}\mathbf{C}\mathbf{E} = g\mathbf{D}, \tag{3.15}$$

where the matrix **E** contains the eigenvectors of the matrix **C** as columns and the diagonal matrix **D** contains the eigenvalues of **C**. Defining the vertical transforms of **h** and **V** as

$$\tilde{\mathbf{V}} = \mathbf{E}^{-1}\mathbf{V} \tag{3.16}$$

$$\tilde{\mathbf{h}} = \mathbf{E}^{-1}\mathbf{h} \tag{3.17}$$

produces the uncoupled equation set

$$\frac{\partial\tilde{\mathbf{V}}}{\partial t} + f\mathbf{k}\times\tilde{\mathbf{V}} + g\nabla\tilde{\mathbf{h}} = \tilde{\mathbf{Q}}_{\mathbf{v}} \tag{3.18}$$

$$g\frac{\partial\tilde{\mathbf{h}}}{\partial t} + \mathbf{D}(\nabla\cdot\tilde{\mathbf{V}}) = \tilde{\mathbf{Q}}_{\mathbf{h}}, \tag{3.19}$$

where $\mathbf{Q}_{\mathrm{v}}$ and $\mathbf{Q}_{\mathrm{h}}$ are the transforms of $\mathbf{Q}_{\mathrm{v}}$ and $\mathbf{Q}_{\mathrm{h}}$ respectively. These equations are uncoupled except through the nonlinear terms on the right sides of the equations. The independent variables in (3.18) and (3.19) are the coefficients of the vertical modes (the eigenvectors contained in **E**). There are as many modes as there are levels in the model.

The vertical modes derived using the linearized NOGAPS equations given by (3.5)-(3.8) for $\overline{\mathbf{T}}$ equal to (218, 218, 218, 228, 241, 254, 267, 276, 283)°K are shown in Fig. 3.1. For comparison, the vertical modes derived by Temperton and Williamson (1981) for $\overline{\mathbf{T}}$ equal to (229, 209, 218, 237, 256, 268, 277, 283, 285)°K are shown in Fig.

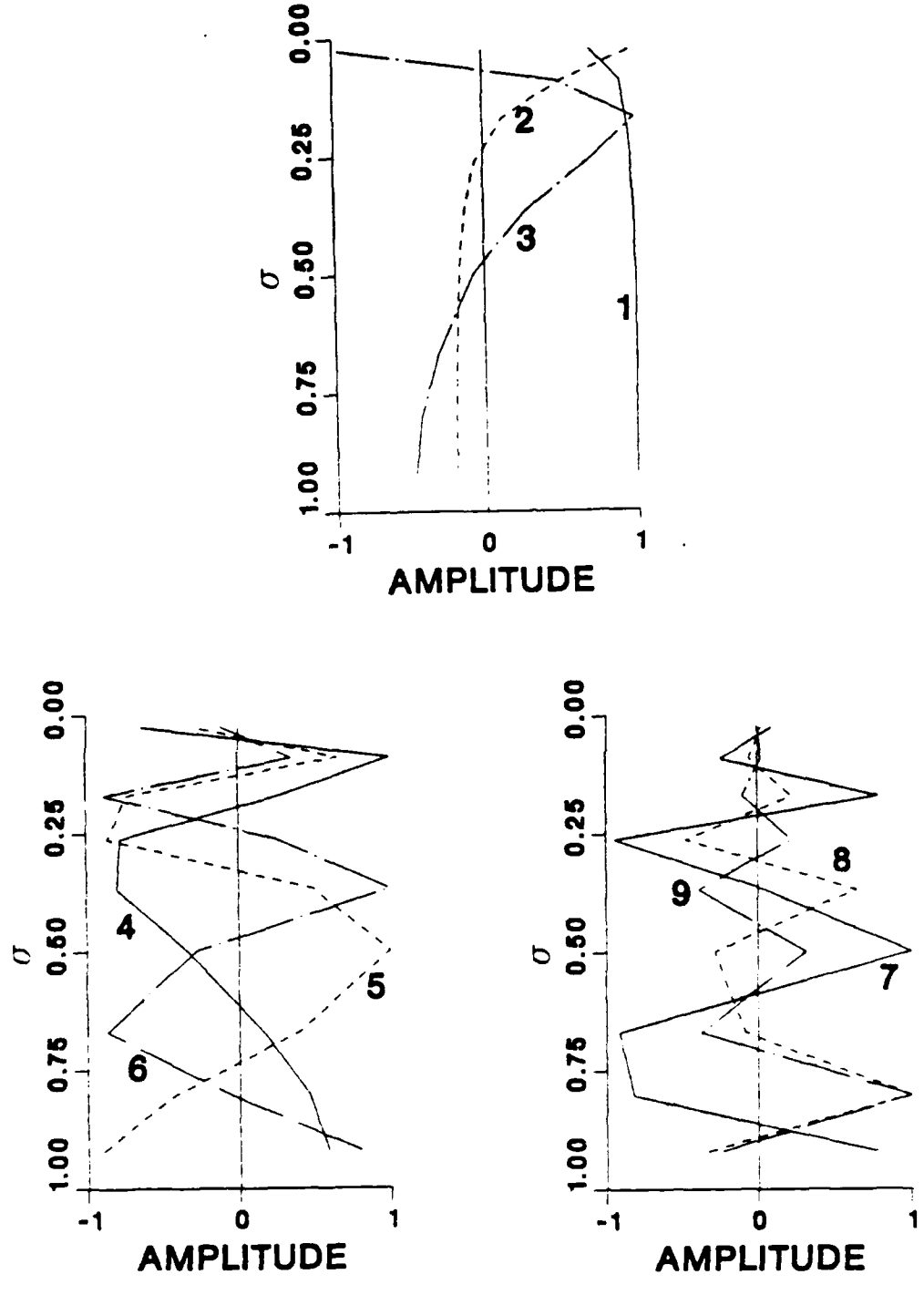

Figure 3.1. Vertical modes for the NOGAPS model with nine levels, $\overline{T}$ equal to (218, 218, 218, 228, 241, 254, 267, 276, 283)°K and a top at 50 mb.

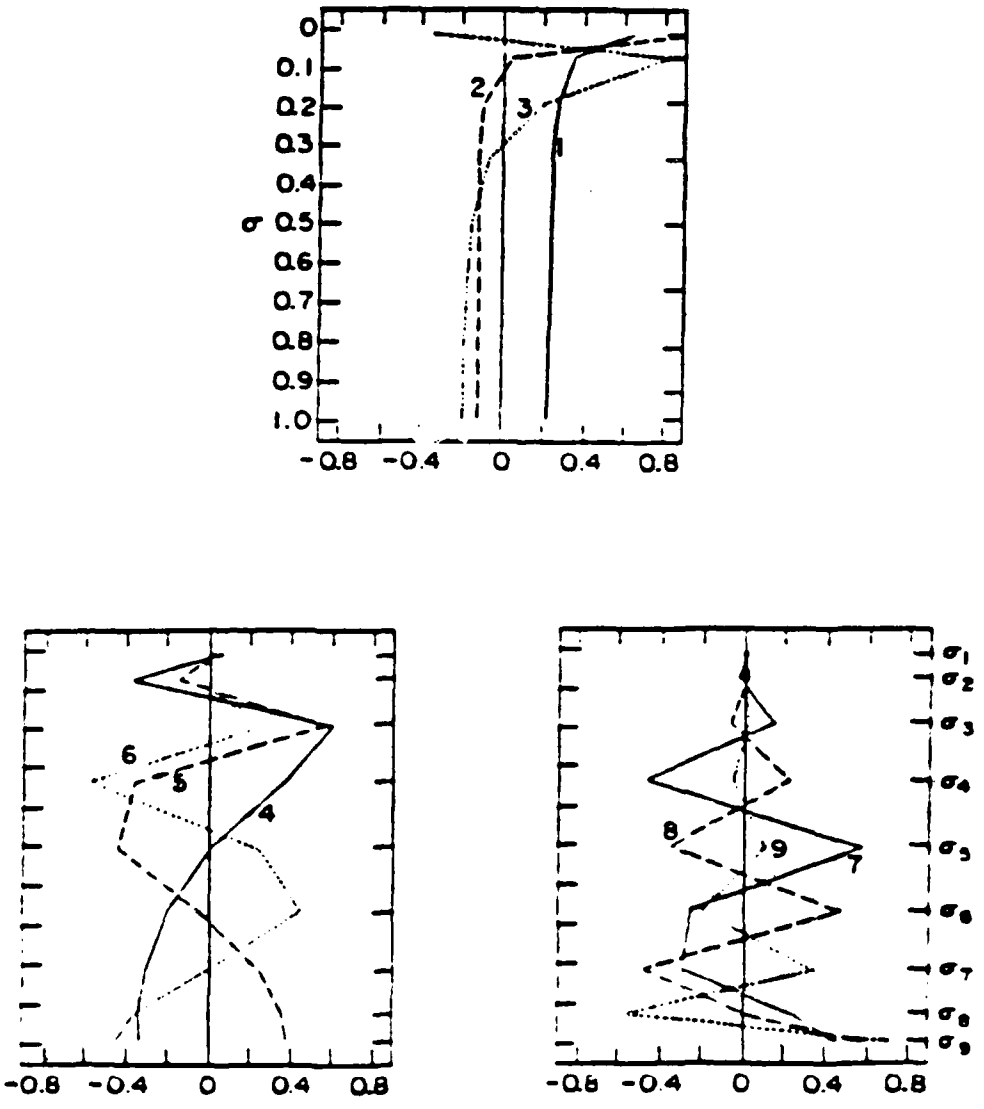

Figure 3.2. Vertical modes from the model used by Temperton and Williamson. The model top is at 0 mb and $\overline{T}$ is equal to (229, 209, 218, 237, 256, 268, 277, 283, 285)°K.

Table 1. Equivalent depths (m) of the vertical modes of the NOGAPS and Temperton and Williamson (T & W) models.

Vertical mode index	NOGAPS	T & W
1	7,829.4	10,153.1
2	972.46	4,701.0
3	186.67	851.40
4	77.86	205.05
5	30.41	64.90
6	13.44	20.06
7	5.629	7.275
8	1.399	2.366
9	.359	.498

3.2. The eigenvalues (equivalent depths) of the vertical modes for this linearization of the NOGAPS model and those derived by Temperton and Williamson (1981) are given in Table 1. These NOGAPS modes are qualitatively very similar to the modes derived by Temperton and Williamson (1981). The general structure (except the sign of the 4th-6th modes are opposite from Temperton and Williamson, but this an arbitrary choice) and the levels at which the crossings occur are similar. However, there are some noticeable differences between the two sets of modes, with the most significant differences occuring in the gravest modes. The NOGAPS barotropic mode (mode one) lacks the characteristic peak at the top of the atmosphere and in fact decreases near the top. The first two baroclinic NOGAPS modes have zero crossings at levels lower than for the modes derived by Temperton and Williamson (1981). Most of these differences can be attributed to the differences between the NOGAPS model and the model used by Temperton and Williamson (1981). One difference between models is the location of the model levels. One of the major differences, in terms of vertical structure, is the location of the model top. The model top in the NOGAPS model is at 50 mb while the top in the model used by Temperton and Williamson (1981) is at 0 mb. Barker (1982) also found that the equivalent depths are sensitive to the location of the model top. Changing the model top from 50 mb to 0 mb increased the equivalent depth of the external mode from 7874 m to 9660 m. Barker found that a consequence of specifying the model top at 50 mb is that all the equivalent depths are smaller than if the top was at 0 mb.

Although most of the difference between the two sets of modes can be attributed to the difference in the model tops, part of this difference is due to an inconsistent

linearization of the hydrostatic equation by Barker. The discretized, unlinearized hydrostatic equation for the NOGAPS model is

$$\boldsymbol{\phi} = \boldsymbol{\phi}_s + \mathbf{GT}, \tag{3.20}$$

where the matrix operator **G** is similar to the one given in Appendix A, except that the full values and not the mean state values are used in the entries of **G**. The **G** matrix defined by Temperton and Williamson (1981) is constant. However, the **G** matrix defined above is not constant. The choice of a model top at a nonzero pressure level makes **G** a function of surface pressure (π in this case), which was not taken into account by Barker (1982) in his linearization of the hydrostatic equation (3.8).

A second set of NOGAPS vertical modes that includes the effect of a variable **G** matrix will now be derived. A more consistent linearization of (3.20) yields

$$\boldsymbol{\phi}' = \boldsymbol{\phi}_s + \overline{\mathbf{G}}\mathbf{T}' + \mathbf{G}'\overline{\mathbf{T}}, \tag{3.21}$$

where

$$\mathbf{G}' = \mathbf{G} - \overline{\mathbf{G}}. \tag{3.22}$$

This linearization of (3.20) has an effect on the matrix **C** from which the vertical modes are derived. Consider the momentum equation

$$\frac{\partial \mathbf{V}}{\partial t} + f\mathbf{k} \times \mathbf{V} + \sigma\pi\boldsymbol{\alpha}\nabla \ln \pi + \nabla\boldsymbol{\phi} = \mathbf{Q}_v. \tag{3.23}$$

Inserting (3.20) in (3.23)

$$\frac{\partial \mathbf{V}}{\partial t} + f\mathbf{k} \times \mathbf{V} + \sigma\pi\boldsymbol{\alpha}\nabla \ln \pi + \nabla\boldsymbol{\phi}_s + \nabla\mathbf{GT} = \mathbf{Q}_v. \tag{3.24}$$

The matrix **G** is a function of π, which is a function of the horizontal coordinates. Expanding $\nabla\mathbf{GT}$ one obtains

$$\frac{\partial \mathbf{V}}{\partial t} + f\mathbf{k} \times \mathbf{V} + \sigma\pi\boldsymbol{\alpha}\nabla \ln \pi + \nabla\boldsymbol{\phi}_s + (\nabla\mathbf{G})\mathbf{T} + \mathbf{G}\nabla\mathbf{T} = \mathbf{Q}_v. \tag{3.25}$$

Following the suggestion of Rosmond (1986) $\nabla\mathbf{G}$ can be written with the chain rule as

$$\pi\frac{d\mathbf{G}}{d\pi}\nabla \ln \pi. \tag{3.26}$$

Using (3.26), (3.25) can be linearized as

$$\frac{\partial \mathbf{V}'}{\partial t} + f\mathbf{k} \times \mathbf{V}' + (\overline{\sigma\pi\boldsymbol{\alpha}} + \overline{\pi}\frac{d\overline{\mathbf{G}}}{d\overline{\pi}}\overline{\mathbf{T}})\nabla \ln \pi + \nabla\boldsymbol{\phi}_s + \overline{\mathbf{G}}\nabla\mathbf{T}' = \mathbf{Q}_v. \tag{3.27}$$

The derivative of **G** with respect to π can be determined analytically since **G** can be written as a function of π. The linearization of the remaining governing equations is unchanged. To obtain a single equation for mass one must define **h** as

$$g\mathbf{h} = (\overline{\sigma\pi\alpha} + \overline{\pi}\frac{d\overline{\mathbf{G}}}{d\overline{\pi}}\overline{\mathbf{T}})\ln\pi + \phi_s + \overline{\mathbf{G}}\mathbf{T}'. \tag{3.28}$$

Using the above definition of **h**, the matrix **C** would be defined as

$$\mathbf{C} = \overline{\mathbf{G}}r + (\overline{\sigma\pi\alpha} + \overline{\pi}\frac{d\overline{\mathbf{G}}}{d\overline{\pi}}\overline{\mathbf{T}})\mathbf{\Pi}^{\mathrm{T}}. \tag{3.29}$$

The matrix **C** defined in (3.29) is clearly different from the **C** defined in (3.13). If **G** were not a function of surface pressure (the model top was at zero), then (3.28) and (3.29) would reduce to (3.11) and (3.13) respectively. Since the matrix **C** in (3.29) is different from that defined in (3.13), the eigenvectors will be different. However, the overall similarities between the vertical eigenvectors and eigenvalues of the NOGAPS model (as derived by Barker, 1982) and those of the model used by Temperton and Williamson (1981) indicate that the effect of the additional term

$$\overline{\pi}\frac{d\overline{\mathbf{G}}}{d\overline{\pi}}\overline{\mathbf{T}} \tag{3.30}$$

in (3.29) is small. The vertical modes obtained from the matrix **C** in (3.29) are shown in Fig. 3.3 and the equivalent depths are given in Table 2. The term (3.30) has been approximated by a centered finite difference as

$$\overline{\pi}\left(\frac{\overline{\mathbf{G}}(\overline{\pi}+\Delta\overline{\pi}) + \overline{\mathbf{G}}(\overline{\pi}-\Delta\overline{\pi})}{2\Delta\overline{\pi}}\right)\overline{\mathbf{T}} \tag{3.31}$$

where $\Delta\pi$ equals 1 mb. The major difference between these modes and those derived previously occurs in the barotropic mode. The characteristic peak that is absent in mode one in Fig. 3.1 is now present. Also, the equivalent depth associated with this mode has increased from 7829 m to 8101 m. The more consistent linearization of the hydrostatic equation leads to a set of vertical modes that are more similar to those derived by Temperton and Williamson (1981).

Although the vertical modes derived with a variable G matrix are more similar (than modes derived without this effect) to modes derived by other authors, they do have some disadvantages. They require the computation and storage of an additional term. In addition, the placement of a model top at 0 mb is clearly a more realistic condition than having the model top at a finite pressure level. The closer the basic state is to the real atmosphere, the better the linear approximation becomes. Thus, it

Table 2. Equivalent depths (m) of the vertical modes of the NOGAPS model that includes the effect of a variable G matrix.

Vertical mode index	Equivalent depth
1	8,101.8
2	914.33
3	198.06
4	73.78
5	31.68
6	12.99
7	5.749
8	1.358
9	.368

would seem that better results would be obtained at less computational and storage expense if the vertical modes were derived with a model top at 0 mb.

Consequently, the modes used in this study are derived from a basic state in which the top of the atmosphere is assumed to be at 0 mb. The equivalent depths for these modes are given in Table 3 and their structure is given in Fig. 3.4. The modes derived with the model top at 0 mb have equivalent depths that are much larger than the NOGAPS modes derived using Barker's linearization or those derived with a variable G matrix. The 0 mb top modes have zero crossing at higher levels than the two other sets of NOGAPS modes and their structure is more similar to the modes derived by Temperton and Willamson.

B. HORIZONTAL MODES

The details of the determination of the horizontal modes of the NOGAPS model have been given by Barker (1982). Only the general method for determining the modes will be given here.

The solutions of the uncoupled equation set (3.18 - 3.19) for each equivalent depth D_ℓ gives the horizontal modes of the model. Equations (3.18) and (3.19) can be written in finite difference form as

$$\delta_t \overline{u}_{i+\frac{1}{2},j} - f_j \overline{(\overline{v})}^{\lambda,\theta}_{i+\frac{1}{2},j} + \frac{g(\delta_\lambda \overline{h})_{i+\frac{1}{2},j}}{a\rho_j \Delta\lambda} = \overline{Q}_{u_{i+\frac{1}{2},j}} \tag{3.32}$$

$$\delta_t \overline{v}_{i,j+\frac{1}{2}} + \frac{\overline{\overline{(f\rho\overline{u})}^{\lambda}_{i,j-\frac{1}{2}}}^{\theta}}{\rho_{j-\frac{1}{2}}} + \frac{g(\delta_\theta \overline{h})_{i,j+\frac{1}{2}}}{a\Delta\theta} = \overline{Q}_{v_{i,j-\frac{1}{2}}} \tag{3.33}$$

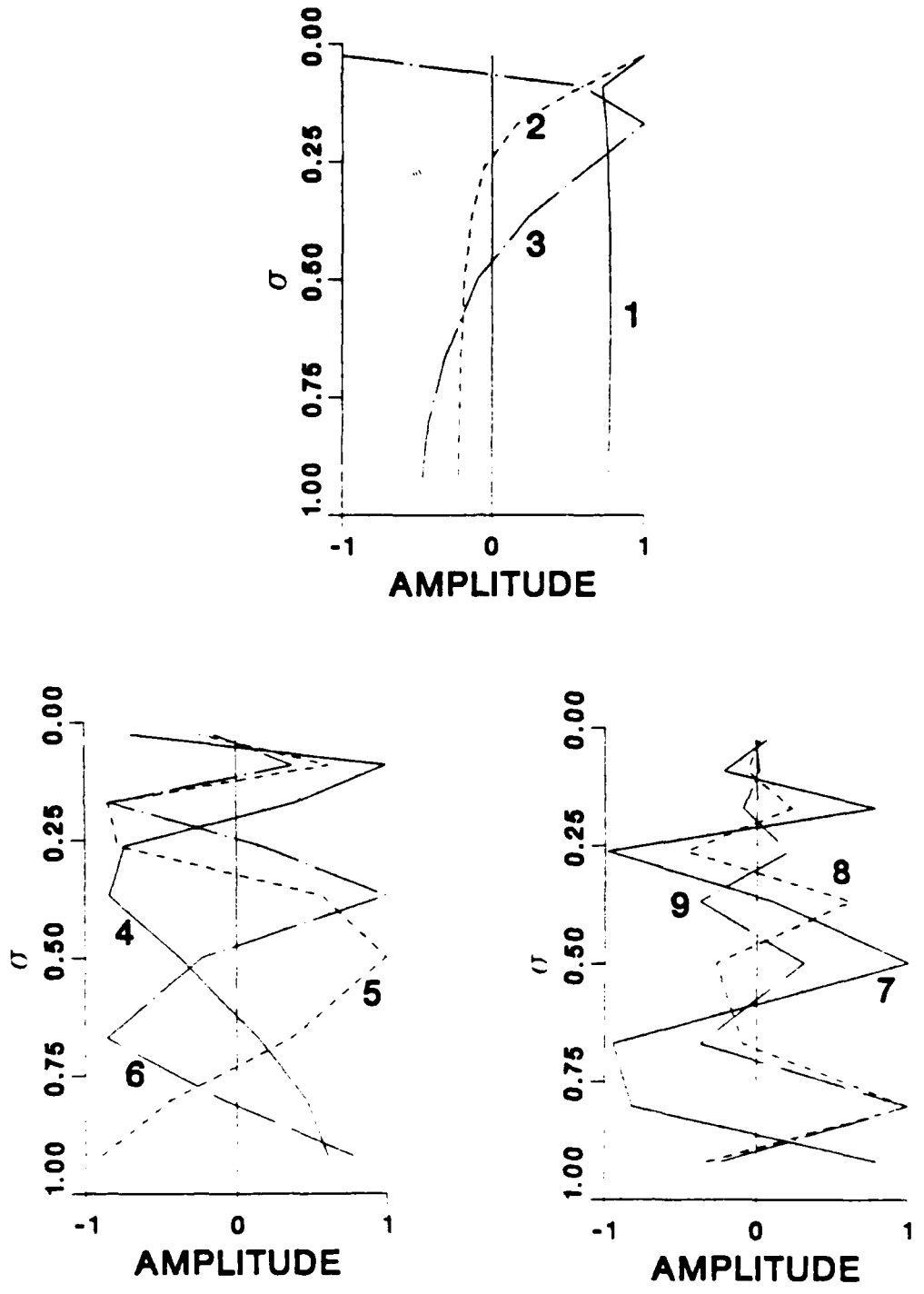

Fig 3.3. As in Figure 3.1, except modes are derived including the effect of a variable G matrix.

Table 3. Equivalent depths (m) of the vertical modes of the NOGAPS model with model top at 0 mb.

Vertical mode index	Equivalent depth
1	9,687.3
2	2,575.5
3	496.85
4	156.01
5	52.99
6	21.85
7	8.960
8	2.253
9	.520

$$\delta_t \overline{h}_{i,j} + D[\frac{(\delta_\theta \overline{v})_{i,j}}{a\Delta\theta} + \frac{(\delta_\lambda \overline{u})_{i,j}}{\rho_j a\Delta\lambda}] = \overline{Q}_{h_{i,j}} \tag{3.34}$$

A vertical mode index (ℓ) is assumed for D and each variable. The finite difference operators are

$$(\delta_z T)_k \equiv T_{k+\frac{1}{2}} - T_{k-\frac{1}{2}} \tag{3.35}$$

$$\overline{(T)}^z_k \equiv \frac{T_{k+\frac{1}{2}} + T_{k-\frac{1}{2}}}{2} \tag{3.36}$$

$$\overline{(T)}^{z,y}_k \equiv \overline{\overline{(T)}^z_k}^y. \tag{3.37}$$

The other variables are defined as follows: a is the earth's radius, $\Delta\lambda$ is the longitudinal grid interval, $\Delta\theta$ is the latitudinal grid interval, u and v are the east and north components of the wind, respectively, i and j are the longitudinal and latitudinal indexes, respectively and ρ is cos θ.

Special definitions of the Coriolis term are used to keep the matrix operator of (3.32)-(3.34) symmetric. A symmetric matrix insures that the corresponding eigenvectors are orthogonal, which allows determination of the inverse of the eigenvector matrix by simply taking the transpose. To achieve symmetry, the Coriolis term in (3.32) is replaced by

$$\frac{f_j^- \rho_{j-\frac{1}{2}} \overline{(\overline{v})}^\lambda_{i+\frac{1}{2},j-\frac{1}{2}} + f_j^+ \rho_{j+\frac{1}{2}} \overline{(\overline{v})}^\lambda_{i+\frac{1}{2},j+\frac{1}{2}}}{2\rho_j} \tag{3.38}$$

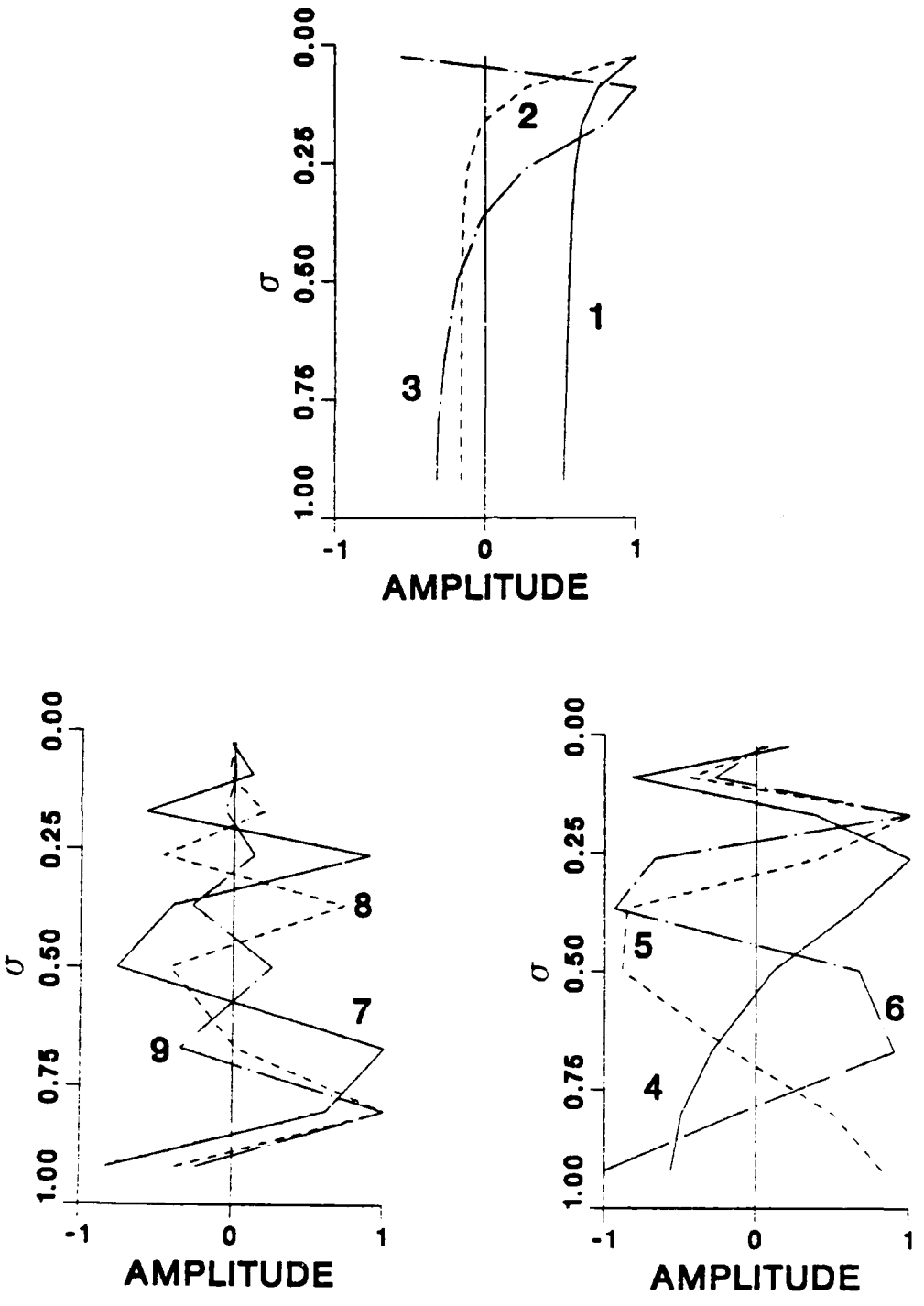

Figure 3.4. Same as Figure 3.1, except model top is at 0 mb.

and the Coriolis term in (3.33) is replaced by

$$\frac{f_j^- \overline{(\overline{u})}^{\bullet}_{i,j} + f_{j-1}^+ \overline{(\overline{u})}^{\bullet}_{i,j-1}}{2} \tag{3.39}$$

where

$$f_j^+ = \frac{\frac{2}{3} f_{j+\frac{1}{2}} + \frac{1}{3} f_{j-\frac{1}{2}}}{\cos\left(\frac{\Delta\theta}{2}\right)} \tag{3.40}$$

and

$$f_j^- = \frac{\frac{1}{3} f_{j+\frac{1}{2}} + \frac{2}{3} f_{j-\frac{1}{2}}}{\cos\left(\frac{\Delta\theta}{2}\right)}. \tag{3.41}$$

These definitions correspond to a potential enstrophy conserving finite difference scheme as derived by Temperton and Williamson (1979).

A dynamical state vector is defined as

$$\overline{\gamma}(\lambda_i, \theta_j, \ell) = \begin{pmatrix} \overline{u}(\lambda_i, \theta_j, \ell) \\ \overline{v}(\lambda_i, \theta_j, \ell) \\ \overline{h}(\lambda_i, \theta_j, \ell) \end{pmatrix} \tag{3.42}$$

where γ represents grid point values of the vertical mode coefficients. These values can be expanded into Fourier modes by

$$\overline{\gamma}(\lambda_i, \theta_j, \ell) = \sum_{m=0}^{I-1} \tilde{\gamma}(m, \theta_j, \ell) e^{im\lambda_i}. \tag{3.43}$$

The inverse of (3.43) is

$$\tilde{\gamma}(m, \theta_j, \ell) = I^{-1} \sum_{i=1}^{I} \overline{\gamma}(\lambda_i, \theta_j, \ell) e^{im\lambda_i}. \tag{3.44}$$

Assuming a wave solution of the form in (3.43) allows (3.32) - (3.34) to be written as

$$\frac{\partial u_j}{\partial t} J'(m) - \frac{1}{\rho_j} \frac{r(m)}{2} [f_j^- \rho_{j-\frac{1}{2}} \tilde{v}_{j-\frac{1}{2}} + f_j^+ \rho_{j+\frac{1}{2}} \tilde{v}_{j+\frac{1}{2}}] + \frac{gik'\tilde{h}_j}{a\rho_j} = \tilde{Q}_u \tag{3.45}$$

$$\frac{\partial v_{j-\frac{1}{2}}}{\partial t} + \frac{r(m)}{2} [f_j^- \tilde{u}_j + f_{j-1}^+ \tilde{u}_{j-1}] J'(m) + \frac{g}{a\Delta\theta} [\tilde{h}_j - \tilde{h}_{j-1}] = \tilde{Q}_v \tag{3.46}$$

$$\frac{\partial h_j}{\partial t} + \frac{D_\ell}{a\rho_j} [ik'\tilde{u}_j + \frac{1}{\Delta\theta} (\tilde{v}_{j+\frac{1}{2}} \rho_{j-\frac{1}{2}} - \tilde{v}_{j-\frac{1}{2}} \rho_{j-\frac{1}{2}})] = \tilde{Q}_h, \tag{3.47}$$

where

$$k'(m) = \frac{\sin\left(\frac{\Delta\lambda}{2}\right)}{\frac{\Delta\lambda}{2}} \tag{3.48}$$

$$r(m) = \cos(\frac{m\Delta\lambda}{2}) \tag{3.49}$$

$$J'(m) = \cos(\frac{\Delta\lambda}{2}) - i\sin(\frac{\Delta\lambda}{2}). \tag{3.50}$$

After applying the symmetric operator

$$\mathbf{S}_\ell = \begin{pmatrix} J'(m) & 0 & 0 \\ 0 & -i & 0 \\ 0 & 0 & (g/D_\ell)^{\frac{1}{2}} \end{pmatrix} \tag{3.51}$$

to γ such that

$$\tilde{\gamma}' = \mathbf{S}_\ell \tilde{\gamma} \tag{3.52}$$

allows Eqs. (3.45) - (3.47) to be written in matrix form as:

$$-i\mathbf{Q}\frac{\partial\tilde{\gamma}'}{\partial t} + \mathbf{L}\tilde{\gamma}' = -i\mathbf{Q}\tilde{\mathbf{H}}'. \tag{3.53}$$

The matrix $\mathbf{Q}$ is diagonal and positive definite with entries related to the $\cos\theta_j$, $\mathbf{L}$ is a matrix depending on the actual finite differences used in the model, and $\mathbf{H}$ is a matrix representing the latitudinal variation of the corresponding nonlinear terms transformed in the same way as u, v and h are to give γ

To complete the computation of the horizontal modes, the matrix equation (3.53) is rescaled using

$$\hat{\gamma} = \mathbf{Q}^{\frac{1}{2}}\tilde{\gamma}', \quad \hat{\mathbf{H}} = \mathbf{Q}^{\frac{1}{2}}\tilde{\mathbf{H}}', \quad \hat{\mathbf{L}} = \mathbf{Q}^{-\frac{1}{2}}\mathbf{L}\mathbf{Q}^{-\frac{1}{2}}. \tag{3.54}$$

If $\mathbf{Y}$ contains the eigenvectors (normal modes) of $\mathbf{L}$, then (3.53) can be written using (3.54) as

$$-i\frac{\partial}{\partial t}[\mathbf{Y}^{-1}\hat{\gamma}] + \mathbf{Y}^{-1}\hat{\mathbf{L}}\mathbf{Y}(\mathbf{Y}^{-1}\hat{\gamma}) = -i\mathbf{Y}^{-1}\hat{\mathbf{H}}. \tag{3.55}$$

The identity

$$\Lambda = \mathbf{Y}^{-1}\mathbf{L}\mathbf{Y}. \tag{3.56}$$

where Λ is a diagonal matrix containing the eigenvalues of $\mathbf{L}$, makes it possible to rewrite (3.55) as

$$\frac{\partial\mathbf{C}}{\partial t} = -i\Lambda\mathbf{C} + \mathbf{r}, \tag{3.57}$$

where

$$\mathbf{C} = \mathbf{Y}^{-1}\hat{\gamma}. \tag{3.58}$$

The nonlinear term is now r and the mode frequencies are Λ.

The components of C, denoted here by $C(m,n,\ell)$, are referred to as the coefficient of the normal mode. Equation (3.57) can be written in component from as

$$\frac{\partial C(m,n,\ell)}{\partial t} = -i\omega C(m,n,\ell) + r(m,n,\ell). \tag{3.59}$$

The elements of C are functions of the vertical, zonal and meridional mode numbers ℓ, m and n, respectively. The mode number n is a measure of the number of zeros between the poles. For each m, ℓ, and n there are three equations for C: One for an eastward propagating gravity wave (EG); one for a westward propagating gravity (WG); wave and one for a westward propagating Rossby wave (R). The symmetric modes (u and h are symmetric about the equator and v is antisymmetric) consist of the odd indexed (n = 1,3,5..) Rossby modes and even indexed gravity modes. The antisymmetric modes (u and h antisymmetric about the equator and v is symmetric) consist of the even indexed Rossby modes and the odd indexed gravity modes. These coefficients are the amplitudes of the various modes required to represent a particular atmospheric state. Corresponding to each horizonal mode is a natural frequency (ω) that is determined as an eigenvalue of the system. The frequencies of various modes corresponding to those given by Dickenson and Williamson (1972), Temperton and Williamson (1981) and Barker (1982) are given in Tables 4 and 5 . The frequencies of all the modes are very similar, with most of small differences being due to the different horizontal resolutions used in each model. The structures for a few selected modes are given in Figs. 3.5 and 3.6. The structures of these modes are also very similar to those derived by other authors (Temperton and Williamson, 1981; Kasahara,1976; Dickenson and Williamson, 1972). Any results obtained here using the modes of the NOGAPS model should be similar to results obtained using modes of other models.

C. EXPANSION OF DATA INTO NORMAL MODES

The amplitude of a given mode is determined by expanding grid point values into normal modes. The first step in the expansion process is to remove the mean state, then combine the thermodynamic variables into one variable, the equivalent geopotential (gh). The data are expanded into vertical modes using (3.16) and (3.17), then into Fourier modes using (3.44) and lastly scaled according to (3.51). The symmetric and antisymmetric components are found by averaging or differencing the values from the two hemispheres. Finally, each scaled Fourier mode of each vertical mode is expanded into meridional modes by (3.58).

Table 4. Frequencies (s^{-1}) of the Rossby modes for the models used by Temperton and Williamson (1981) (T&W), Dickenson and Williamson (1972) (D&W), for the NOGAPS model with model top at 50 mb (B) and for the NOGAPS model with model top at 0 mb (M). D = 10 km for (T&W) and (D&W), D = 8,101 m for (B) and D = 9,682 m for (M). Horizontal grid intervals are specified in degrees.

n	T&W, 10	D&W, 2.5	B 2.4 x 3	M 2.4 x 3
0	6.11×10^{-5}	6.14×10^{-5}	5.93×10^{-5}	6.14×10^{-5}
1	1.44×10^{-5}	1.45×10^{-5}	1.32×10^{-5}	1.43×10^{-5}
2	8.46×10^{-6}	8.73×10^{-6}	8.16×10^{-6}	8.68×10^{-6}
3	5.72×10^{-6}	5.87×10^{-6}	5.61×10^{-6}	5.86×10^{-6}
4	3.98×10^{-6}	4.17×10^{-6}	4.05×10^{-6}	4.18×10^{-6}
5	2.87×10^{-6}	3.08×10^{-6}	3.03×10^{-6}	3.11×10^{-6}
6	2.14×10^{-6}	2.36×10^{-6}	2.34×10^{-6}	2.39×10^{-6}
7	1.63×10^{-6}	1.86×10^{-6}	1.86×10^{-6}	1.89×10^{-6}
8	1.27×10^{-6}	1.49×10^{-6}	1.51×10^{-6}	1.52×10^{-6}
9	1.01×10^{-6}	1.22×10^{-6}	1.24×10^{-6}	1.25×10^{-6}
10	8.10×10^{-7}	1.02×10^{-6}	1.04×10^{-6}	1.05×10^{-6}
11	6.62×10^{-7}	8.58×10^{-7}	8.83×10^{-7}	8.89×10^{-7}
12	5.52×10^{-7}	7.30×10^{-7}	7.58×10^{-7}	7.62×10^{-7}
13	4.70×10^{-7}	6.27×10^{-7}	6.57×10^{-7}	6.60×10^{-7}
14	4.11×10^{-7}	5.43×10^{-7}	5.74×10^{-7}	5.77×10^{-7}
15	3.75×10^{-7}	4.73×10^{-7}	5.06×10^{-7}	5.08×10^{-7}
16	3.13×10^{-7}	4.14×10^{-7}	4.49×10^{-7}	4.50×10^{-7}

For each ℓ and zonal wavenumber $m \neq 0$, there are 111 modes in the NOGAPS model for the symmetric case and 112 for the antisymmetric case. These modes may be divided into three sets (sets of 37 each for the symmetric case, two sets of 37 and one set of 38 for the antisymmetric case). The modes associated with the 37 largest negative eigenvalues are usually referred to as westward-gravitational (WG) modes. The 37 modes whose eigenvalues are positive are refered to as eastward-gravitational (EG) modes. The remaining modes, all with negative or zero values are referred to as Rossby or rotational (R). In a linearized model, these modes describe westward- and

Table 5. As in Table 4, except for eastward-gravitational modes.

n	T&W, 10	D&W, 2.5	B 2.4 x 3	M 2.4 x3
0	-5.44×10^{-5}	-5.38×10^{-5}	-4.71×10^{-5}	-5.29×10^{-5}
1	-1.31×10^{-4}	-1.30×10^{-4}	-1.18×10^{-4}	-1.28×10^{-4}
2	-1.87×10^{-4}	-1.86×10^{-4}	-1.69×10^{-4}	-1.84×10^{-4}
3	-2.35×10^{-4}	-2.36×10^{-4}	-2.13×10^{-4}	-2.33×10^{-4}
4	-2.79×10^{-4}	-2.83×10^{-4}	-2.55×10^{-4}	-2.80×10^{-4}
5	-3.22×10^{-4}	-3.29×10^{-4}	-2.97×10^{-4}	-3.27×10^{-4}
6	-3.63×10^{-4}	-3.75×10^{-4}	-3.38×10^{-4}	-3.73×10^{-4}
7	-4.01×10^{-4}	-4.21×10^{-4}	-3.80×10^{-4}	-4.20×10^{-4}
8	-4.36×10^{-4}	-4.66×10^{-4}	-4.22×10^{-4}	-1.51×10^{-4}
9	-4.69×10^{-4}	-5.10×10^{-4}	-4.63×10^{-4}	-4.66×10^{-4}
10	-4.98×10^{-4}	-5.54×10^{-4}	-5.05×10^{-4}	-5.13×10^{-4}
11	-5.23×10^{-4}	-5.97×10^{-4}	-5.47×10^{-4}	-5.60×10^{-4}
12	-5.44×10^{-4}	-6.38×10^{-4}	-5.88×10^{-4}	-6.06×10^{-4}
13	-5.61×10^{-4}	-6.79×10^{-4}	-6.29×10^{-4}	-6.52×10^{-4}
14	-5.72×10^{-4}	-7.19×10^{-4}	-6.70×10^{-4}	-6.98×10^{-4}
15	-5.94×10^{-4}	-7.57×10^{-4}	-7.11×10^{-4}	-7.44×10^{-4}
16	-5.94×10^{-4}	-7.94×10^{-4}	-7.51×10^{-4}	-7.89×10^{-4}

eastward-propagating gravity waves, and westward-propagating Rossby waves, respectively. Consistent with the above categorization, Kelvin waves are EG modes and mixed Rossby-gravity waves are R modes. For each ℓ, there are 113 zonally symmetric ($m = 0$) modes in the NOGAPS model. The modes may be divided among the types R, WG and EG. All of the R modes for $m=0$ are stationary in the linearized model.

In the real atmosphere or in nonlinear models, the normal modes from the linearized equations are no longer independent solutions and their behavior is not necessarily wave-like. However, each mode may be considered as describing a particular dynamical structure. The behavior of these modes is altered by the inclusion

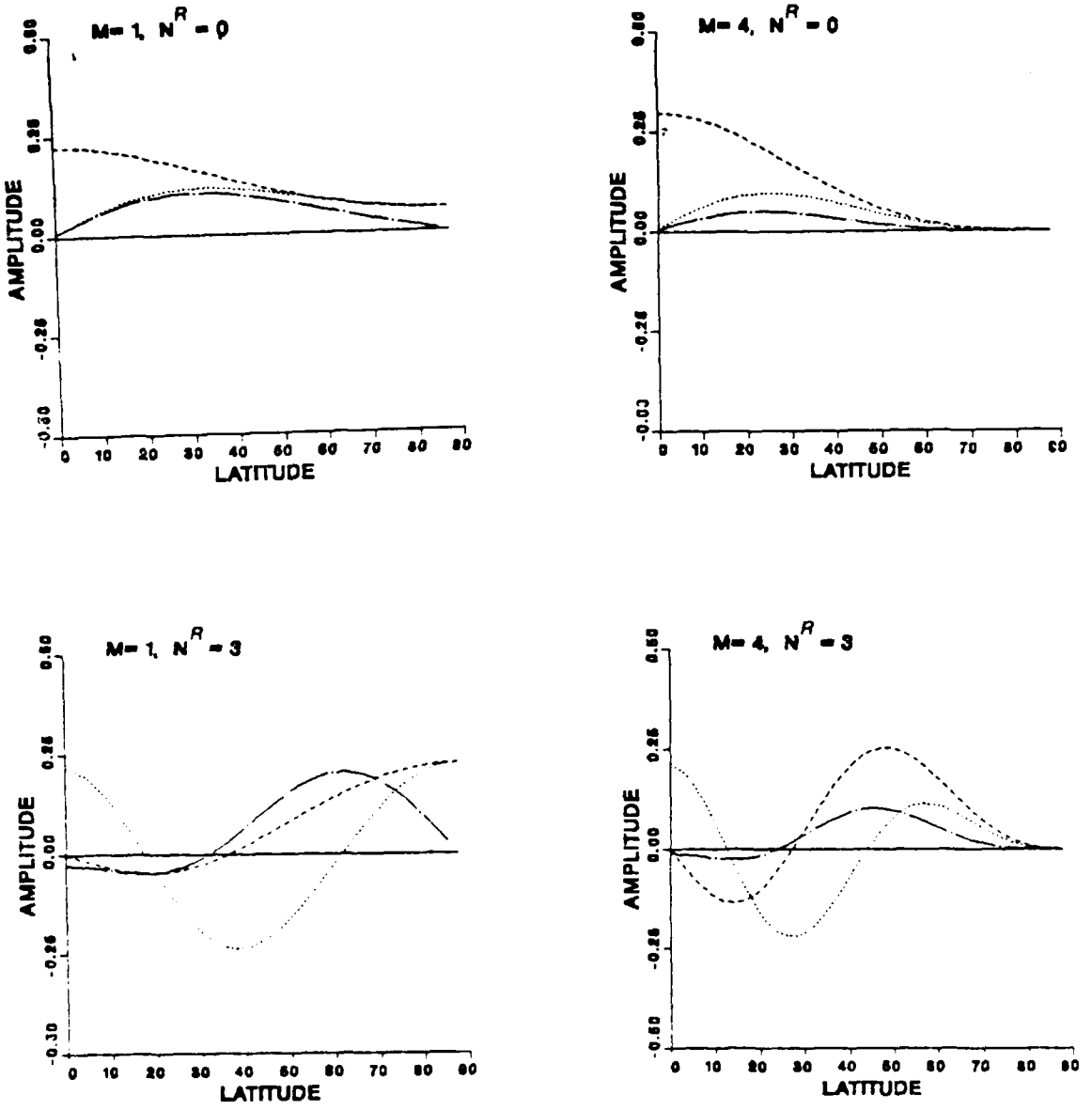

Figure 3.5. Structure of the u component (dotted), v component (dashed), and the h component for selected rotational modes (R) of the model in this study. M is the zonal wavenumber and N is the meridional mode number.

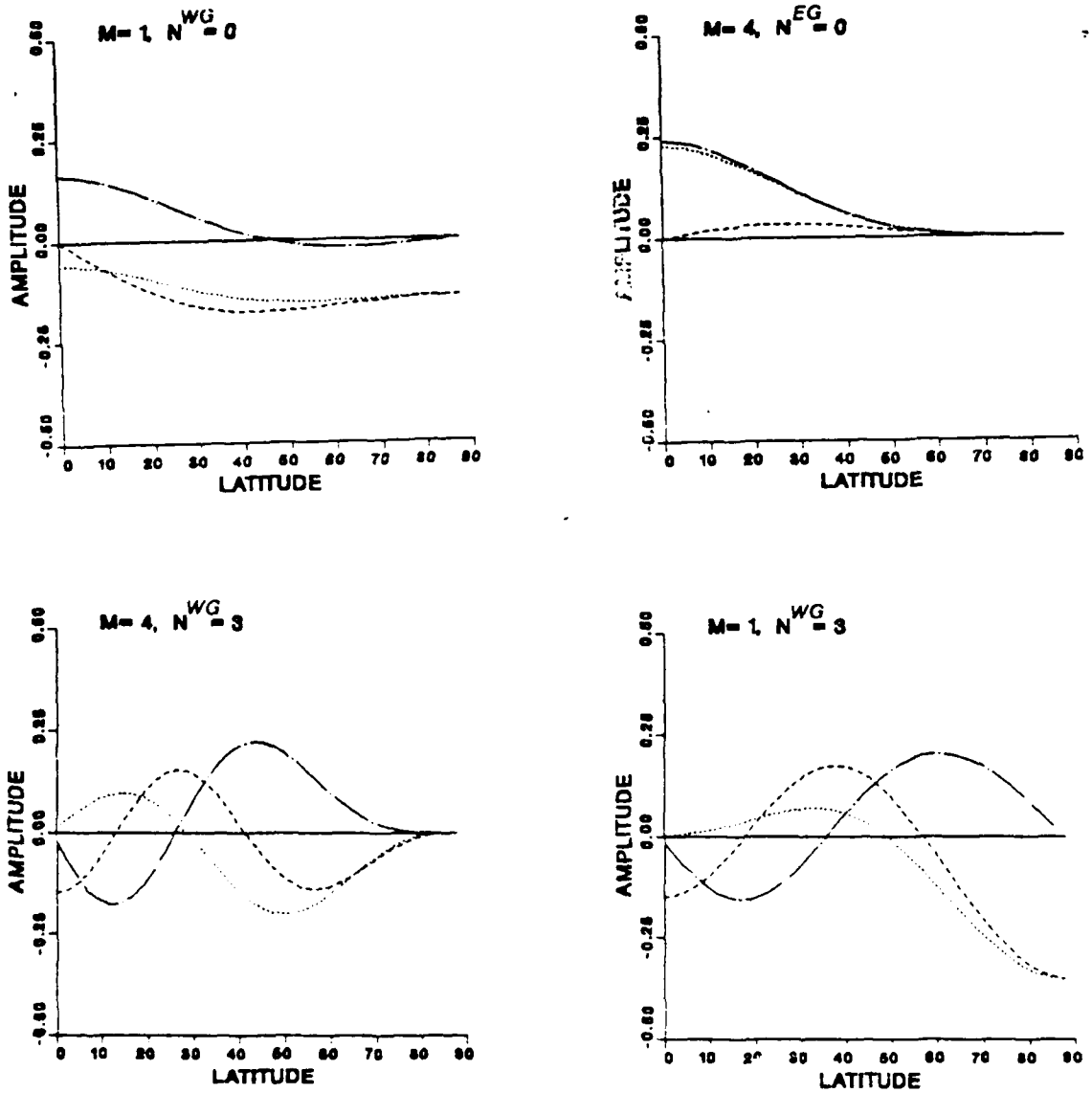

Fig 3.6. As Figure 3.5, except for selected gravitational modes (EG, WG).

of those terms/physical processes that are absent in the linearized models: nonlinear advective terms and diabatic terms (which include friction). These terms couple the behavior of the modes in a nonlinear model. The eigenvalue associated with each mode in a nonlinear model is not the only frequency the mode may have, but it may be considered as the mode's natural or resonant frequency. Whether a mode with that frequency is observed depends on the strength of the nonlinear and diabatic forcing.

For the modes of equivalent depth D_ℓ, the structures of the modes have been normalized so that the sum of the kinetic plus available potential energies per unit mass of the corresponding fields is given by

$$E_\ell = \frac{1}{2} \sum_{n \in S_\ell} C_n C_n^* \tag{3.60}$$

where C_n is the amplitude of the mode designated by the index n and the asterisk denotes a complex conjugate. The sum is over all modes of a given equivalent depth D_ℓ (denoted by the set S_ℓ). For each value of ℓ, each mode contributes independently to E_ℓ because the modes are mutually orthogonal for each ℓ.

The vertical modes of the NOGAPS model are not orthogonal. Therefore, it is not true that

$$E' = \sum_{\ell=1}^{9} E_\ell \tag{3.61}$$

is the total kinetic plus available potential energy of all the modes. However, E' is positive definite and increases in value as the E_ℓ increase. Although its is not the precise energy, it does have utility.

D. NORMAL MODE ANALYSIS

In the nonlinear, diabatic, discrete-time NOGAPS model the prognostic equation of a coefficient may be written as

$$\frac{\Delta C_n}{\Delta t} = -i\omega C_n + N_n + Q_n \tag{3.62}$$

where $\Delta C_n \Delta t$ is the discrete time tendency of a particular vertical, zonal, meridional EG, WG, or R mode, $-i\omega C_n$ represents the linear terms in the model, $i=\sqrt{-1}$, N_n represents the adiabatic nonlinear terms, and Q_n is a sum of diabatic terms. The focus of this study is on the prognostic equation for the R modes and the nonlinear interactions which may occur through the adiabatic nonlinear term.

The procedure for determining the different terms in (3.62) for the R modes is relativity simple. The linear term for a particular mode n is determined by multipling

the coefficient of a mode by its natural frequency. The coefficient for a mode is determined from initialized NOGAPS analyses using the procedure described in section C of this chapter. The discrete time tendency is determined from a one-time step integration of the NOGAPS model. First the coefficients for the modes are determined at the initial time (t). Then the model is integrated over one time step (Δt) and the coefficients at $t + \Delta t$ are determined. The discrete time tendency is then given by

$$\frac{C_n(t + \Delta t) - C_n(t)}{\Delta t} \tag{3.63}$$

where Δt is equal to four minutes. The determination of the time tendency was found not to be sensitive to the time step used. In addition, for the Rossby modes, one would not expect $\Delta C/\Delta t$ to vary greatly from one time step to another. This in fact has been demonstrated by Errico (1984). However, for the gravitational modes, $\Delta C/\Delta t$ may vary largely in the initial stages of a model integration. This variation of $\Delta C/\Delta t$ for the gravitation mode will depend on the initialization method used. For the Rossby modes, the procedure for determining the time tendency should be adequate for the purposes of this study.

The nonlinear adiabatic term is determined by subtracting the linear term from the discrete time tendency that has been determined from an **adiabatic** one-time step integration. Errico (1981) was able to derive explicit expressions for the Ns of a simple, nonlinear, f-plane, primitive equation, two layer model. For this simple model, the Ns can be written in terms of the sums of quadratic functions of the modal amplitudes. These sums represent interactions between rotational (geostrophic), rotational and gravitational (ageostrophic) and gravitational modes of different wavenumbers. The complex NOGAPS model does not lend itself to such a simple decomposition. Thus the nonlinear adiabatic term is determined numerically using the NOGAPS model and the procedure described above.

Using a numerical procedure, Errico (1984) was able to decompose the adiabatic nonlinear terms of the modal equations of a gobal primitive equation spectral model into three different groups: $N_n(R)$, $N_n(G)$ and $N_n(R*G)$. The first depends only on the rotational mode coefficients, the second only on the gravitational mode coefficients, and the last only on the sums of products of each type of mode with the other. Because of the highly divergent nature of the gravational modes, $N_n(R*G)$, may be likened to interactions between the divergent component of the motion and the rotational component. For a simple f-plane model, $N_n(R*G)$ would represent terms such as the advection of momentum by the divergent wind.

The adiabatic nonlinear terms for the modal equations of the NOGAPS model are not decomposed into $N_n(R)$, $N_n(G)$, and $N_n(R^*G)$. However, Errico (1984) has shown for the long time solutions to the NCAR Community Climate Model, $N_n(R)$ is an order of magnitude larger than $N_n(R^*G)$ and $N_n(G)$ for all but the smallest vertical scale rotational modes ($\ell = 8,9$). For the smallest vertical scale R modes $N_n(R^*G) \sim N_n(R)$. For rotational modes, one would expect that if nonlinear interactions occur through the adiabatic nonlinear term that they would to a first order approximation, be due to interactions between rotational modes (except for the smallest scale vertical modes i.e. $\ell = 8,9$).

The diabatic term is determined by subtracting the discrete time tendency determined from the adiabatic one-time step integration from the discrete time tendency determined from a one-time step integration which included diabatic parameterizations (e.g. cumulus, sensible heating parameterizations etc).

In addition to allowing the examination of possible nonlinear interactions through the adiabatic nonlinear term, (3.62) can be used to gain insight into the general dynamical nature of a given mode. This insight may be gained by comparing the relative magnitudes of the different terms. For example, it is possible to determine if a mode is balanced, i.e., the time tendency of the mode is small compared to the other terms. If a mode is not balanced, it may be possible to ascertain which terms are most important in determining the time tendency of a given mode.

IV. A SCALE ANALYSIS AND A SIMPLE ANALYTIC MODEL

To interpret the results from the complex NOGAPS model, one must first have a good understanding of the linear and nonlinear dynamics of planetary scale modes. To highlight the difference between the results presented in the next chapter and those predicted by linear theory, a linear and nonlinear scale analysis of the shallow water equations is presented. A simpler analytic model will also be developed in this section. This simple model will be used to show what terms are represented by the adiabatic nonlinear term and how synoptic waves may affect planetary waves.

A. SCALE ANALYSIS

Some important dynamical features of planetary scale Rossby modes can be illustrated by a simple scale analysis of the shallow water equations with a variable Coriolis parameter. The shallow water equations are adequate for this purpose because the primitive equations can be represented through the normal mode as a set of shallow water equations for each equivalent depth (assuming V is not a function of the vertical coordinate). The shallow water equations to be scale analyzed are

$$\frac{\partial \mathbf{V}}{\partial t} + \mathbf{V} \cdot \nabla \mathbf{V} + \nabla \phi + f\mathbf{k} \times \mathbf{V} = 0 \tag{4.1}$$

and

$$\frac{\partial \phi}{\partial t} + \mathbf{V} \cdot \nabla \phi + \overline{\phi} \nabla \cdot \mathbf{V} + \phi \nabla \cdot \mathbf{V}. \tag{4.2}$$

The nonlinear terms have been retained to show how nonlinear interactions may have a significant affect on planetary scale motions. In a strictly shallow water context, $\overline{\Phi}$ would be considered the mean height of the fluid and would be fixed. In a normal mode context, $\overline{\Phi}$ is the equivalent depth and is different for each vertical mode considered. Note that Φ is the departure of the geopotential from $\overline{\Phi}$.

Two length scales are chosen to demonstrate how synoptic scale motions (L_2) affect planetary scale Rossby motions (L_1). In addition, two different time scales, an advective scale ($T = L, V$) and one appropriate for a free planetary scale Rossby wave, will be used. The latter time scale is determined by L_1/C, where $C = \beta\overline{\Phi}/f^2$ is the phase speed of the fastest Rossby mode. Using two length scales and the time scale associated with this fast Rossby mode makes the scale analysis presented in this section

different from those of other authors (Burger, 1958; Haltiner and Williams, 1980) who used an advective time scale and a single planetary length scale. The scales used in the following analyses are:

$$f = 10^{-4}s^{-1}, \quad L_1 = 10^7 m, \quad , L_2 = 10^6 m, \quad V = 10 ms^{-1} \tag{4.3}$$

1. Single length scale analysis

Using the planetary length scale given above and assuming an advective time scale, the equation of motion (4.1), with the exception of the pressure gradient force, is scaled as

$$\frac{\partial \mathbf{V}}{\partial t} + \mathbf{V} \cdot \nabla \mathbf{V} + \nabla \phi + f\mathbf{k} \times \mathbf{V} = 0 \tag{4.4}$$

$$\frac{V^2}{L_1} \qquad \frac{V^2}{L_1} \qquad \frac{\phi}{L_1} \qquad fV$$

or after multiplication by L_1

$$V^2 \qquad V^2 \qquad \phi \qquad fV$$

so that the values are

$$10^3 \qquad 10^2 \qquad \phi \qquad 10^4$$

If the equation is to be balanced, the pressure gradient force must balance the coriolis force i.e. the scaling is geostrophic, so that Φ scales to 10^4.

Using geostrophic scaling for ϕ, an advective time scale and a single planetary length scale, the geopotential equation (4.2) is

$$\frac{\partial \phi}{\partial t} + \mathbf{V} \cdot \nabla \phi + \bar{\phi} \nabla \cdot \mathbf{V} + \phi \nabla \cdot \mathbf{V} \tag{4.5}$$

$$\frac{V\phi}{L_1} \qquad \frac{V\phi}{L_1} \qquad \frac{\Phi V}{L_1} \qquad \frac{V\phi}{L_1}$$

and after multiplication by L_1

$$V\phi \qquad V\phi \qquad \Phi V \qquad V\phi$$

For the above analysis, Φ is the scale value of $\bar{\phi}$ and it represents the scale of the equivalent depth. The appropriate value of Φ for the fast time scaling is $10^5 m^2 s^{-2}$ (this is the approximate value for the equivalent depth of the barotropic mode). Using this value of Φ and fast time scale in (4.5) reveals that the time tendency and the divergence terms are of the same order. For the slow time scaling, if one assumes $\Phi = 10^5$ then the first-order equation for (4.5) is $\nabla \cdot \mathbf{V} = 0$. However, most of the

planetary scale modes with a natural period (i.e, the period determined from the natural frequency) that is approximately equal to the slow time scale do not have an equivalent depth equal to 10^5. A more appropriate equivalent depth for these modes is $\overline{\Phi} = 10^4$. Using the slow time scale and the more appropriate value of Φ shows all the terms in (4.5) to be the same magnitude. The results obtained using the advective time scaling and the more appropriate value for the equivalent depth are similar to the results obtained by other authors (Burger, 1958; Haltiner and Williams, 1980).

The first-order system obtained using the fast time scale is quite different from that obtained using the slow time scale. The fast time scale system is linear, the winds are geostrophic and the time variation is given solely by the divergence term in (4.5). The slow time scale system is nonlinear, the winds are also geostrophic, but the time variation is determined by advection of the mass field as well as by the divergence term.

2. **Multi-length scale analysis**

To accomplish a multi-length scale analysis, the synoptic length scale (L_2) is used whenever a derivative is taken in the nonlinear terms. Planetary scaling (L_1) is used in the other terms. A more formal procedure to determine nonlinear interactions would be to transform the equations using the appropriate transform based on the geometry: Fourier transforms for cartesian geometry or spherical harmonics for spherical geometry. After transformation of the equations, the nonlinear terms would appear as interaction coefficients that represent explicitly the scale interactions. For scale analysis purposes, this interaction can be illustrated by using only two length scales (L_1, L_2) in the nonlinear terms. Using multiple length scales in the scaling of (4.1) yields results similar to those obtained using a single length scale except the advection term is an order of magnitude larger. However, this term is still an order of magnitude smaller than the largest term in the equation.

Using multiple length scales in the scaling of (4.2) gives the same results as using a single length scale if one assumes geostrophic synoptic scaling for Φ i.e $\Phi = fVL_2$. The overall effect of including nonlinear interactions for the fast Rossby waves is small. The momentum advection term in (4.1) is an order of magnitude larger but it is still an order of magnitude smaller than the largest term in (4.1). Because of the assumption of geostrophic synoptic scaling for Φ in the nonlinear analysis of (4.5), there is no difference between the linear and nonlinear scaling of this equation. For the fast time scaling, the time tendency in (4.5) is still driven by the divergence term and for the slow scaling (with $\overline{\Phi} = 10^4$) all the terms are still the same magnitude.

It would appear from the analysis using the slow scaling and $\Phi = 10^4$ that nonlinear interactions from the advection of the synoptic scale momentum fields may not be as important as the nonlinear advection of the mass field. This result is consistent with geostrophic adjustment theory, which indicates that the atmospheric response to a mass perturbation for scales larger than the Rossby radius $\sqrt{\Phi}/f$ is greater than for a given wind perturbation. The planetary length scale used in this analysis is an order of magnitude larger than the Rossby radius. Since the Rossby radius decreases as the equivalent depth ($\bar{\Phi}$) decreases, one would expect mass perturbations to be even more important for the smaller equivalent depth planetary scale baroclinic modes.

Additional information on the dynamics of planetary scale Rossby modes can be obtained by scale analyzing the quasi-geostrophic potential vorticity equation. This equation can be derived from (4.1) and (4.2). The potential vorticity equation for this model is

$$\frac{\partial \zeta}{\partial t} - \frac{f}{\bar{\phi}}\frac{\partial \phi}{\partial t} + \mathbf{V}\cdot\nabla\zeta - \frac{f}{\bar{\phi}}\mathbf{V}\cdot\nabla\phi + v\beta = 0$$

$$\frac{CV}{L_1^2} \quad \frac{f^2CV}{\bar{\phi}} \quad \frac{V^2}{L_2^2} \quad \frac{f^2V^2}{\bar{\phi}} \quad \frac{Vf}{L_1} \qquad (4.6)$$

$$\frac{C}{L_1 f} \quad \frac{fCL_1}{\bar{\phi}} \quad \frac{L_1 V}{fL_2^2} \quad \frac{fVL_1}{\bar{\phi}} \quad 1$$

where the nonlinear scaling for this equation is based on fast time scaling using $\Phi = 10^5$. For this scaling, these nondimensional quantities have the values:

$$\frac{C}{L_1 f} \sim \frac{1}{10} \quad \frac{fCL_1}{\bar{\phi}} \sim 1 \quad \frac{L_1 V}{fL_2^2} \sim 1 \quad \frac{fVL_1}{\bar{\phi}} \sim \frac{1}{10}.$$

Note that the nonlinear interaction through the advection of vorticity is now part of the first-order system. This implies that nonlinear momentum interactions could be important. Again, this result is consistent with geostrophic adjustment theory because for these modes $\bar{\Phi} = 10^5$ the Rossby radius is approximately the same order of magnitude as the planetary length scale.

If the nonlinear terms are dropped and the geostrophic relation for V is inserted, (4.6) can be written in cartesian coordinates as

$$-\frac{f}{\bar{\phi}}\frac{\partial \beta}{\partial t} + \frac{\beta}{f}\frac{\partial \phi}{\partial x} = 0. \qquad (4.7)$$

Insert the wave solution $\Phi = exp\, i\mu(x\text{-}ct)$ into (4.7) then

$$C = -\frac{\beta\bar{\phi}}{f^2} \tag{4.8}$$

This agrees with the value of C that is used in this scale analysis. However, the effect of the nonlinear terms may be such that this phase speed is not observed for this mode, so that it is probably an overestimate of the speed of this mode. One final point to be made from this analysis is that the importance of the mass field interactions will increase as the equivalent depth ($\bar{\Phi}$) decreases.

B. A SIMPLER ANALYTIC MODEL

The normal modes of the NOGAPS model are quite complex and are not easily interpreted. A simpler analytic model will be developed in this section to illustrate what terms/effects are represented by the nonlinear term of a mode. Using this model, it will be shown how waves of a particular vertical and horizontal scale can affect waves of different scales. The results from this quasi-geostrophic model will be used to interpret the more complex NOGAPS model.

Following Haltiner and Williams (1980), the quasi-geostrophic equations are

$$\frac{\partial\zeta}{\partial t} + \mathbf{V}_\psi \cdot \nabla(\zeta + \beta_0 y) - f_0 e^z \frac{\partial}{\partial Z}(e^{-z}\dot{Z}) = 0 \tag{4.9}$$

$$\frac{\partial}{\partial t}\frac{\partial\phi'}{\partial Z} + \mathbf{V}_\psi \cdot \nabla\frac{\partial\phi}{\partial Z} + \Gamma(Z)\dot{Z} = 0 \tag{4.10}$$

$$\nabla^2\phi' - f\zeta = 0 \tag{4.11}$$

where

$$\nabla = \mathrm{i}\frac{\partial}{\partial x} + \mathrm{j}\frac{\partial}{\partial y} \tag{4.12}$$

$$\mathbf{V}_\psi = f_0^{-1}\mathbf{k} \times \nabla\phi = \mathbf{k} \times \nabla\psi \tag{4.13}$$

$$\zeta = f_0^{-1}\nabla^2\phi \tag{4.14}$$

$$\Gamma(Z) = \frac{\partial}{\partial Z}\left(\frac{\partial\bar{\phi}}{\partial Z} + \kappa\bar{\phi}\right) = \frac{H^2 g}{T}\left(\frac{g}{C_p} - \frac{1}{H}\frac{\partial T}{\partial Z}\right). \tag{4.15}$$

The vertical coordinate (Z) of this system is defined and related to the more familiar pressure coordinate system in Appendix B. The vertical velocity of this system is given by Z. Now making the Boussinesq approximation (e^{-Z} = constant) and assuming static stability (Γ) is constant, then (4.9)-(4.11) may be written

$$\frac{\partial}{\partial t}\nabla^2\psi + \mathbf{k}\times\nabla\psi\cdot\nabla\nabla^2\psi + \frac{\partial\psi}{\partial x}\beta_0 - f_0\frac{\partial\dot{Z}}{\partial Z} = 0 \tag{4.16}$$

$$\frac{\partial}{\partial t}\frac{\partial\psi}{\partial Z} + \mathbf{k}\times\nabla\psi\cdot\nabla\frac{\partial\psi}{\partial Z} + \frac{\Gamma}{f_0}\dot{Z} = 0. \tag{4.17}$$

If the above is linearized about a basic state of rest and $\dot{Z} = 0$ at the surface ($Z = 0$) and at the top of the atmosphere ($Z = Z_T$), then the vertical modes for this system are

$$\Phi_\ell(Z) = A_\ell \cos\frac{\ell\pi Z}{Z_T} \tag{4.18}$$

The derivation of these modes is given in Appendix B. To transform (4.16) and (4.17) let

$$\psi = \sum_{-\infty}^{\infty}\psi_\ell(x,y,t)e^{i\ell\frac{\pi Z}{Z_T}} \tag{4.19}$$

$$\dot{Z} = \sum_{-\infty}^{\infty}\dot{Z}_\ell(x,y,t)e^{i\ell\frac{\pi Z}{Z_T}} \tag{4.20}$$

where $\Psi_\ell = \psi_{-\ell}$ and $\dot{Z}_\ell = -\dot{Z}_{-\ell}$ Substituting the above expressions into (4.16) and (4.17), multiplying by $e^{-(i\ell\pi Z/Z_T)}$, and integrating from $Z=0$ to $Z=Z_T$ gives the following transformed equations

$$\frac{\partial}{\partial t}\nabla^2\psi_\ell + \sum_j \mathbf{k}\times\nabla\psi_j\cdot\nabla\nabla^2\psi_{\ell-j} + \frac{\partial\psi_\ell}{\partial x}\beta_0 + f_0\ell\dot{Z}_\ell = 0 \tag{4.21}$$

$$\ell\frac{\partial\psi_\ell}{\partial t} + \sum_j(\ell-j)\mathbf{k}\times\nabla\psi_j\cdot\nabla\psi_{\ell-j} + \frac{\Gamma}{f_0}\dot{Z}_\ell = 0, \tag{4.22}$$

where the boundary conditions require $\dot{Z}_\ell = 0$ if $\ell = 0$ ($\ell=0$ in this system corresponds to $\ell=1$ for the NOGAPS mode, i.e., the barotropic mode). The second terms in (4.21) and (4.22) represent the nonlinear interactions between vertical modes j and ℓ-j that will affect a given mode ℓ. The interaction term in (4.21) represents interaction between the momentum fields, while the interaction between the mass fields (temperature advection) is represented by the interaction term in (4.22).

It will be useful to look at two cases. For the first case $\ell = 0$ (barotropic case), so that (4.21) and (4.22), reduce to one equation

$$\frac{\partial}{\partial t}\nabla^2\psi_0 + \sum_j \mathbf{k} \times \nabla\psi_j \cdot \nabla\nabla^2\psi_{-j} + \frac{\partial\psi_0}{\partial x}\beta_0 = 0 \tag{4.23}$$

As expected, this equation closely resembles the barotropic quasi-geostrophic vorticity equation, except that the simple advection term is represented as the nonlinear interaction term. The only interactions that are allowed come from the momentum advection terms. The interaction through the mass advection term is eliminated because of the boundary conditions $\dot{Z} = 0$ at the top and bottom of the model. The boundary condition at the bottom is not the same as in the NOGAPS model where the vertical motion is not necessarily zero at the bottom. One consequence of the boundary condition $\dot{Z} = 0$ at the top and bottom of the simple model is that the vertical structure of the barotropic mode is strictly constant. Also, since the equivalent depth is proportional to $1/\ell$, the equivalent depth of the barotropic mode is infinite. If the equivalent depth (Φ) is infinite then from (4.6) it can be seen that mass advection term is zero. The equivalent depth associated with the barotropic mode of the NOGAPS model is not infinite. Thus, one would not expect that interactions through the mass advection term would be completely eliminated. However, the scale analysis of (4.6) indicated that for an equivalent depth that is approximately equal to that of the barotropic mode of the NOGAPS model, that interactions through this term would be small. It remains to be seen if the results for the barotropic mode of this simple model apply to results obtained with the more complex NOGAPS model.

The second case is just the general baroclinic case where $\ell \neq 0$. For example, if $\ell = 3$ then (4.21) and (4.22) become

$$\frac{\partial}{\partial t}\nabla^2\psi_3 + \sum_j \mathbf{k} \times \nabla\psi_j \cdot \nabla\nabla^2\psi_{3-j} + \frac{\partial\psi_3}{\partial x}\beta_0 + f_0 3\dot{Z}_\ell = 0 \tag{4.24}$$

$$3\frac{\partial\psi_3}{\partial t} + \sum_j (3-j)\mathbf{k} \times \nabla\psi_j \cdot \nabla\psi_{3-j} + \frac{\Gamma}{f_0}\dot{Z}_3 = 0, \tag{4.25}$$

Thus, interaction may occur for baroclinic modes through the temperature advection term and through the momentum advection term. For mode number 3 to be affected by nonlinear interactions, mode ψ_1 will interact with ψ_2, ψ_5 with ψ_{-2}, etc.

Horizonal wave interaction will now be examined using Fourier transforms. The following derivation closely follows the method used in Lorenz (1960) and Haltiner and Williams (1980). If we assume periodic boundary conditions in both x and y

$$\psi_\ell(x+\frac{2\pi}{k}, y+\frac{2\pi}{g}, t) = \psi_\ell(x, y, t) \tag{4.26}$$

$$\dot{Z}_\ell(x+\frac{2\pi}{k}, y+\frac{2\pi}{g}, t) = \dot{Z}_\ell(x, y, t) \tag{4.27}$$

then the horizontal variations of ψ_ℓ and Z_ℓ can be represented using orthogonal basis functions of the form:

$$\varphi_{mn}(x,y) = e^{i(mkx+ngy)}. \tag{4.28}$$

Using the above, ψ and Z are represented as

$$\psi(x,y,Z,t) = \sum_\ell \sum_m \sum_n C_{\ell,m,n}(t) e^{i(mkx+ngy)} e^{i\frac{\ell\pi Z}{Z_T}} \tag{4.29}$$

$$\dot{Z}(x,y,Z,t) = \sum_\ell \sum_m \sum_n D_{\ell,m,n}(t) e^{i(mkx+ngy)} e^{i\frac{\ell\pi Z}{Z_T}}, \tag{4.30}$$

where k and g are the periods in the x and y directions respectively. Therefore, (4.21) and (4.22) can be transformed to

$$\frac{\partial C_{\mathbf{M},\ell}}{\partial t} = \frac{imk\beta C_{\mathbf{M},\ell}}{\mathbf{M}\cdot\mathbf{M}} + \sum_j \sum_{\mathbf{H}} (\mathbf{M}-\mathbf{H})\cdot(\mathbf{M}-\mathbf{H})\mathbf{k}\cdot\mathbf{H}\times\mathbf{M}\, C_{\mathbf{M}-\mathbf{H},j} C_{\mathbf{H},\ell-j} \tag{4.31}$$
$$+ \frac{f_0 \ell}{\mathbf{M}\cdot\mathbf{M}} D_{\mathbf{M},\ell}$$

$$\frac{\partial C_{\mathbf{M},\ell}}{\partial t} = \sum_j \sum_{\mathbf{H}} \frac{(\ell-j)}{\ell} (\mathbf{M}-\mathbf{H})\cdot(\mathbf{M}-\mathbf{H})\mathbf{k}\cdot\mathbf{H}\times\mathbf{M}\, C_{\mathbf{M}-\mathbf{H},j} C_{\mathbf{H},\ell-j} \tag{4.32}$$
$$- \frac{\Gamma}{f_0 \ell} D_{\mathbf{M},\ell},$$

where $\mathbf{M} = mk\mathbf{i} + ng\mathbf{j}$, $\underline{\nabla}\underline{\nabla} = \underline{\nabla}$ and $\mathbf{H}$ is a dummy index. The interaction terms in the above equations represent interactions between vertical as well as horizontal modes. The horizontal modes interact in the same manner as do the vertical modes. That is, zonal wavenumber 7 may interact with zonal wavenumber 8 to affect zonal wavenumber 1.

Eliminating $D_{\mathbf{M},\ell}$ between (4.31) and (4.32) gives the spectral form of the potential vorticity equation

$$\frac{\partial C_{\mathbf{M},\ell}}{\partial t} = \frac{imk\beta_0 C_{\mathbf{M},\ell}}{A_2} + (1+\frac{f_0^2 \ell}{\Gamma}) \sum_j \sum_{\mathbf{H}} \frac{A_1}{A_2} C_{\mathbf{M}-\mathbf{H},j} C_{\mathbf{H},\ell-j}, \tag{4.33}$$

where

$$A_1 = (\mathbf{M} - \mathbf{H}) \cdot (\mathbf{M} - \mathbf{H})\mathbf{k} \cdot \mathbf{H} \times \mathbf{M}$$

and

$$A_2 = (\mathbf{M} \cdot \mathbf{M}) + \frac{f_0^2 \ell^2}{\Gamma} \quad .$$

The spectral form of the quasi-geostrophic vertical motion equation is obtained by eliminating $\partial C_{\mathbf{M},\ell}/\partial t$ between (4.31) and (4.32) to give

$$D_{\mathbf{M},\ell} = -\frac{imk\ell\beta_0 C_{\mathbf{M},\ell}}{(\mathbf{M} \cdot \mathbf{M})} + [(\ell - j) - \frac{\ell}{\mathbf{M} \cdot \mathbf{M}}]\frac{A_1}{A_3} + \sum_j \sum_{\mathbf{H}} C_{\mathbf{M}-\mathbf{H},j} C_{\mathbf{H},\ell-j} \quad (4.34)$$

where

$$A_3 = (\frac{f_0^2 \ell^2}{\mathbf{M} \cdot \mathbf{M}} + \frac{\Gamma}{f_0}) \quad .$$

Using (4.33) and (4.34) some analogies to the normal modes of the NOGAPS can now be made.

The spectral form of the quasi-geostrophic potential vorticity equation (4.33) is of the form as (3.62) i.e

$$\frac{\Delta C_n}{\Delta t} = -i\omega C_n + N_n \quad (4.35)$$

where

$$\omega = \frac{imk\ell\beta_0}{A_2} \quad (4.36)$$

and

$$N_n = (1 + \frac{f_0^2 \ell}{\Gamma}) \sum_j \sum_{\mathbf{H}} \frac{A_1}{A_2} C_{\mathbf{M}-\mathbf{H},j} C_{\mathbf{H},\ell-j} \quad (4.37)$$

Thus (4.33) may be likened to the prognostic equation for the rotational modes of the more complex NOGAPS model. For this simple model the adiabatic nonlinear term (N_n) is written as the sum of quadratic products of the modal coefficients and it represents interactions between the rotational modes of different wavenumbers. Note that there is no prognostic equation for $D_{\mathbf{M},\ell}$. $D_{\mathbf{M},\ell}$ may be likened to the coefficient of a gravitational mode for the more complex NOGAPS model. The equation for $D_{\mathbf{M},\ell}$ is purely diagnostic and the amplitude of $D_{\mathbf{M},\ell}$ is determined solely by the rotational components of the motion (this is consistent with the initial assumption of quasi-geostrophic conditions). A final point to be made from (4.33) and (4.34) is that

N_n for the quasi-geostrophic equations does not contain interactions between the divergent and rotational components of the motion.

It is desirable to form the kinetic and potential energy equations for these modes. The kinetic energy for this system is given by

$$K = \int_0^{2\pi/k} \int_0^{2\pi/s} \int_0^{2\pi} \nabla\psi \cdot \nabla\psi \, dZ \, dx \, dy = \frac{1}{2} \sum_{\ell} \sum_{\mathbf{M}} \mathbf{M} \cdot \mathbf{M} C_{\mathbf{M},\ell} C_{-\mathbf{M},-\ell} \quad (4.38)$$

using the above and (4.16), the kinetic energy equation for this system may be written as

$$\frac{\partial K}{\partial t} = \frac{1}{2} \sum_{\ell} \sum_{\mathbf{M}} C_{-\mathbf{M},-\ell} \sum_{j} \sum_{\mathbf{H}} (\mathbf{M}-\mathbf{H}) \cdot (\mathbf{M}-\mathbf{H}) \mathbf{k} \cdot \mathbf{H} \times \mathbf{M} C_{\mathbf{M}-\mathbf{H},j} C_{\mathbf{H},\ell-j} \quad (4.39)$$

$$+ f_0 \ell C_{\mathbf{M},-\ell} D_{\mathbf{M},\ell}$$

$$+ C_{\mathbf{M},\ell} \sum_{j} \sum_{\mathbf{H}} (-\mathbf{M}-\mathbf{H}) \cdot (-\mathbf{M}-\mathbf{H}) \mathbf{k} \cdot \mathbf{H} \times (-\mathbf{M}) C_{-\mathbf{M}-\mathbf{H}} C_{\mathbf{H},-\ell-j}$$

$$- f_0 \ell C_{-\mathbf{M},-\ell} D_{-\mathbf{M},-\ell}$$

A potential energy equation may be formed by assuming the potential energy is proportional to

$$P = \sum_{\ell} \sum_{\mathbf{M}} \frac{f_0 \ell^2}{\Gamma} C_{\mathbf{M},\ell} C_{-\mathbf{M},-\ell} \quad (4.40)$$

Using the above and (4.22), the potential energy equation for this system may be written as

$$\frac{\partial P}{\partial t} =$$

$$\sum_{\ell} \sum_{\mathbf{M}} \frac{f_0^2 \ell^2}{\Gamma} C_{-\mathbf{M},-\ell} \sum_{j} \sum_{\mathbf{H}} (\ell - j)(\mathbf{M} - \mathbf{H} \cdot (\mathbf{M}-\mathbf{H}) \mathbf{k} \cdot \mathbf{H} \times \mathbf{M} C_{\mathbf{M}-\mathbf{H},j} C_{\mathbf{H},\ell-j} \quad (4.41)$$

$$+ f_0 \ell C_{\mathbf{M},-\ell} D_{\mathbf{M},\ell}$$

$$- \frac{f_0^2 \ell^2}{\Gamma} C_{\mathbf{M},\ell} \sum_{j} \sum_{\mathbf{H}} (\ell - j)(-\mathbf{M} - \mathbf{H} \cdot (-\mathbf{M}-\mathbf{H}) \mathbf{k} \cdot \mathbf{H} \times (-\mathbf{M}) C_{-\mathbf{M}-\mathbf{H}} C_{\mathbf{H},-\ell-j}$$

$$- f_0 \ell C_{-\mathbf{M},-\ell} D_{-\mathbf{M},-\ell}$$

Based on (4.39) and (4.41), the amount of kinetic or potential energy transferred to a given mode $C_{\mathbf{M},\ell}$ is proportional to the amplitude of that mode times the pair of interacting modes $C_{\mathbf{M}-\mathbf{H},j} C_{\mathbf{H},\ell-j}$. Also note that the potential energy as defined in

The scale analysis and simple analytic model results presented in this chapter indicate how the dynamics of planetary-scale waves could be affected by synoptic-scale waves and how this effect might vary with vertical mode. However, the simple system of equations used here do not address the other important aspects of the dynamics of planetary-scale waves. For example, the importance of forcing by diabatic processes and nonlinear interactions which involve the divergent component of the wind are not addressed by the quasi-geostrophic equations. For any given time, these neglected effects could be small, but in a climatic sense (time mean) they may be important. The adiabatic nonlinear term (N_n) for the rotational modes of the NOGAPS model will include interactions between different scales of the highly divergent gravitational modes and the rotational modes. However, for the long-time solution to the NCAR Community Climate Model, Errico (1984) has shown that the adiabatic nonlinear term that represents interactions between the gravitational modes and rotational modes is generally an order of magnitude smaller than the adiabatic term that contains only interactions between rotational modes (except for the shallowest vertical modes $\ell = 8,9$).

While the results of the simple analytic model do not contain all the possible interactions between modes, one would expect the results to be valid as a first order approximation to the more complex NOGAPS model. In addition, the possible importance of diabatic process and forcing by the divergent part of the motion do not negate the possible importance of synoptic-scale interactions through the adiabatic nonlinear term.

V. RESULTS

The first experiment of this study is designed to determine the dynamical importance of synoptic-scale nonlinear interactions on planetary scale Rossby modes. In the first part of this experiment, 19 days of 12UTC initialized NOGAPS analyses taken every five days from 16 January 1986 to 16 April 1986 are projected onto the normal modes of the model and the magnitudes of the terms given in (3.62) are determined. In addition, the energy spectrum as a function of meridional mode number for each vertical mode is determined. Mean magnitudes of the terms for zonal wavenumbers 1, 2 and 3, are obtained by averaging the real and imaginary parts of the respective terms over the period and then taking the magnitude of that average. An alternative way to compute these would be to take the magnitude and then average. The latter method has been used by most other authors (Errico, 1984; Kasahara and Puri, 1981). Similarities between the time-averaged energy spectra computed in this study and those computed by other authors indicate the difference in averaging techniques produces no qualitative difference in the spectra. Only the time-averaged spectra are computed by averaging the real and imaginary parts. All other averages are computed by taking the magnitude first and then averaging.

Since the vertical modes are not orthogonal, the energy spectrums as a function of vertical modes cannot be precisely compared. However, the meridional energy spectrum for each vertical mode is exact since the meridional modes are orthogonal. Due to the large number of modes associated with each zonal wavenumber (there are nine vertical modes and 37 meridional modes associated with each), it is necessary to limit the number of modes to be examined. The choice of modes to be examined should be based on the energetics and dynamics of these modes. The energy spectrum of these modes should give some indication as to which modes (meridional and vertical), if any, are the most important.

A. ENERGETICS AND DYNAMICS OF PLANETARY SCALE MODES

The choice of which vertical modes to examine cannot be based solely on the energy spectrum determined in this study because the vertical modes are not completely orthogonal, although the larger scale modes are nearly orthogonal. Instead, one must also rely on previous studies. Little work has been done in the area of the atmospheric

energetics of normal modes, although some related work has been done using empirical orthogonal functions.

The partial basis for the choice of which vertical modes to examine comes from Kasahara and Puri (1981) and Ko (1985). Kasahara and Puri (1981) analyzed Northern Hemisphere National Meteorological Center (NMC) daily data for the month of January 1977 using completely orthogonal normal modes. They found that the kinetic energy was the largest for the external mode ($\ell = 1$) and then it generally decreased as a function of vertical mode number, although a substantial amount of energy existed in the fourth and fifth vertical modes. They also noted that there was more kinetic energy in the smaller scale vertical modes than in other studies that used empirical orthogonal functions to represent the vertical structure of the atmosphere. An important conclusion of their study is that higher resolution (more vertical modes) is needed to clearly resolve the planetary scales. This conclusion was based on an analysis of the kinetic energy spectra that showed significant kinetic energy in the medium scale vertical modes of planetary-scale waves.

Ko (1985) analyzed 30 days of perpetual January simulations from the National Center for Atmospheric Research (NCAR) Community Climate Model. His results, in terms of the kinetic energy spectra, were similar to those of Kasahara and Puri (1981). Ko also examined the total and potential energy spectra. He found that a large percentage of the total and available potential energy was contained in the medium scale vertical modes ($\ell = 4$-6). Vertical modes 4 and 5 were found to contain the largest percentage of total and available potential energy. Those modes also contained about the same percentage of kinetic energy as the barotropic and first baroclinic modes.

The results of Kasahara and Puri (1981) and Ko (1985) indicate that at a minimum, the ℓ = 1-4 vertical modes need to be examined. Kasahara and Puri (1981) presented some statistics in regards to the energy spectra as a function of meridional mode number, but no conclusions were made as to the required meridional resolution needed to clearly resolve the planetary scales.

Because the meridional modes used in this study are orthogonal for a given vertical mode, it is possible to examine the energy spectra as a function of meridional mode number and draw definite conclusions. The energy spectra for a time average of the sum of symmetric (odd indexed) Rossby meridional modes of zonal wavenumber 1, 2 and 3 for the nine vertical modes of the model are given in Figs. 5.1 - 5.5. The energy spectra for the large-scale vertical modes ($\ell = 1$-3) have a peak in the energy

around meridional mode number 1-6 with a rapid decrease there-after. The spectra for the medium-scale vertical modes ($\ell = 4,6$) are much flatter than the spectra for the large-scale vertical modes. The $\ell = 4$ mode still shows a slight peak around meridional mode number 9, but the rapid decrease in the spectrum does not occur until meridional mode number 19. The spectrum of the $\ell = 5$ mode is generally flat until meridional mode number 33, while the spectra of the $\ell = 6$ mode is generally flat through meridional mode 57. The general pattern for the $\ell = 7$ mode is that the energy is spread uniformly over most meridional scales. The smallest vertical scale modes ($\ell = 8,9$) have a minimum in energy near meridional mode 17 and then the energy increases until mode number 41 where the spectra become relatively flat. The corresponding energy spectra for the antisymmetric (even indexed) Rossby modes (not shown) are very similar. These results are qualitatively consistent with those of Ko (1985) and Kasahara and Puri (1982), although there are of course quantitative differences. These differences can be attributed to the difference between the modes used, the averaging technique used and to the differences in the data analyzed. It appears from the energy spectra that no clear choice of which meridional modes to be examined can be made. While it is true for certain vertical modes that energy is concentrated in particular meridional modes, this pattern does not hold for all vertical modes. Clearly some additional criteria are required to reduce the number of modes examined.

It is possible to establish some additional criteria based on the dynamics of the different modes. The focus of this study is on planetary scale waves and these waves have certain dynamical properties that were illustrated by the scale analysis presented in Chapter 4. The analysis using the single length scale and the fast time scale (this time scale is appropriate for the large-scale barotropic meridional modes; $\ell = 1$, $n = 0$-3) shows the time tendency to be driven solely by linear effects. The multi-length scale analysis using the fast time scale also indicated that the linear terms should be the same order of magnitude as the largest term in (3.62). The scale analysis for the slower time scales also indicated that the linear term was the same order as the largest term. This slow time scale is appropriate for the baroclinic modes.

The importance of the linear term (same order magnitude as the largest term) can be used as a criteria for the selection of the modes to be examined. Only those modes that show the linear term to be important should be examined. The amplitudes of the terms in (3.62) are given as a function of meridional and vertical mode numbers in

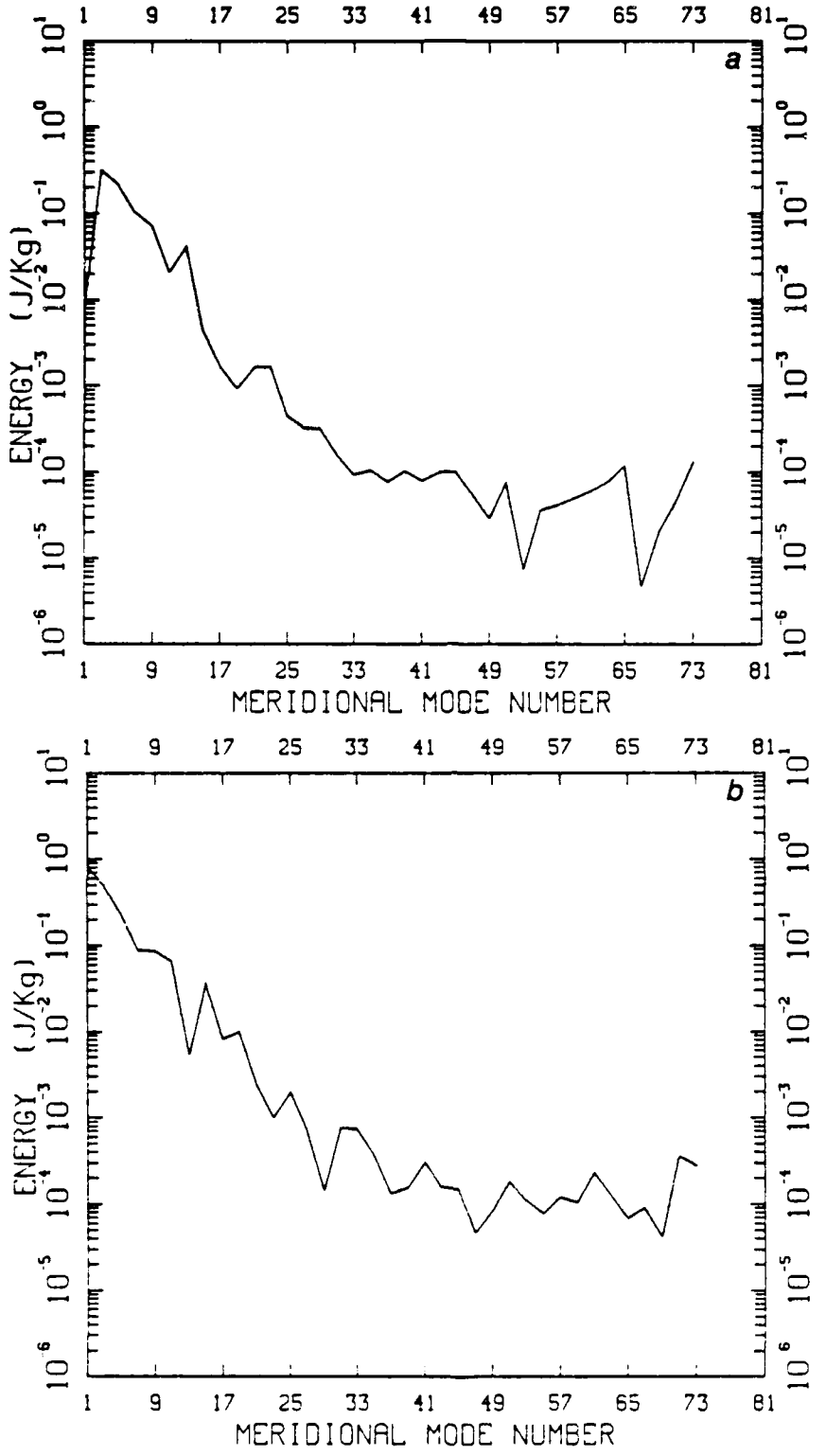

Figure 5.1. Energy spectra for an average of zonal wavenumbers 1-3 for (a) the barotropic ($\ell = 1$) rotational mode and (b) 1st baroclinic rotational mode ($\ell = 2$) as a function of the odd (symmetric) meridional mode numbers.

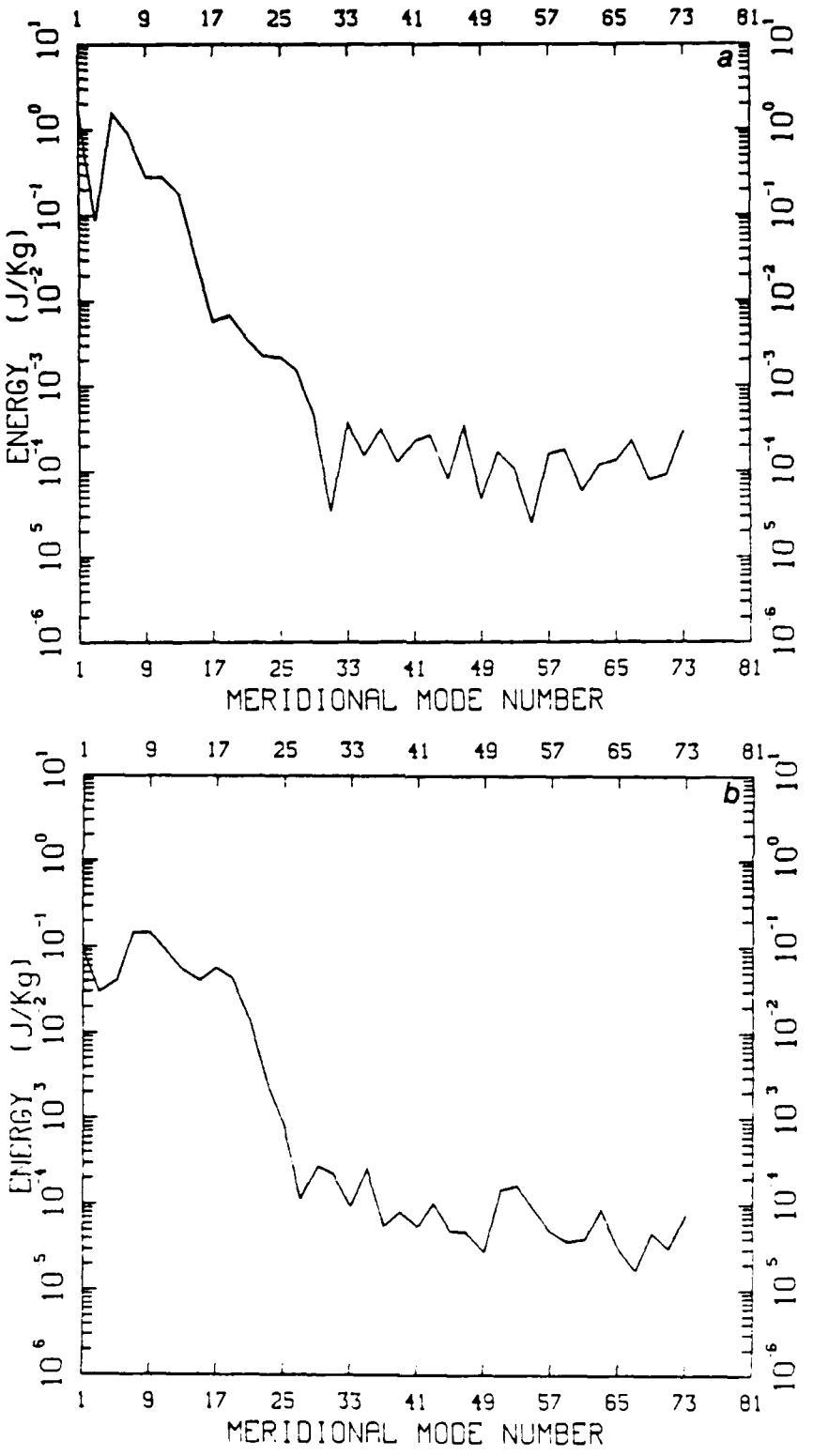

Figure 5.2. As in Figure 5.1, except for (a) $\ell = 3$ and (b) $\ell = 4$.

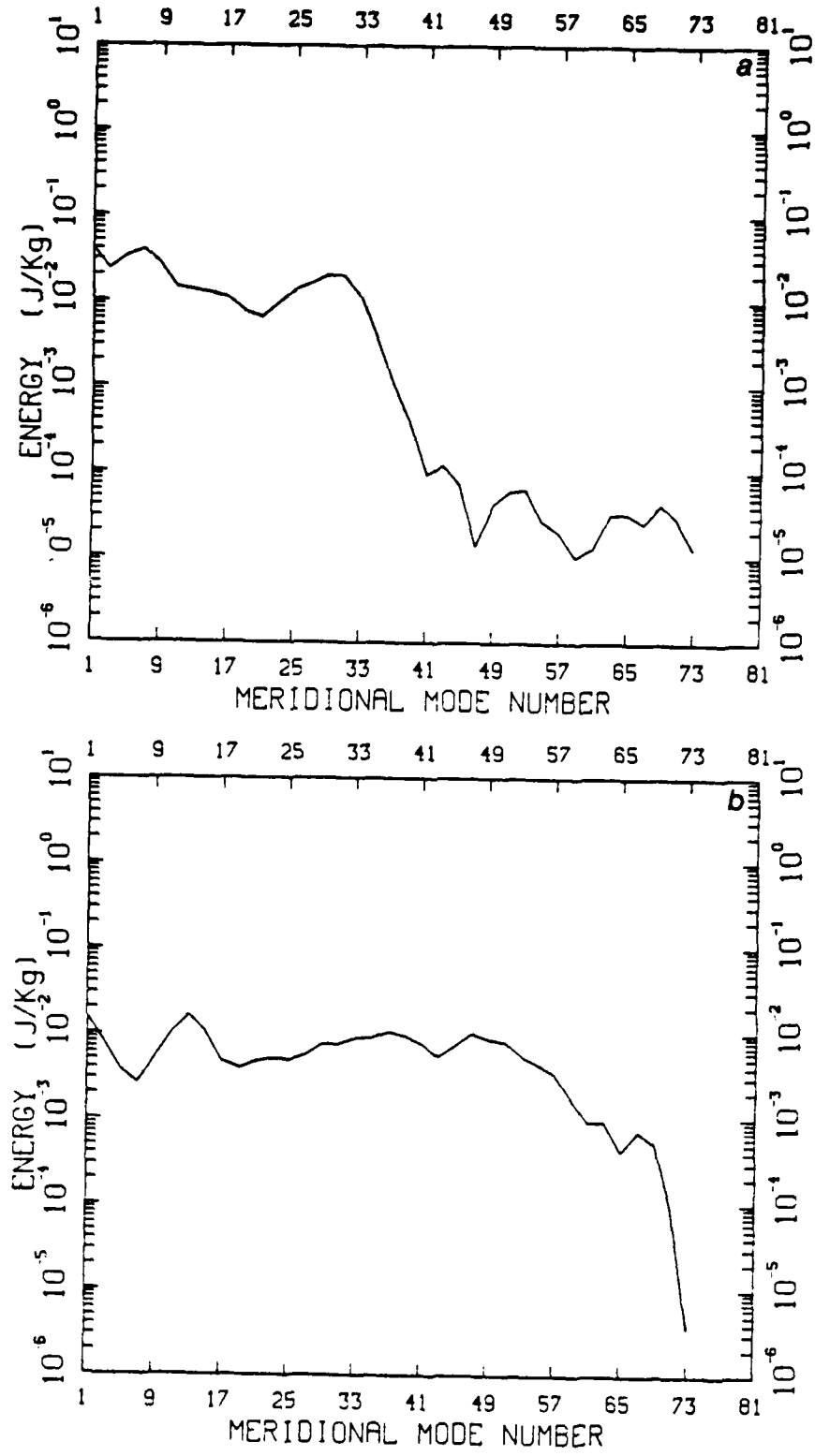

Figure 5.3. As in Figure 5.1, except for (a) $\ell = 5$ and (b) $\ell = 6$.

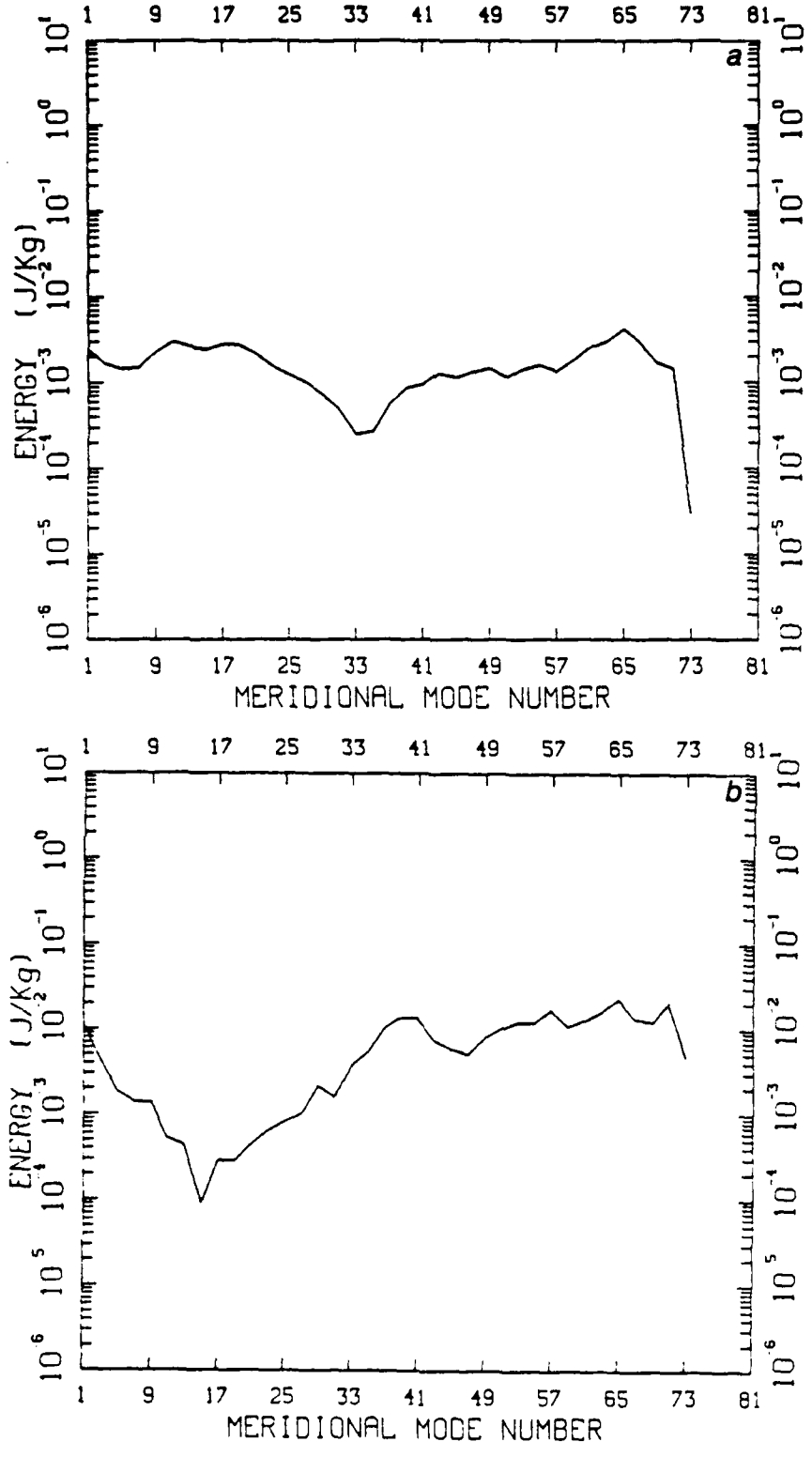

Figure 5.4. As in Figure 5.1, except for (a) $\ell = 7$ and (b) $\ell = 8$.

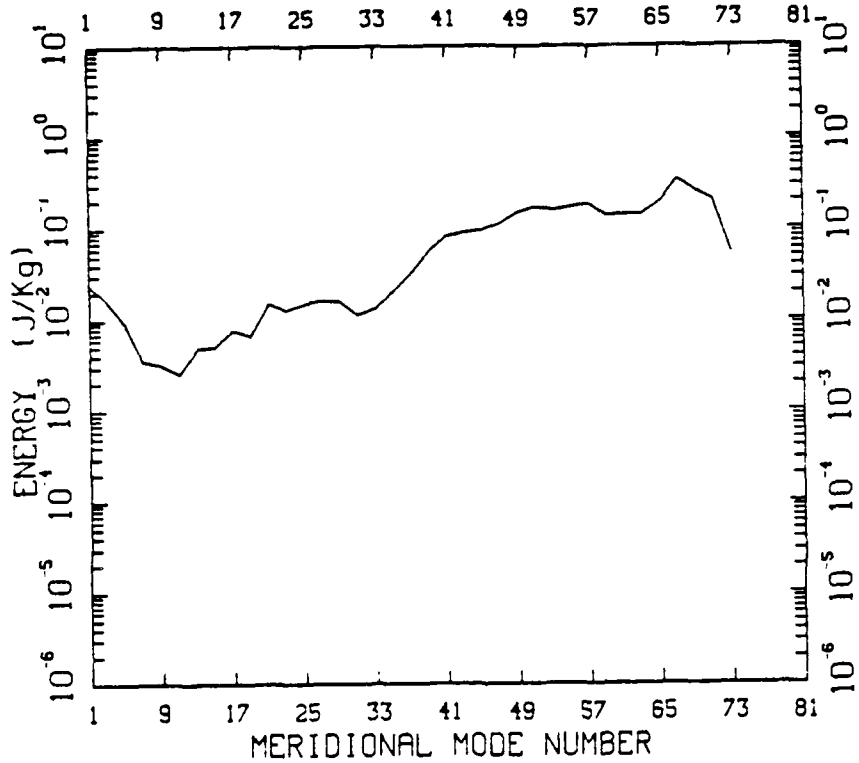

Figure 5.5. As in Figure 5.1, except for $\ell = 9$.

Figs. 5.6 - 5.10 for a time average of the symmetric zonal wavenumber 1 case (results are similar for wavenumbers 2 and 3). The importance of the linear term is evident for the $n \leq 3$ meridional modes for the first four vertical modes. The linear term is important up to meridional mode 8 for the barotropic mode, and up to meridional mode 4 for the third vertical mode. For the smaller scale vertical modes ($\ell = 7$-9) modes, the linear term is no longer important for any meridional scale. In general, it can be said that the importance of the linear term decreases with increasing vertical mode number. Based on the meridional wavenumber arguments given above and the analysis of the importance of the linear term as a function of vertical as well as meridional mode number it would seem reasonable to limit this study to the examination of the first four meridional modes ($n = 0$-3).

From Figs. 5.1 - 5.5 it can be seen that the energy contained in the $n \leq 3$ modes decreases as a function of vertical mode. In general the energy contained in the $n \leq 3$ modes is of the order $1 - 10^{-1}$ while the energy contained in the $n \leq 3$ modes for $\ell \geq 5$ modes is of the order $10^{-2} - 10^{-3}$ The comparison of the amount of energy contained in the $n \leq 3$ meridional modes is not exact (the vertical modes of the NOGAPS model are not completely orthogonal). However, the variation of the energy in these modes with vertical mode is very consistent with the results of Kasahara and Puri (1982) and Ko (1985). Based on the above comparison of the energy contained in the different vertical modes for the $n \leq 3$ meridional modes and the consistency of these results with those of other authors, it would seem reasonable to limit this study to the examination of the first four vertical modes of the $n = 0$-3 meridional modes.

Another reason for not examining the smaller scale vertical modes (which cannot be addressed by the analysis of Figs. 5.1-5.5 and 5.6-5.10 is the possible dependence of the adiabatic nonlinear on the divergent part of the motion. Errico (1984) has shown for the long-time solution to a primitive equation model that N(G*R) is the same order of magnitude as the N(R*R). The N(G*R) term depends highly on the divergent part of the motion. Since the divergent part of the NOGAPS analyses is just the model first-guess divergence, any results obtained concerning nonlinear interactions may be more indicative of the model rather than the actual atmosphere. The dependency of the interactions on the model is an important subject in its own right, but it is a subject beyond the scope of this work.

The choice of of the modes to be examined (the $\ell = 1$-4 , $n = 0$-3 modes) does eliminate some modes with energies similar to the chosen modes and modes that show

the linear term to be important, but the set chosen should be sufficient for the purpose of this study which is to show that nonlinear interactions with cyclone waves can be an important factor in the dynamics of planetary waves.

Before examining the results of the experiment that is designed to determine the importance of synoptic-scale nonlinear interactions, it is necessary to establish the importance of the adiabatic nonlinear term in the dynamics of planetary waves. While it may be shown that synoptic-scale interactions are an important part of the adiabatic nonlinear term, this effect would not be significant unless this term is important in general (of the same magnitude as the other terms). As can be seen from Figs. 5.6 - 5.10 the adiabatic nonlinear term is at least the same order as the largest term for a given meridional mode and it is often the largest term. For the largest scale vertical modes, all of the terms (linear, nonlinear adiabatic, diabatic and time tendency) are nearly the same magnitude for the largest scale meridional modes (n = 1-3). This result is interesting considering the single length scale analysis carried out using the fast time scale (which is appropriate for the $\ell = 1$, n = 0-3 modes) showed the time tendency to be driven by the linear term. The multi-scale analysis did show that the nonlinear term could be important. For most of the remaining meridional modes, the time tendency for the largest vertical scales is driven by the adiabatic nonlinear term, with the diabatic term becoming important for the smallest scale meridional modes.

The importance of the diabatic term for the largest vertical scale meridional modes has not been shown before. In the only other study of this kind, Errico (1984) did not investigate the planetary scales in detail and his focus was mainly on the balance for the gravity modes. In addition, he averaged modes by frequency, which could have obscured some of the detail of the planetary scales. The results that he presented did show the adiabatic nonlinear term to be important for the higher frequency Rossby modes, but he did not show the diabatic term to be important for the Rossby modes except for the higher vertical modes. Although it beyond the scope of this study to examine in detail the affects of diabatic terms on planetary waves, the importance of the diabatic term, as shown in Figs. 5.6 - 5.10, does deserve some comment.

It is not surprising that this term might be important for planetary scales given the general belief that the quasi-stationary component of planetary waves is forced in part by differential heating due to land-sea contrasts. A note of caution must be added here. As is the case with most models, the diabatic processes of the NOGAPS model

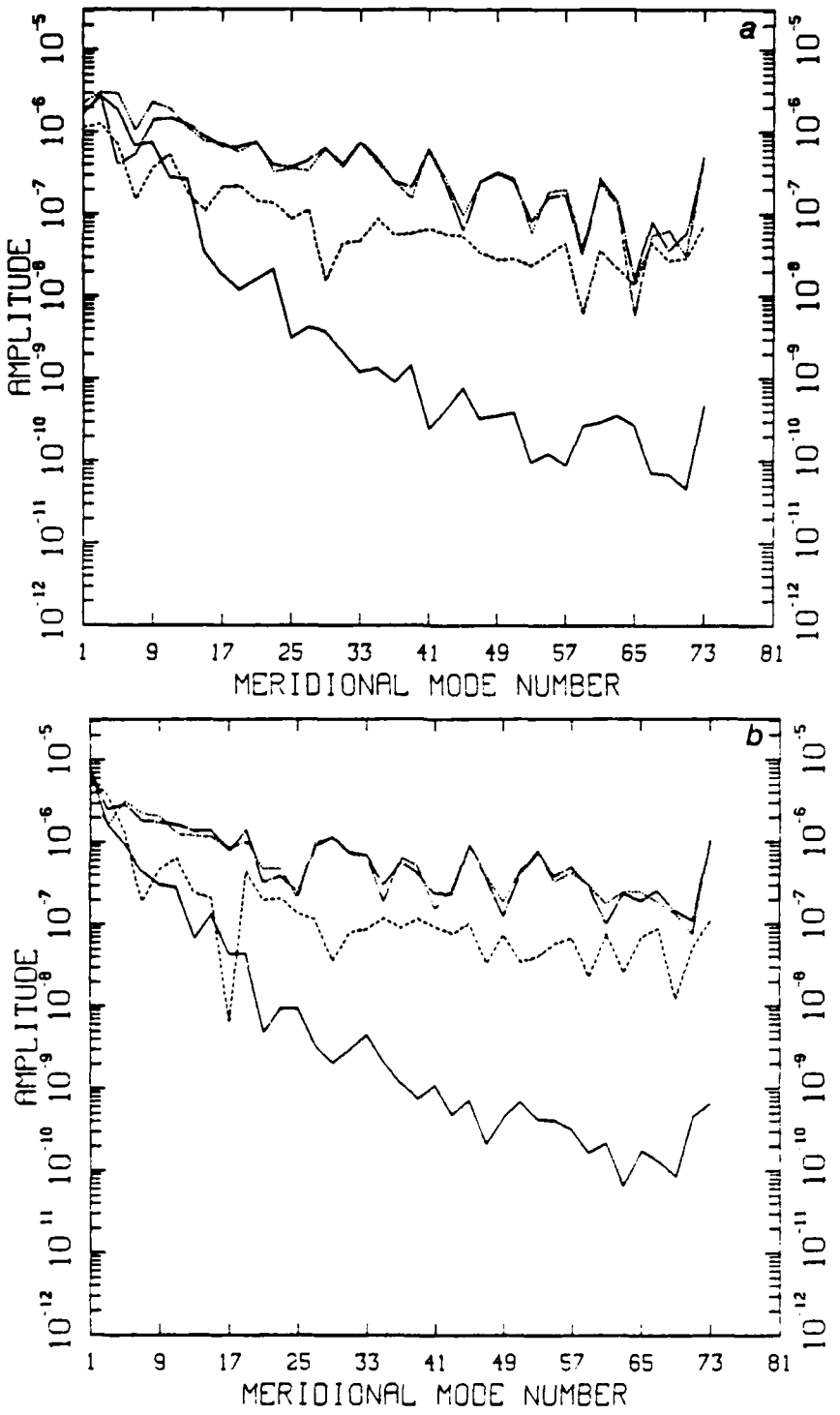

Figure 5.6. Magnitude of $\Delta C_n/\Delta t$ (dotted line), $-i\omega C_n$ (solid), N_n (dash-dot), and Q_n (dashed) for (a) the barotropic ($\ell = 1$) rotational mode and (b) the 1st baroclinic Rotational mode ($\ell = 2$) as a function of meridional mode number (n) for zonal wavenumber 1.

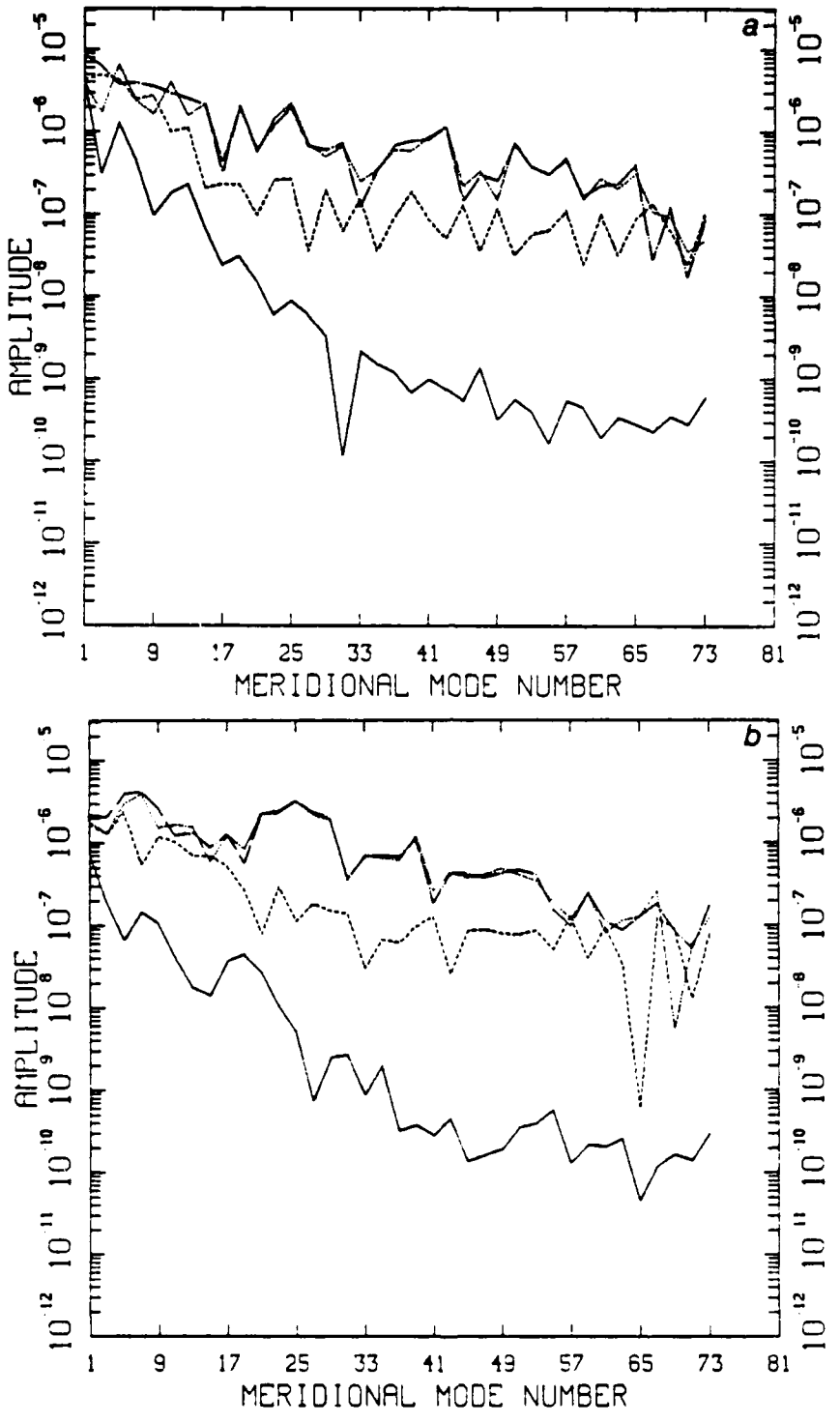

Figure 5.7. As in Figure 5.6, except for (a) $\ell = 3$ and (b) $\ell = 4$.

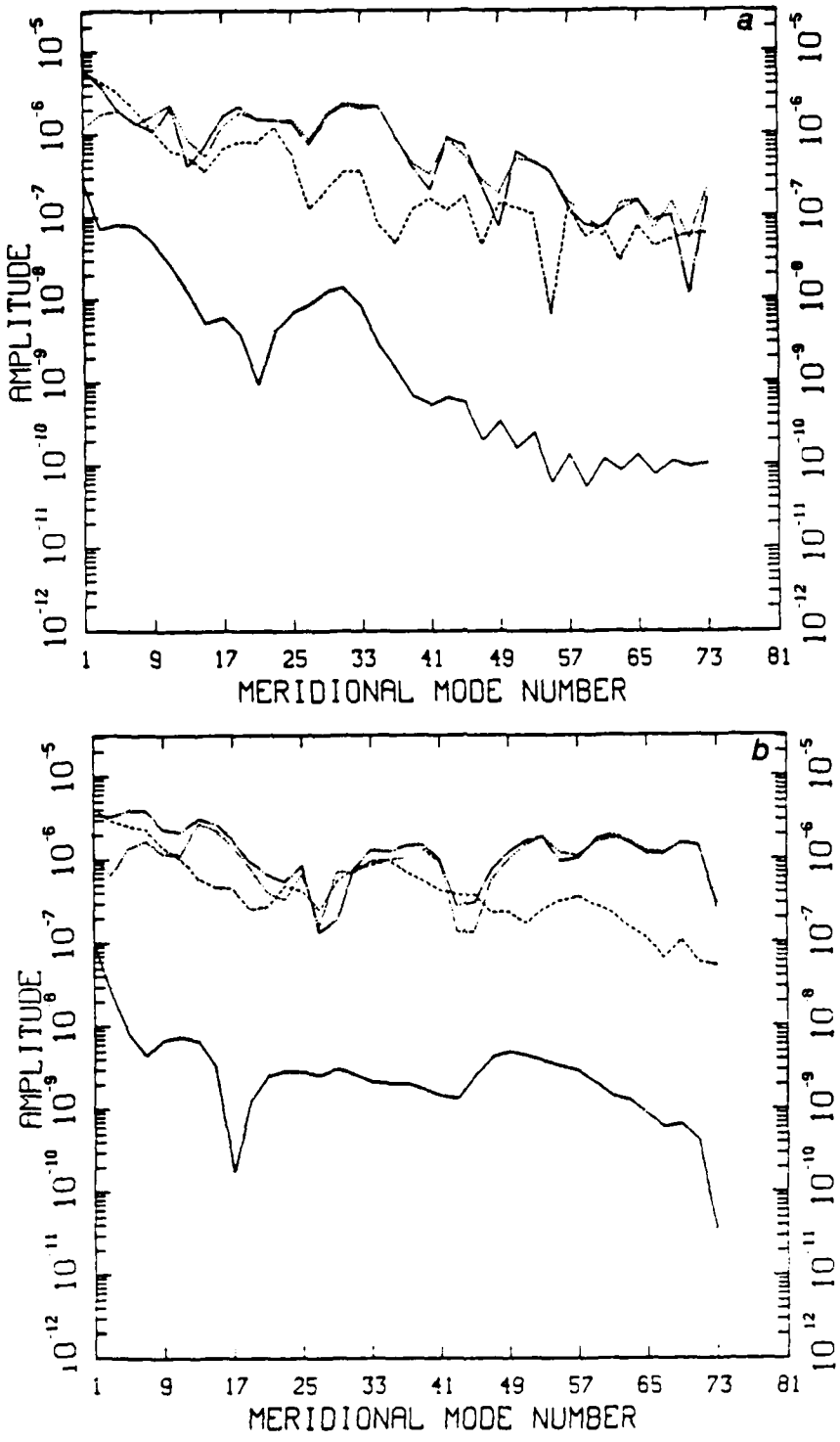

Figure 5.8. As in Figure 5.6, except for (a) $\ell = 5$ and (b) $\ell = 6$.

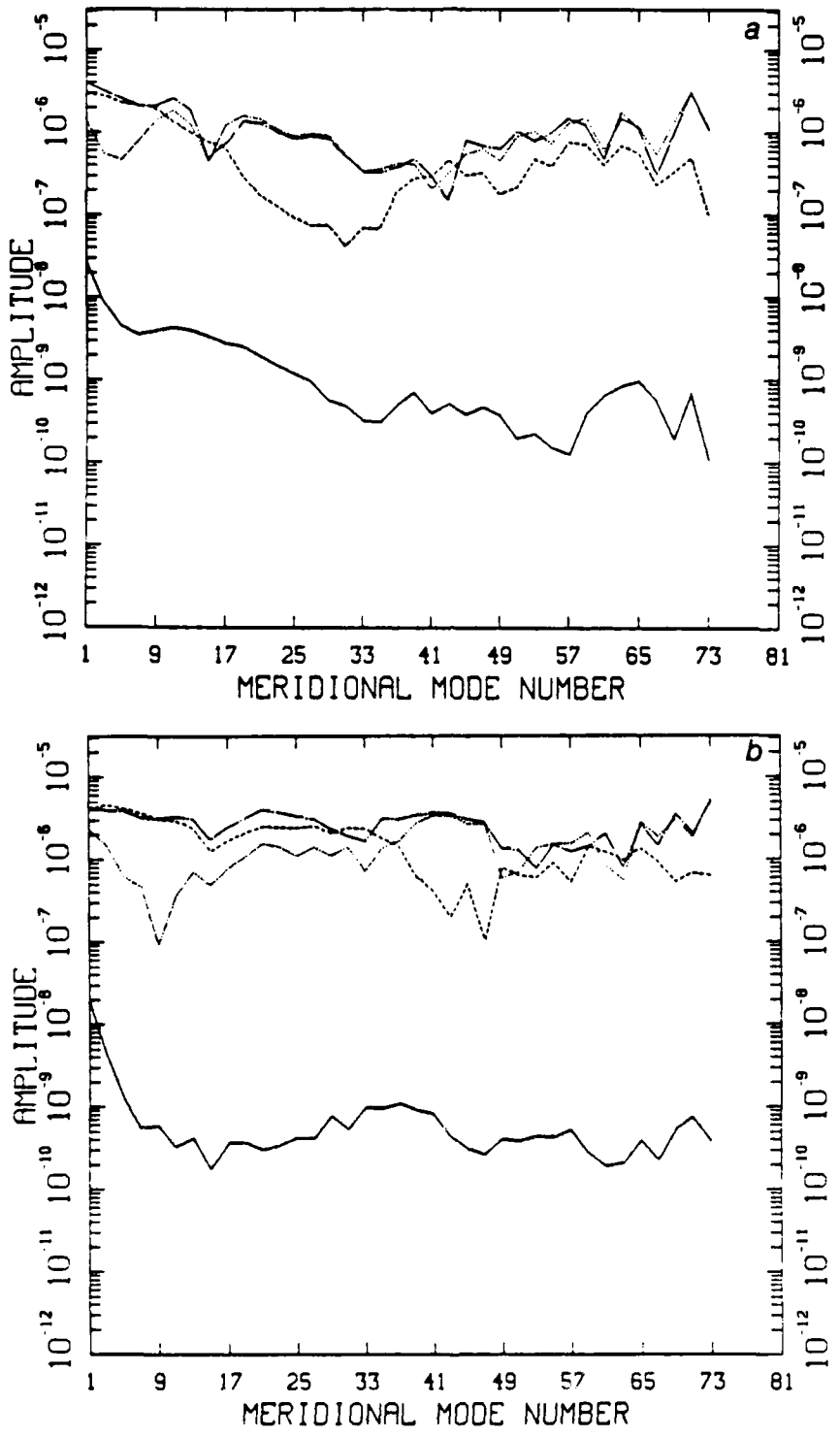

Figure 5.9. As in Figure 5.6, except for (a) $\ell = 7$ and (b) $\ell = 8$.

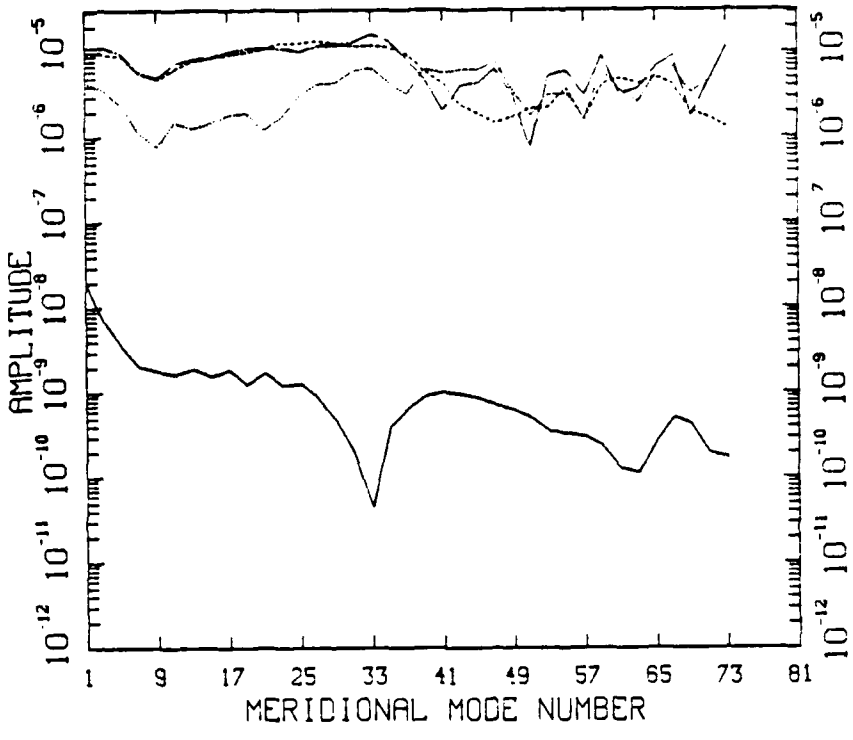

Figure 5.10. As in Figure 5.6, except for $\ell = 9$.

are parameterizations of the actual atmospheric diabatic processes. Thus results obtained here may be different from other models with different parameterizations. In addition, the diabatic term is not decomposed into different components (sensible heating, latent heating, frictional dissipation, radiational heating), so it is not possible to determine which diabatic processes contribute the most to this term. For the larger meridional scales, it is possible that the majority of this term is due to heating. For the smaller scales, dissipation may be important.

B. THE EFFECT OF SYNOPTIC SCALES ON PLANETARY SCALES

Based on the dynamics and energetics of the different modes and on scale considerations, the focus will be on zonal wavenumbers 1-3, vertical modes 1-4 and meridional modes 0-3. For this part of the experiment, the data (u, v, T, ln p_s) for each of the 19 days of 12UTC NOGAPS analyses taken every 5 days from 16 January 1986 to 16 April 1986 are spectrally filtered. The data are taken only every 5 days so that each day is statistically independent. Also, graphs of the data taken every 5 days are easier to interpret than those that have daily data plotted. When average magnitudes and energies are computed later, 85 days of data taken over the same period will be used.

To eliminate the synoptic waves, the data are filtered by transforming to spectral space using a fast Fourier transform routine, setting the coefficients of zonal wavenumbers 7-15 to zero and transforming back to physical space. The magnitudes of the adiabatic nonlinear term (N_n) from both the unfiltered and filtered data are computed and the difference between the nonlinear terms from the unfiltered and filtered data is calculated. The magnitude of this difference represents the contribution of the synoptic scales to the nonlinear term of the given planetary scale, hereafter referred to as N_{ns}.

Figures 5.11 - 5.14 are plots of N_n and N_{ns} versus time for an average of meridional modes n = 0-3 of the ℓ = 1-4 modes of zonal wavenumbers m = 1-3. The general pattern that emerges from an examination of Figs. 5.11 - 5.14 is that for all vertical modes N_{ns} is the same order of magnitude as N_n, but it is generally smaller than N_n (here after referred to as the total nonlinear term). On no day is N_{ns} larger than N_n (which could occur if the interactions from waves other than m = 7-15 acted to oppose the interactions from the m = 7-15 waves). On a number of days, the synoptic-scale contribution to the total nonlinear term is significant (N_{ns} is a large percentage of N_n).

For a given day, the significance of the synoptic-scale contribution to the total term can be illustrated by the ratio of N_{ns} to N_n. Figures 5.15 - 5.18 are plots of the percent magnitude of the synoptic-scale contribution to the total nonlinear term as a function of time. The synoptic-scale contribution to the magnitude of the total nonlinear term will be considered significant for any given day if this contribution is at least 30 percent of the total. This is somewhat arbitrary, because a smaller value could be important if $\Delta C/\Delta t$ is smaller than the nonlinear term. However, the 30% value does highlight days on which the synoptic-scale contribution to the nonlinear term is large. The number of days where the magnitude of the synoptic-scale contributions is greater than 30 percent varies with vertical mode. The number of significant days is greatest for fourth vertical mode. In general, the larger scale vertical modes (ℓ = 1-3) have the smallest number of significant days. The strength of the synoptic-scale contribution to the total nonlinear term varies with vertical mode number in the same manner as the number of significant days. The synoptic-scale contribution to the total is strongest for medium-scale fourth vertical mode. For this mode, the synoptic-scale contribution to the total nonlinear term exceeds 50 percent for a number of days. There is a slight variation of the synoptic-scale contribution to the total nonlinear term with zonal wavenumber. Zonal wavenumber 3 is the most affected zonal wave number. The fourth vertical mode for this zonal wavenumber exceeds the 30 percent criteria for 12 of the 19 days and on three of these days the synoptic-scale contributions exceeds 50 percent.

From the above analysis, it is clear that synoptic-scale interactions can be significant for a particular day, but the analysis does not show the time average effect of the synoptic scales on planetary scales. Table 6 gives the average magnitude of the difference between the total nonlinear term and the nonlinear term computed from the filtered data as a percentage of the average magnitude of the total nonlinear term. The averages for these terms are computed as

$$\overline{N}_{me} = \left[\frac{1}{4K} \sum_{k=1}^{K} \sum_{n=0}^{3} N_n(t_k) N_n^*(t_k) \right]^{\frac{1}{2}} \qquad (5.1)$$

where K is the number of days in the data set and four is the number of meridional modes. To insure greater statistical significance, a larger sample size is used to compute the averages given in Table 6. For these averages, the total term (N_n) and the synoptic part (N_{ns}) are determined from **85 days** of 12Z initialized NOGAPS analyses **taken every day** from 16 January 1986 to 16 April 1986. The following days were missing from the data set: 17, 21 and 23 January and 9 and 21 March.

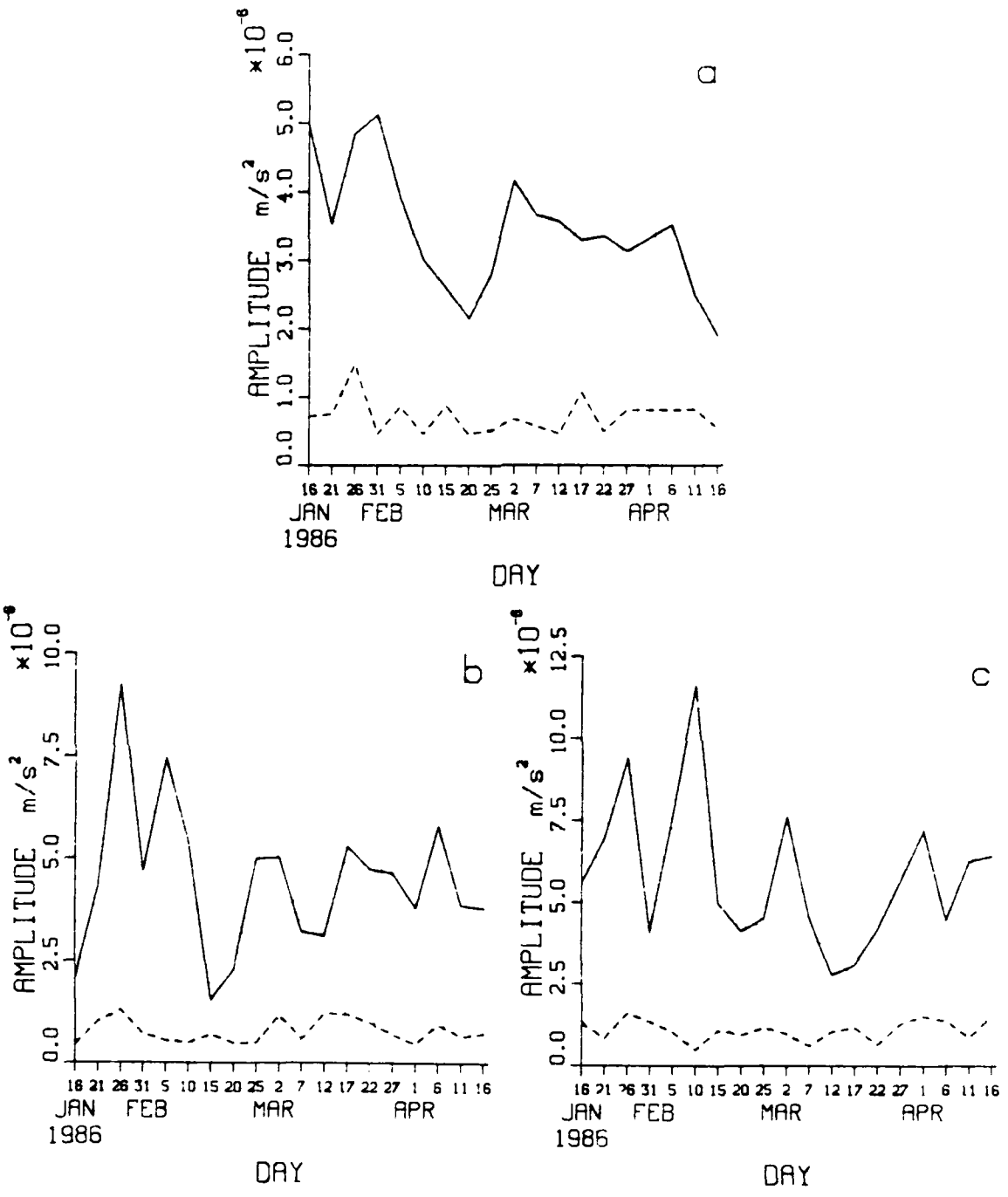

Figure 5.11. Magnitudes of N_n (solid) and the synoptic scale contribution to N_n (dashed) as a function of time for zonal wavenumbers (a) 1, (b) 2, and (c) 3 for the barotrophic mode ($\ell = 1$).

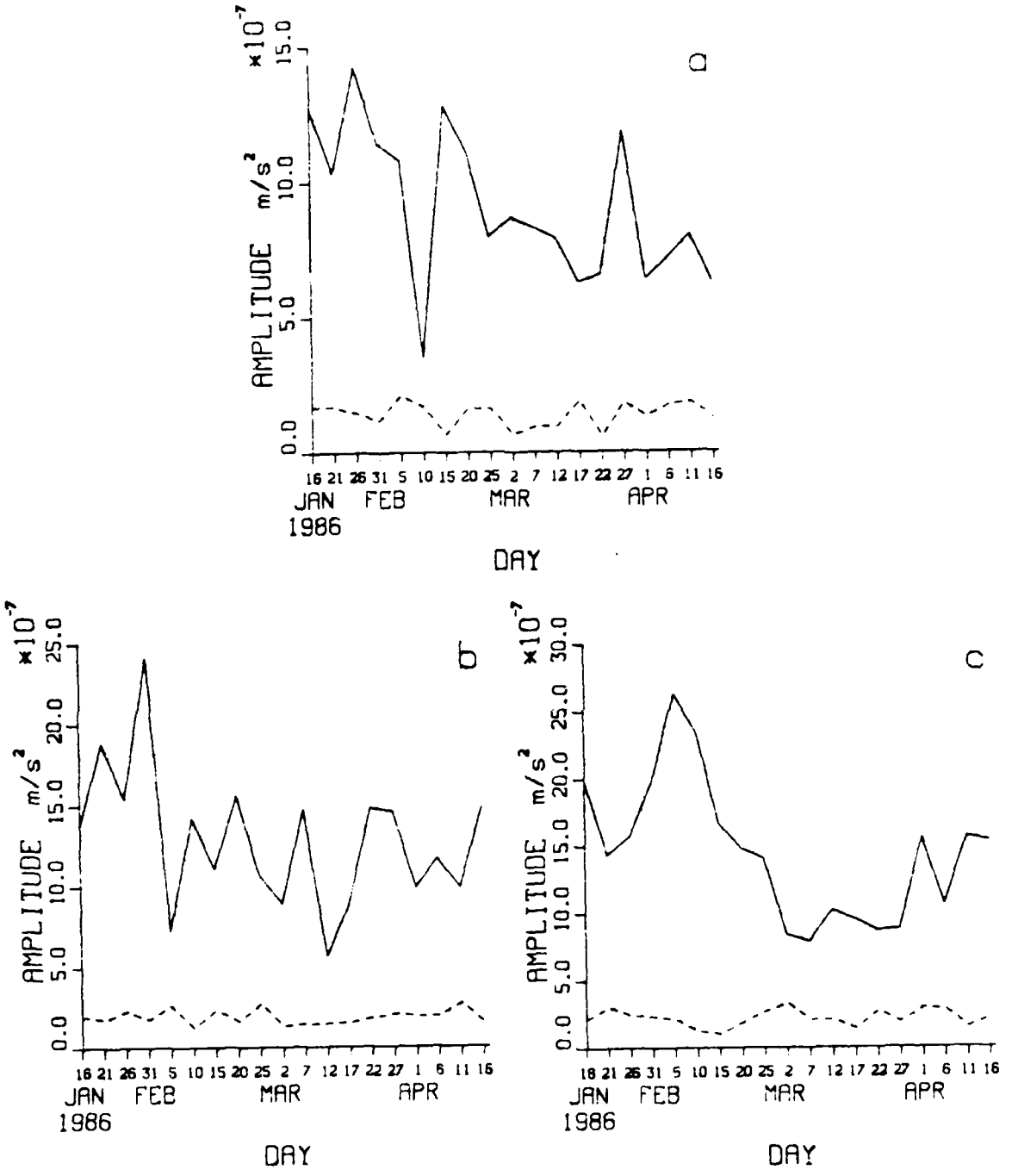

Figure 5.12. As in Figure 5.11, except for $\ell = 2$.

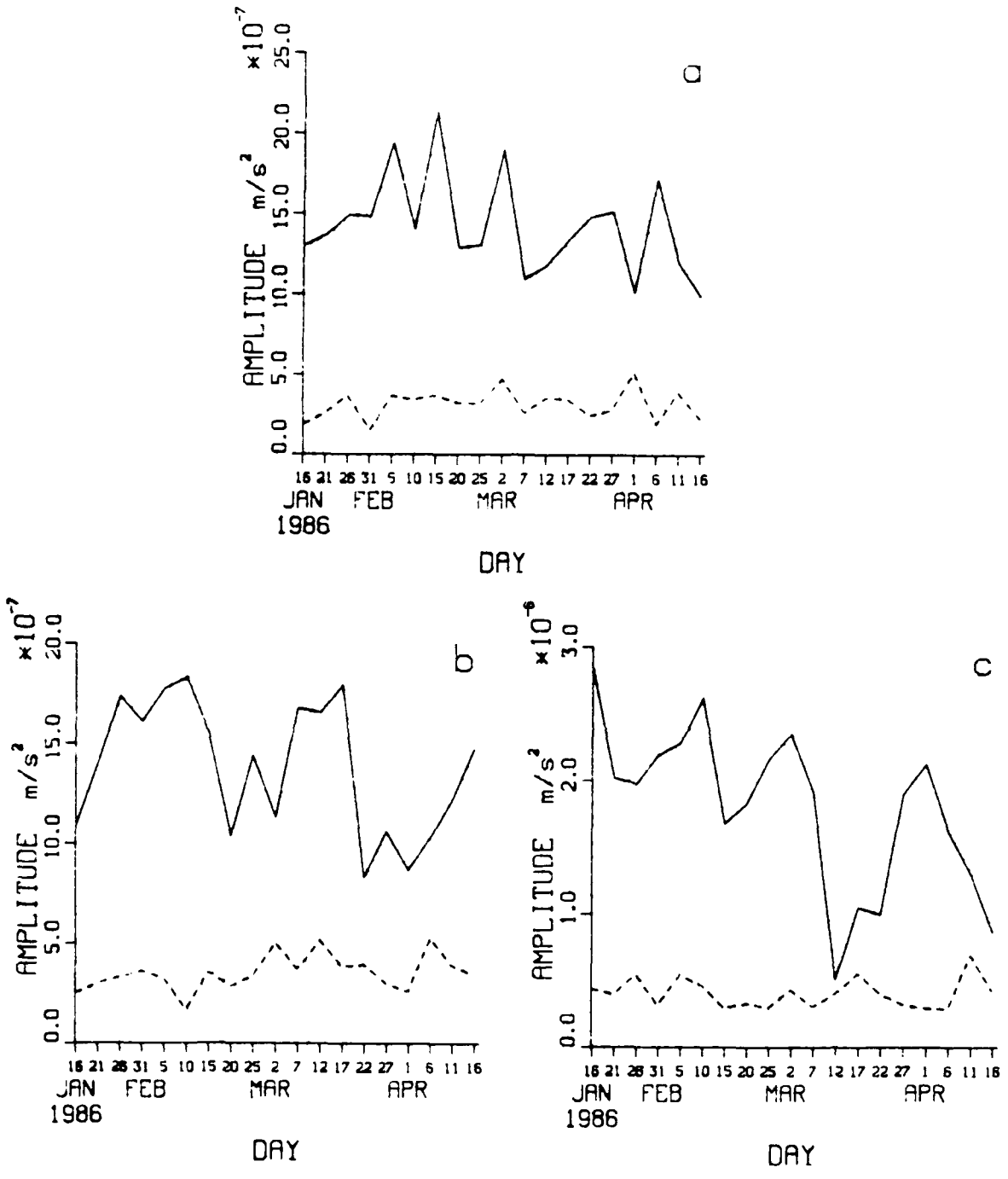

Figure 5.13. As in Figure 5.11, except for $\ell = 3$.

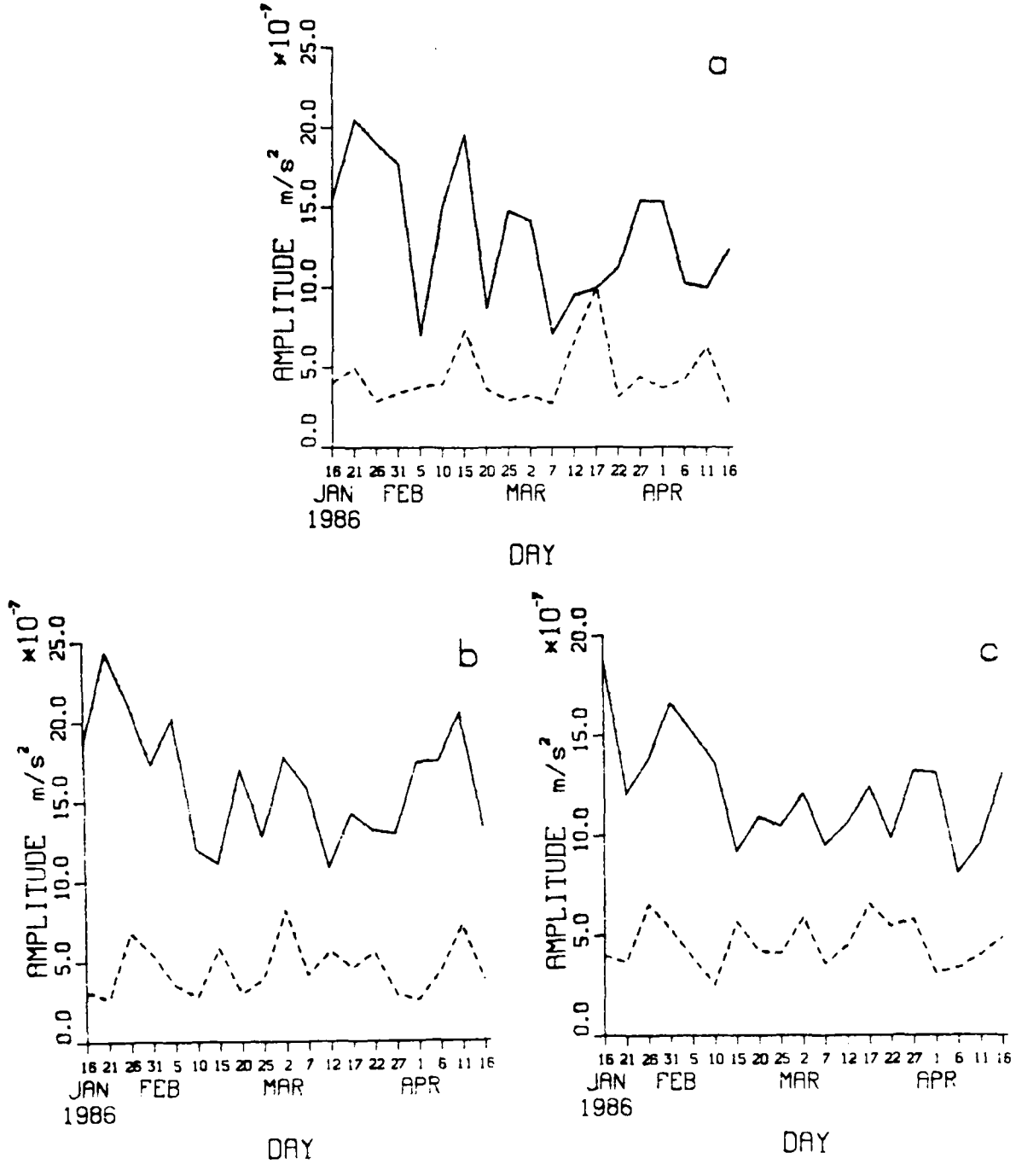

Figure 5.14. As in Figure 5.11, except for $\ell = 4$.

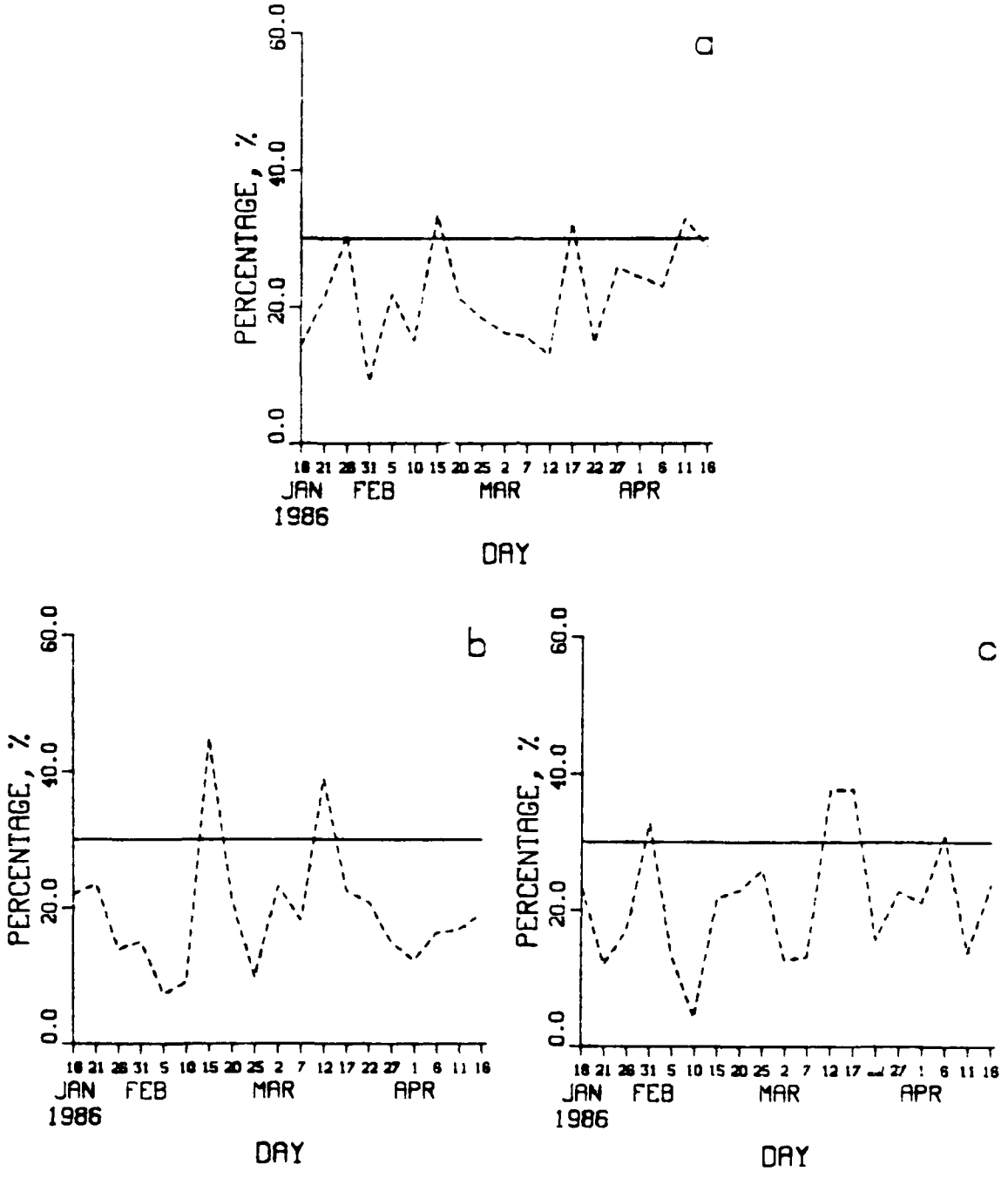

Figure 5.15. Synoptic-scale contribution to the total nonlinear term for the barotropic mode ($\ell = 1$) as a percentage of the total nonlinear term for zonal wavenumbers m = 1-3 (a-c). The 30% level is indicated for use as a benchmark.

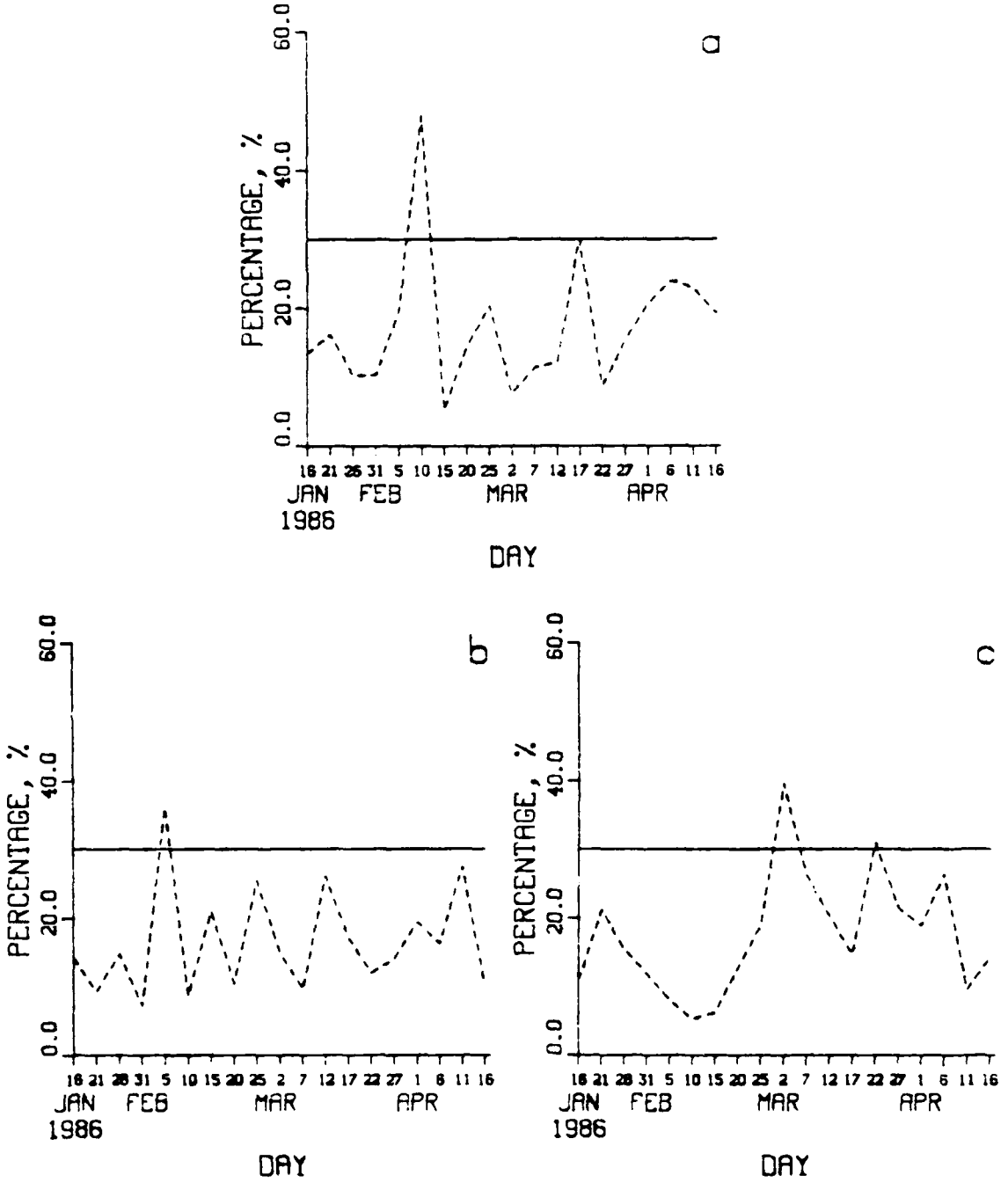

Figure 5.16. As in Figure 5.15, except for $\ell = 2$.

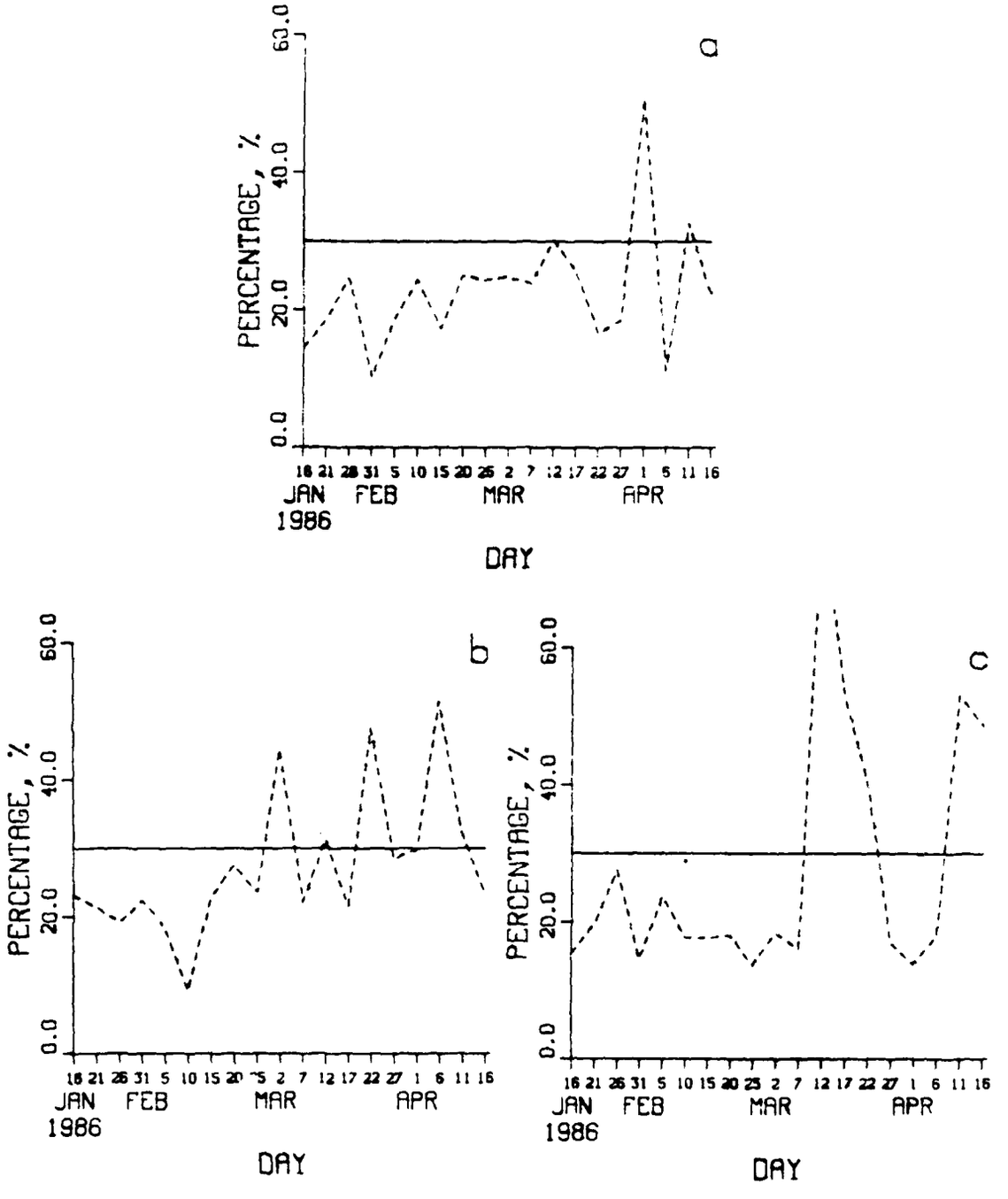

Figure 5.17. As in Figure 5.15, except for $\ell = 3$.

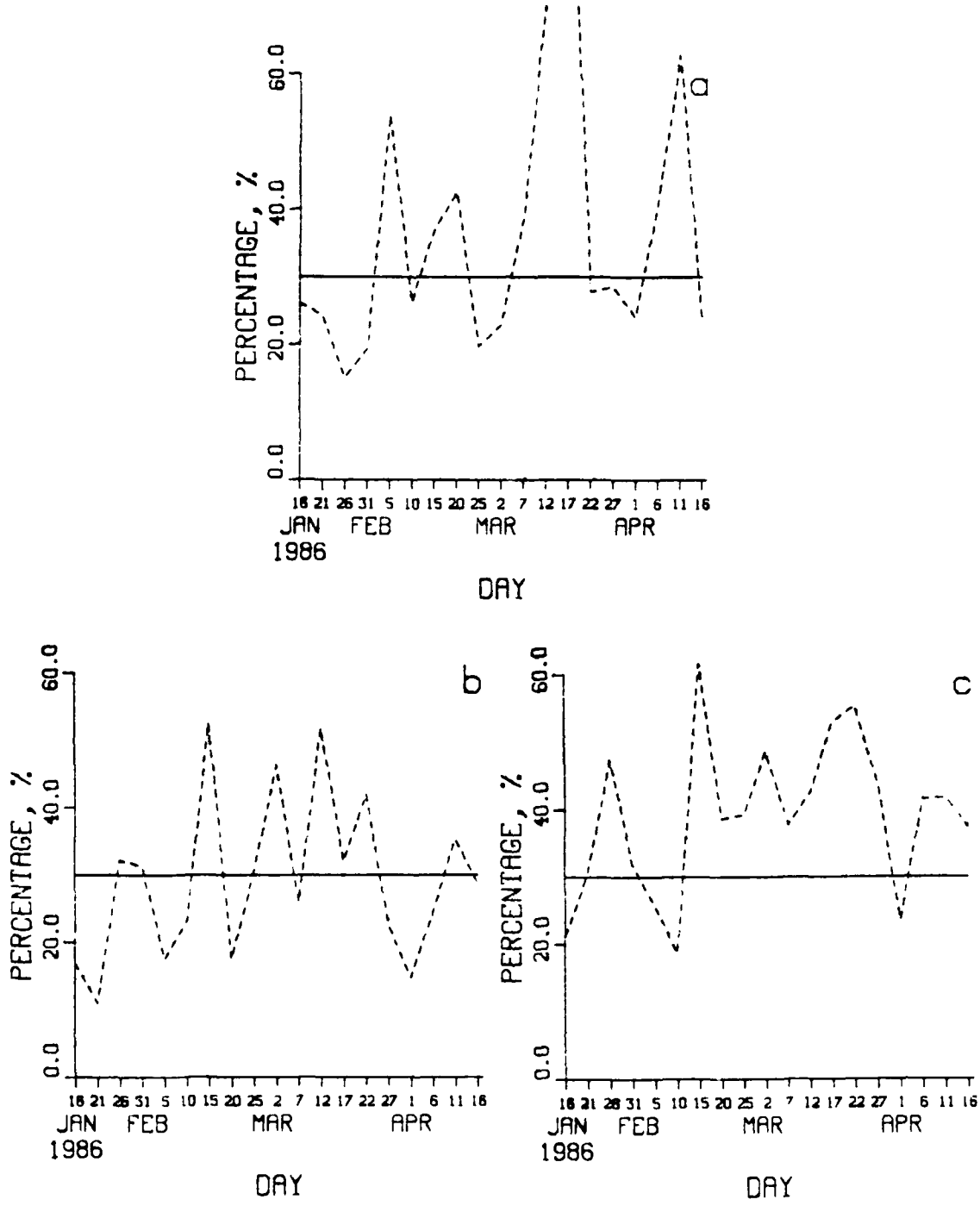

Figure 5.18. As in Figure 5.15, except for $\ell = 4$.

Table 6. Time averaged (over 85 days, taken between 16 January and 16 April 1986) synoptic-scale contribution to the total nonlinear term as a percentage of the total for an average of meridional modes n = 0-3.

Vertical mode index	Zonal Wavenumber		
	1	2	3
1	20	18	17
2	17	14	16
3	24	25	24
4	35	28	42

For a given zonal wavenumber, the magnitude of the time averaged synoptic-scale contributions is a largest percentage of the total nonlinear term for the fourth vertical mode. The nonlinear term of the second vertical mode appears to have the smallest contribution from synoptic scales. For the medium-scale vertical modes, zonal wavenumber 3 has the largest synoptic-scale contribution to the planetary scales in terms of the percent magnitudes.

It is clear from the above analysis that the synoptic-scale contributions to the magnitude of the total nonlinear term can be significant for a given day (N_{ns} can be as large as 60% of N_n) and are significant in a time-averaged sense.

The result that the synoptic scales tend to have a significant impact on the magnitude of the total nonlinear term is important, but it is not the whole story. For the most affected mode ($\ell = 4$, $m = 3$), the nonlinear interaction from synoptic scales is 42% of the total. However, this leaves nearly 60% of the total unaccounted for. The rest of the term is due to interactions with scales other than those represented by wavenumbers 7-15. This includes interaction of the planetary scales with the zonal mean state ($m = 0$). Although these other interactions are significant, it is beyond the scope of this study to examine them. The purpose of this study is to establish that interactions with cyclone waves can be an important factor in the dynamics of planetary waves.

Another point that has not been considered is the relationship of the days when N_{ns} is a large percentage of N_n to the general importance of N_n on those days. It is

important to establish that on the days when the synoptic-scale contribution to the total nonlinear term is a large, the total nonlinear term is of importance, i.e., it is of the same magnitude as the other terms in (3.62). To accomplish the above, one must examine the non-time averaged variations of the terms given in (3.62). In addition, such an examination will also serve to illustrate the dynamical differences between the different vertical modes at these planetary scales.

The terms in (3.62) are plotted in Figs. 5.19 - 5.22 for an average of meridional modes n=0-3 versus time for the data taken every five days. The time variations of barotropic mode (Fig. 5.19) are quite interesting. For all three zonal wavenumbers, the general dynamic pattern is a tendency for balance between the adiabatic nonlinear term and the linear term. The time tendency of these modes is generally less than the nonlinear or linear term, and the diabatic term also has a small contribution to the barotropic mode. On the days on which the nonlinear and linear terms are not in partial balance, the time tendency is driven by the linear term. For these days, it appears as if the heating is partially balancing the nonlinear term. For all the days examined, the contribution of the nonlinear to the barotropic mode term is at least the same order of magnitude as the other terms. It was previously shown (Fig. 5.15) that the synoptic-scale contribution to the total nonlinear term for the barotropic mode is small. However, the synoptic-scale contribution to the overall dynamics of the planetary-scale barotropic modes could be more important than the small magnitude might indicate. This contribution could be an important factor in maintaining the partial balance found in this mode or it could be the dynamic ingredient that keeps these modes from obtaining a complete balance. The above could also be true of the diabatic term which also has a small magnitude for the barotropic modes.

The above description of the dynamical nature of the barotropic mode is also generally true for the second vertical mode (Fig. 5.20). The dynamics of the third (Fig. 5.21) and fourth (5.22) vertical modes are quite complex. No one term or two terms seem to dominate. The diabatic term is of increased importance for these modes, but it is by no means dominant. The linear term is of lesser importance for these modes than it is for the first two vertical modes, but it still makes a significant contribution to the time tendency. There is no hint of a simple balance between two leading terms for these modes. For both of these modes, it generally true that the diabatic, adiabatic nonlinear and linear terms are additive so that the time tendency is the largest term.

Two important points are illustrated by the above analysis

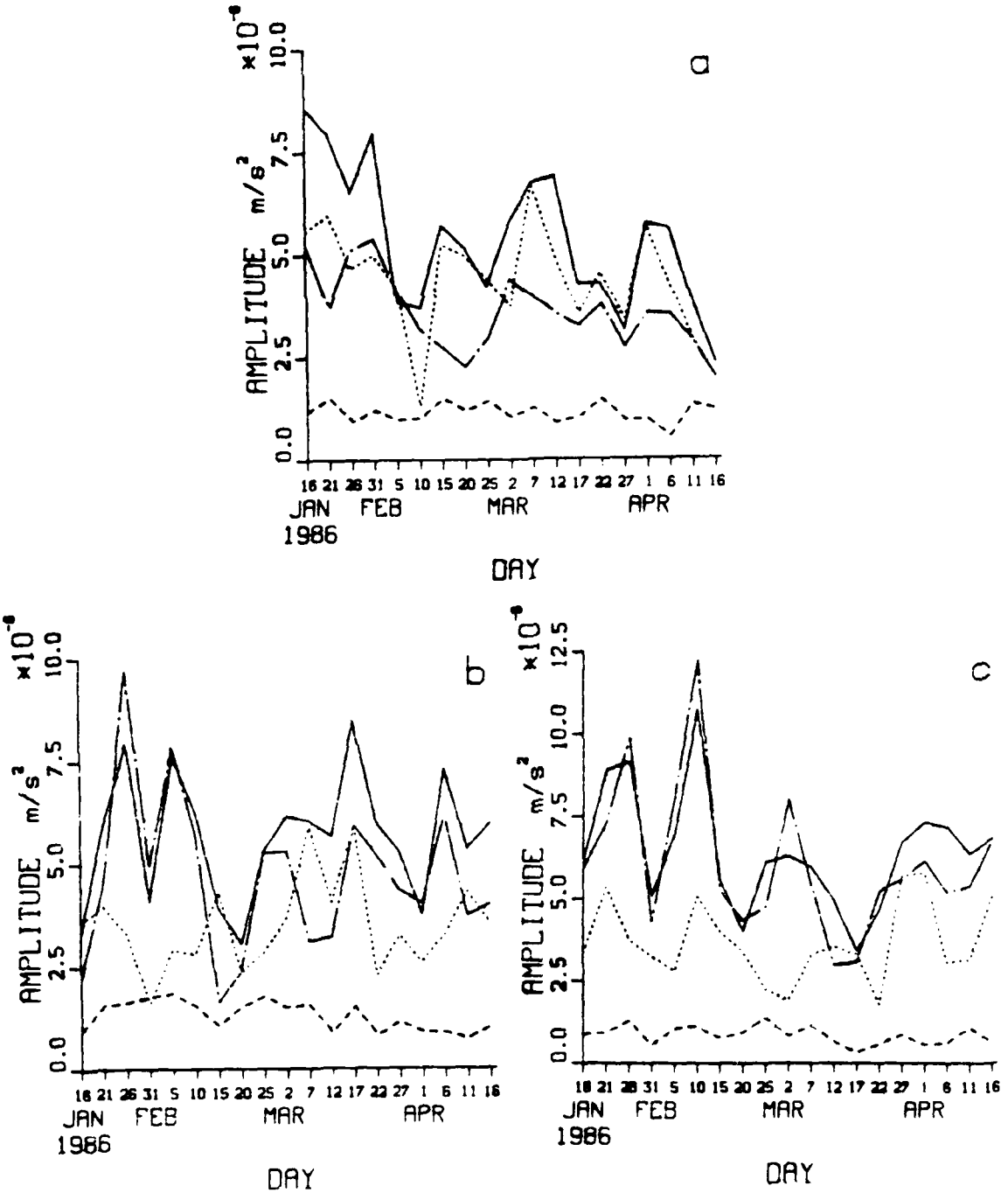

Figure 5.19. Magnitude of $\Delta C_n/\Delta t$ (dotted), $-i\omega C_n$ (solid), N_n (dash-dot), and Q_n (dashed) for the barotropic ($\ell = 1$) modes of zonal wavenumbers 1-3 (a-c) for each fifth day of the period.

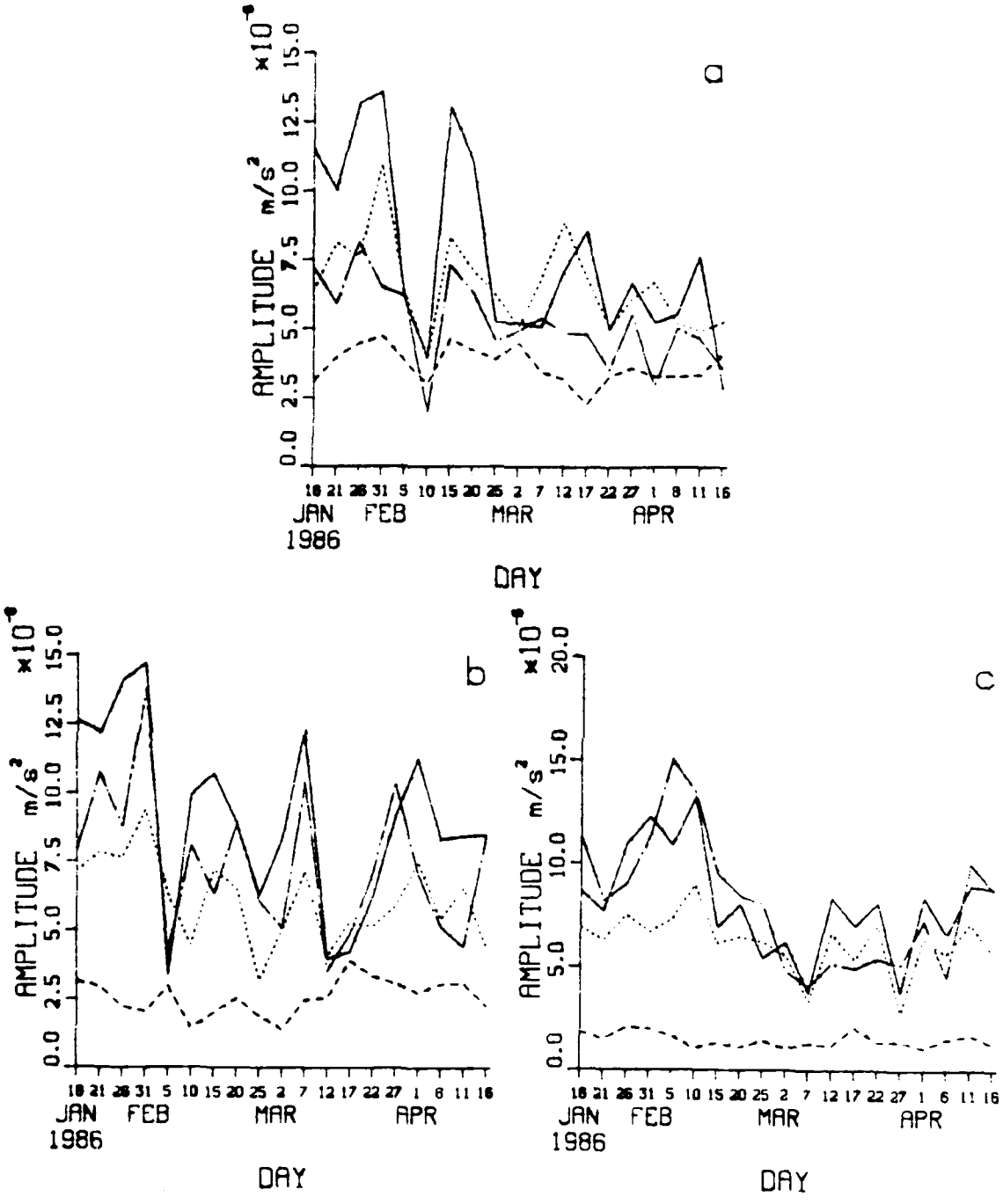

Figure 5.20. As in Figure 5.19, except for $\ell = 2$.

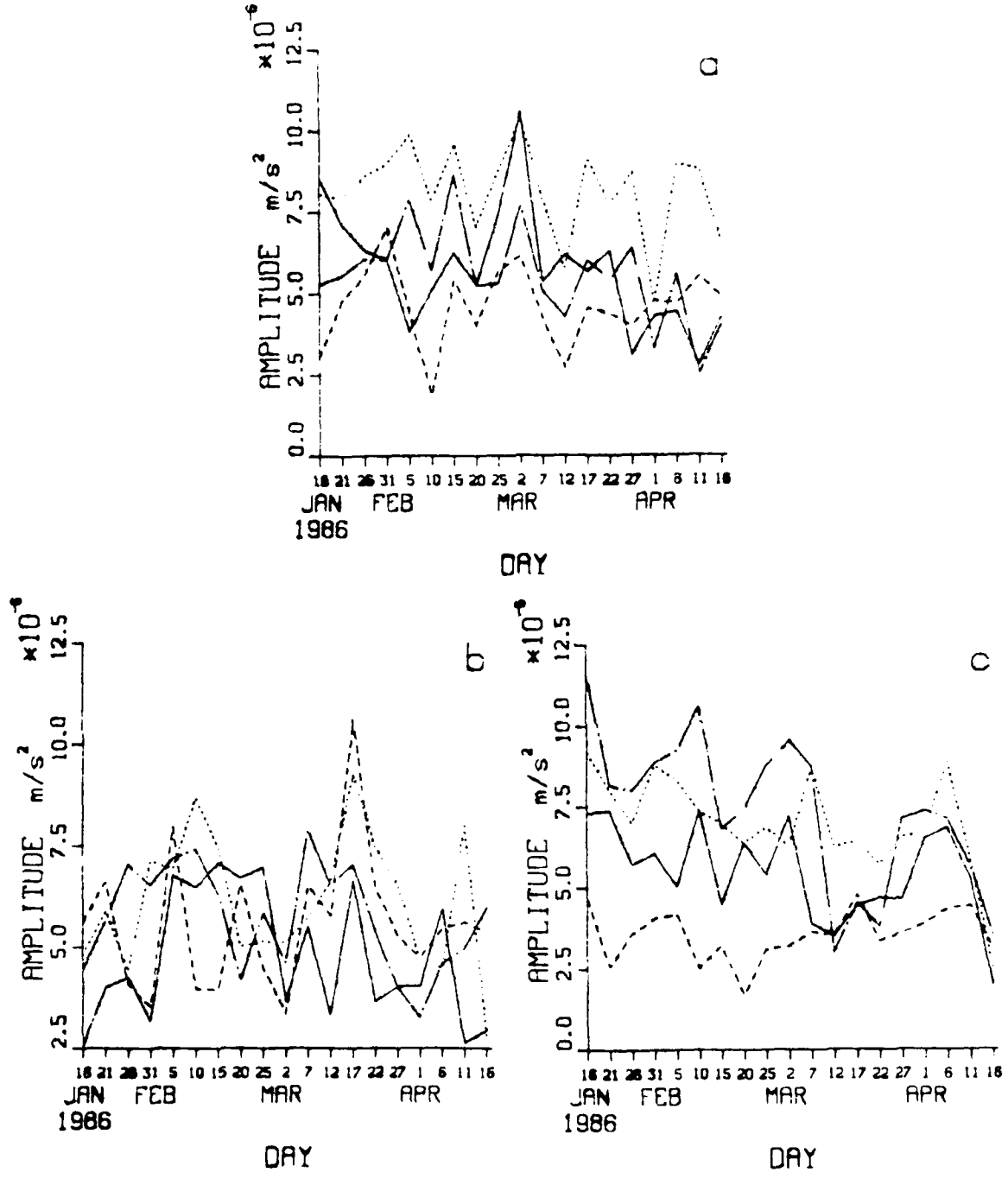

Figure 5.21. As in Figure 5.19, except for $\ell = 3$.

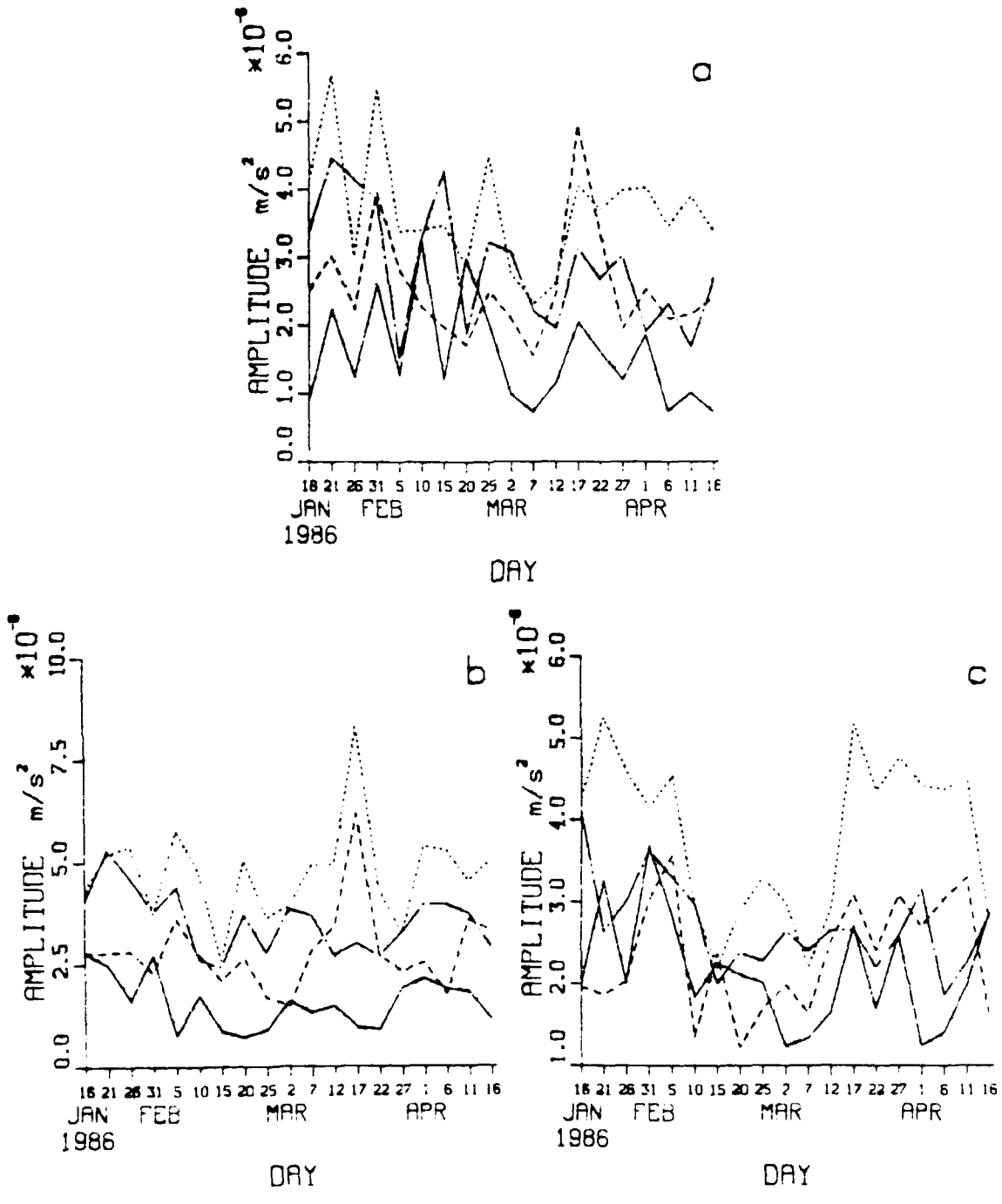

Figure 5.22. As in Figure 5.19, except for $\ell = 4$.

- For the vertical mode that is most affected by synoptic-scale interactions ($\ell = 4$), the dynamics are the most complex. The nonlinear term is on average important for this mode, but this importance varies significantly over the period being examined.
- The time tendencies of the barotropic and first baroclinic modes are generally smaller than the nonlinear term due to the partial balance between the linear and nonlinear terms. Thus, synoptic-scale contributions can be more important in determining the time tendency of these modes than their small percentage of the total nonlinear term may indicate.

To establish the importance of synoptic-scale interactions for these modes, it is necessary to compare the magnitude of the synoptic-scale contribution to the total nonlinear term to the magnitude of the time tendency. The magnitude of the synoptic-scale contribution to the total nonlinear term as a percentage of the magnitude of the time tendency are given in Figs. 5.23 - 5.26 for the $\ell = 1$-4 vertical modes of zonal wavenumbers 1-3. In addition, the synoptic-scale contribution to the total nonlinear term is plotted to allow comparisons on the days when the synoptic scales make up a large percentage of the total nonlinear term. For the barotropic mode (and especially for the barotropic mode of zonal wavenumber 3), the synoptic-scale contribution is a larger percentage of the time tendency than it is of the total nonlinear term. For example, the synoptic-scale contribution to the total nonlinear term of the barotropic mode of zonal wavenumber 2 on the 26th and 31st of January is only about 12-14% of the total nonlinear term, but 38-40% of the time tendency. This result implies that for the barotropic modes, the synoptic-scale contributions are more important than the small value of N_{ns}/N_n would indicate. The result is also true, although to a lesser extent, for the second vertical mode (Fig. 5.24) of zonal wavenumbers 1 and 2. For vertical modes 3 and 4 (Figs. 5.25 - 5.26), the general pattern is that the synoptic-scale contributions to the total nonlinear term are a larger percentage of that term than of the time tendency. This is an indication that the nonlinear term is no longer the dominant term for these modes. Rather, the nonlinear term it is only one of three terms that contribute to the time tendency and that these terms are additive. The lack of any balance for the $\ell = 3,4$ modes is an indication that the linear term is no longer large enough to balance the nonlinear term. However, the fourth vertical mode is still the most affected by synoptic scales. The number of days for which the magnitude of the synoptic-scale contributions to the total nonlinear term is greater than 30 percent of the magnitude of the time tendency is generally less than the number of days for which the synoptic-scales contributions are greater than 30 percent of the total

nonlinear term. However, there are still more significant days for the fourth vertical mode than any other vertical mode.

C. ENERGY RELATIONSHIPS

It is clear from the above analysis that synoptic scales can play an important role in the dynamics of planetary scale waves. It is also clear that these interactions are important in a time mean sense (Table 6). The analysis in the previous section is very good at highlighting this importance, but it does not show how the energy flows between synoptic scales and planetary scales. Are the scale interactions acting to decrease or increase the amplitudes (energy) of these modes? This question will be addressed in the this section. It will also be very important to determine the average energy transfers that can be compared with other studies (e.g. Tanaka et al., 1986). Most of these studies considered either kinetic or potential energy transfers, while total energy energy transfers are treated in this study.

The sum of kinetic plus available potential energy in a particular mode is given simply by

$$C_n C_n^* \tag{5.2}$$

where C_n is the amplitude of the mode designated by the index n and $(\ )^*$ indicates the complex conjugate. Thus, an equation for the time tendency of the total energy of a given mode can be obtained by multiplying (3.62) by C_n^* , and adding this to the product of the complex conjugate of (3.62) times C_n. The contribution of N_n to the time tendency of the energy of a mode n for $m \neq 0$ is given by

$$2\ \mathrm{Re}\,(C_n N_n^*) \tag{5.3}$$

where Re indicates the real part of the expression. The relation given in (5.3) indicates that the energy tendency generated by N_n or N_{ns} depends on the phasing between C_n and N_n or N_{ns}. If the synoptic-scale forcing is out of phase with the planetary scale mode, then a large magnitude of N_{ns} does not necessarily imply a large energy transfer to the planetary mode. However, this might still indicate an important contribution to the phase speed of the planetary wave.

The synoptic-scale contribution to the energy tendency produced by the nonlinear term is computed by taking the difference of the tendencies as computed in

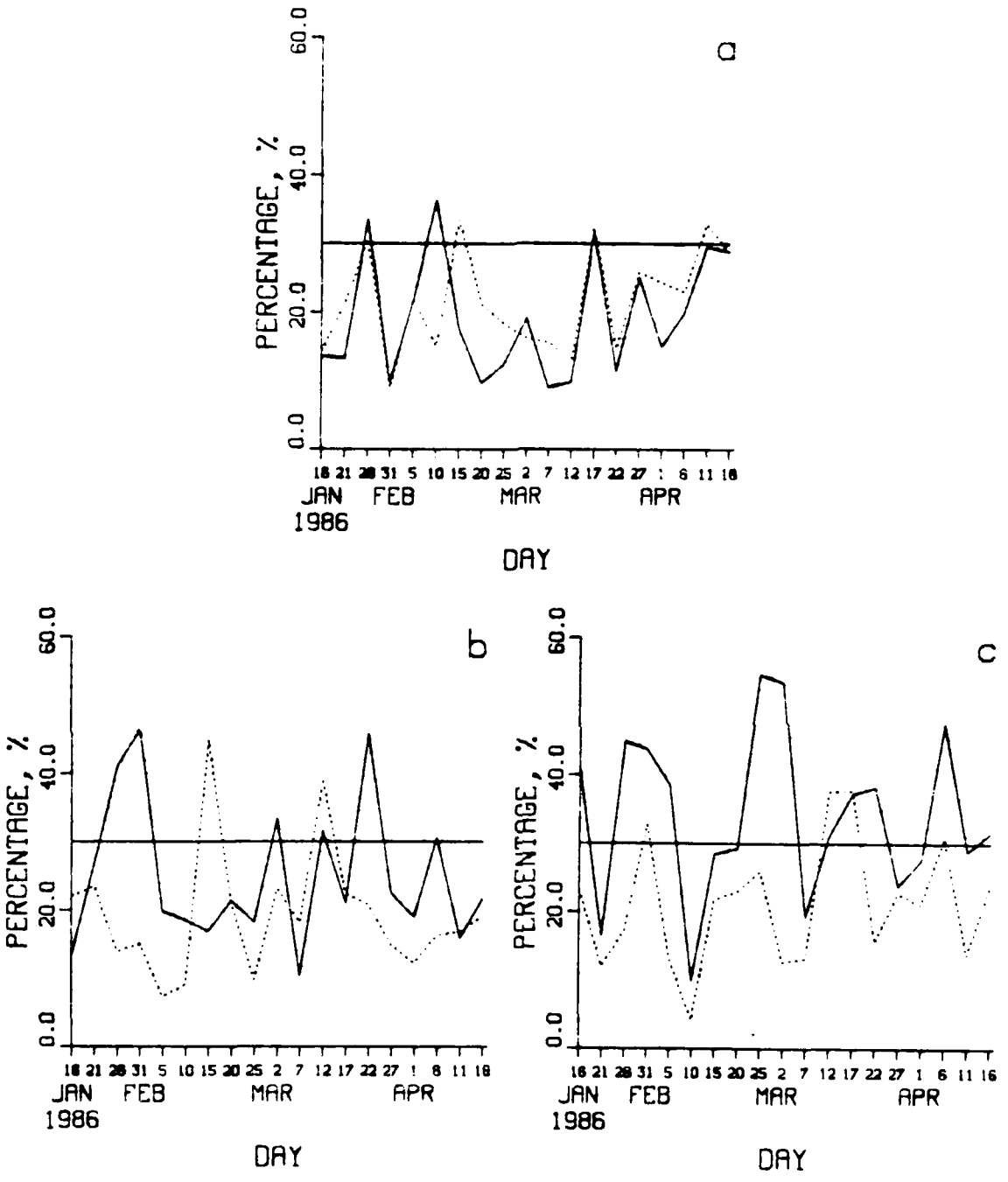

Figure 5.23. Synoptic-scale contribution to the total nonlinear term of the barotropic mode ($\ell = 1$) as a percentage of the magnitude of the time tendency (solid) and of the total nonlinear term (dashed) for zonal wavenumbers m = 1-3 (a-c).

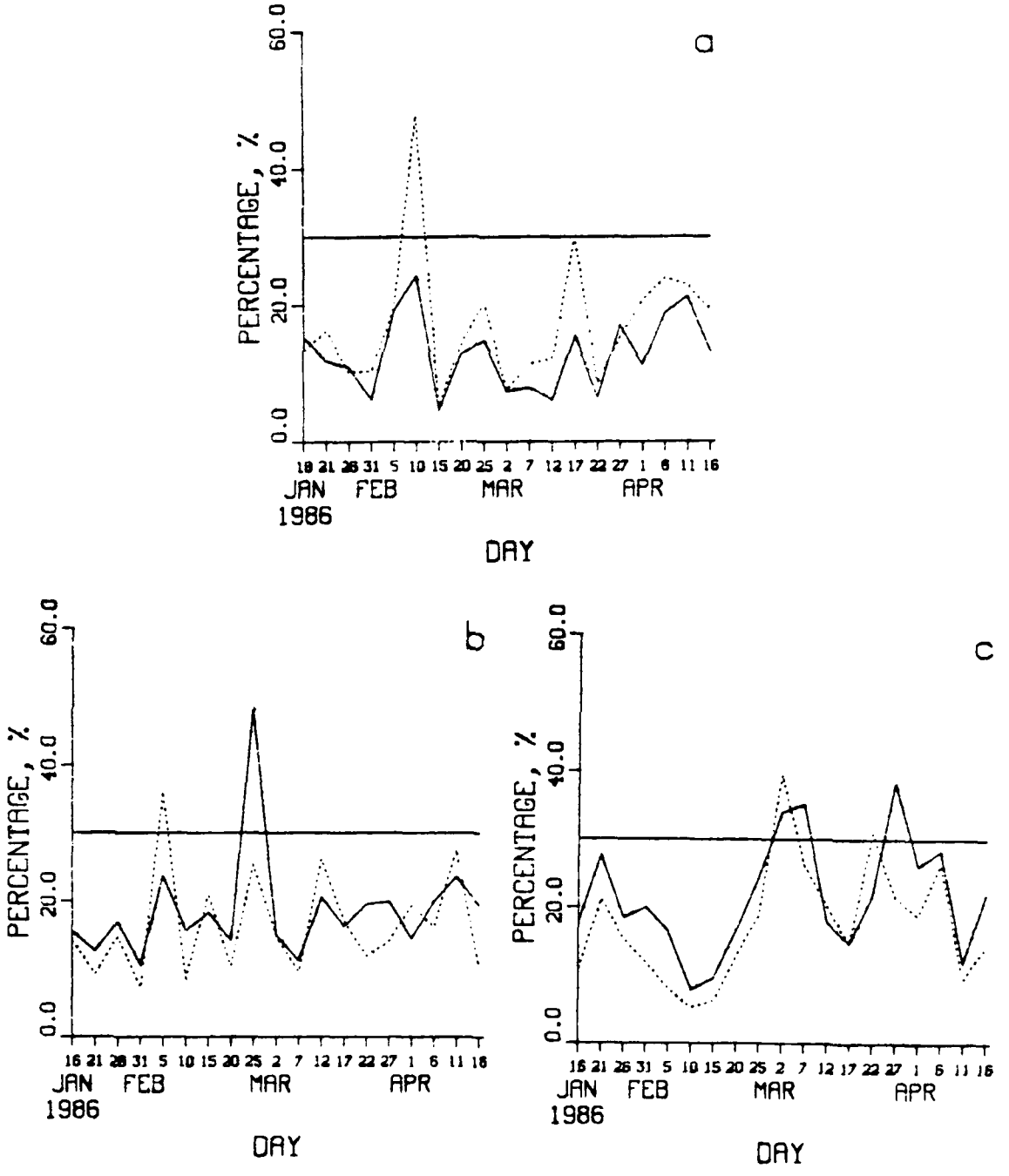

Figure 5.24. As in Figure 5.23, except for $\ell = 2$.

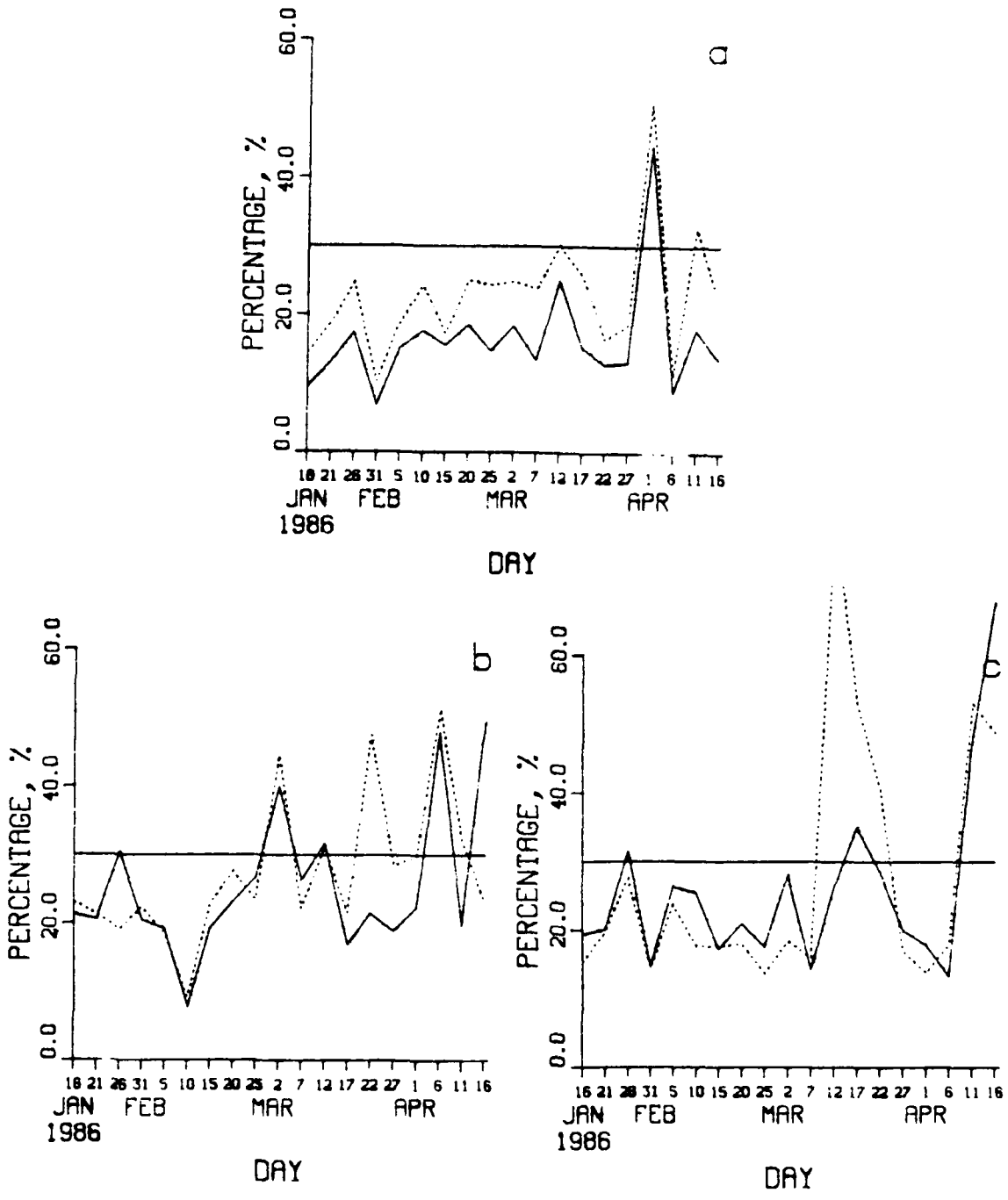

Figure 5.25. As in Figure 5.23, except for $\ell = 3$.

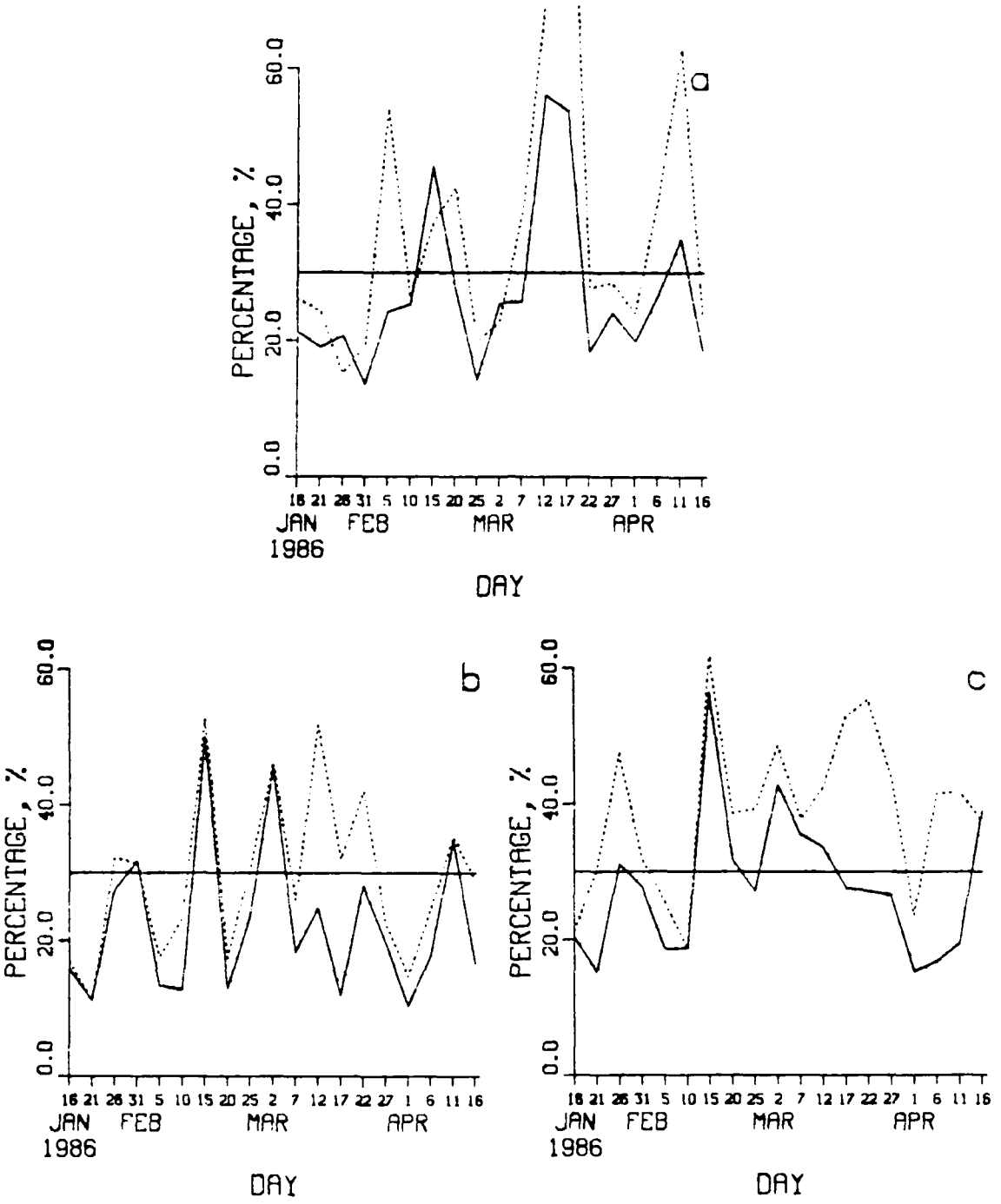

Figure 5.26. As in Figure 5.23, except for $\ell = 4$.

(5.3) from the filtered and unfiltered data. The energy tendency that is associated with the synoptic-scale contribution to the nonlinear term is shown in Figs. 5.27 - 5.30 for the $\ell = 1$-4 vertical modes of zonal wavenumbers 1-3. Also included on these plots are the contributions of the total nonlinear term. For the barotropic mode of zonal wavenumber 1 (Fig. 5.27), there is clearly a bias for the synoptic-scale contribution to the energy tendency to be positive. That is, the synoptic scales are interacting such that they are increasing the energy of the barotropic mode on 16 of the 19 days that were analyzed. The above pattern is evident to a lesser extent for the barotropic modes of zonal wavenumbers 2 and 3. For the $\ell = 2,3$ modes (Figs. 5.28-5.29), there is a tendency for the synoptic scales to take energy away from the planetary scale. This tendency appears to be strongest for the $\ell = 3$ modes. For example, on only two of the 19 days are the synoptic scales transfering energy to zonal wavenumbers 3 and 2 scales. The fourth (Fig. 5.30) vertical mode has the largest contribution from synoptic scales to planetary scales in terms of the percentage of the total energy tendency due to the nonlinear term. For most of the days examined, the synoptic-scale contribution to the energy tendency is positive for all three zonal wavenumbers.

Table 7 gives the time-averaged synoptic-scale contribution to the energy tendencies of the nine vertical modes of zonal wavenumbers 1-3. Energy flow from synoptic scales to planetary scales would be indicated by a positive value. Once again, to insure greater statistical significance the averages in Table 7 are computed from 85 days of 12UTC initialized NOGAPS analyses

The general pattern that is evident from Table 7 is that barotropic ($\ell = 1$), and third baroclinic ($\ell = 4$) modes have a positive contribution from synoptic scales to the energy tendency for all three zonal wavenumbers. The synoptic scale contribution for the $\ell = 2,3$ modes are consistently negative for all three zonal wavenumbers. The synoptic-scale contribution to the energy tendency is generally largest for the barotropic mode and smallest for the $\ell = 4$ mode. The relative importance of the energy flow from synoptic to planetary scales for a particular vertical mode is not truely indicated by energy tendencies given in Table (7). For example, the barotropic mode has a larger synoptic-scale contribution to energy tendency than does the $\ell = 4$ mode, but the barotropic mode contains a larger amount of energy than does the $\ell = 4$ mode. However, the most important point to be made from Table (7) is not the strength of the synoptic-scale contribution, but rather the pattern of this contribution. Based on the the pattern of energy flow from synoptic to planetary scales, one can hypothesize some possible mechanisms for these interactions.

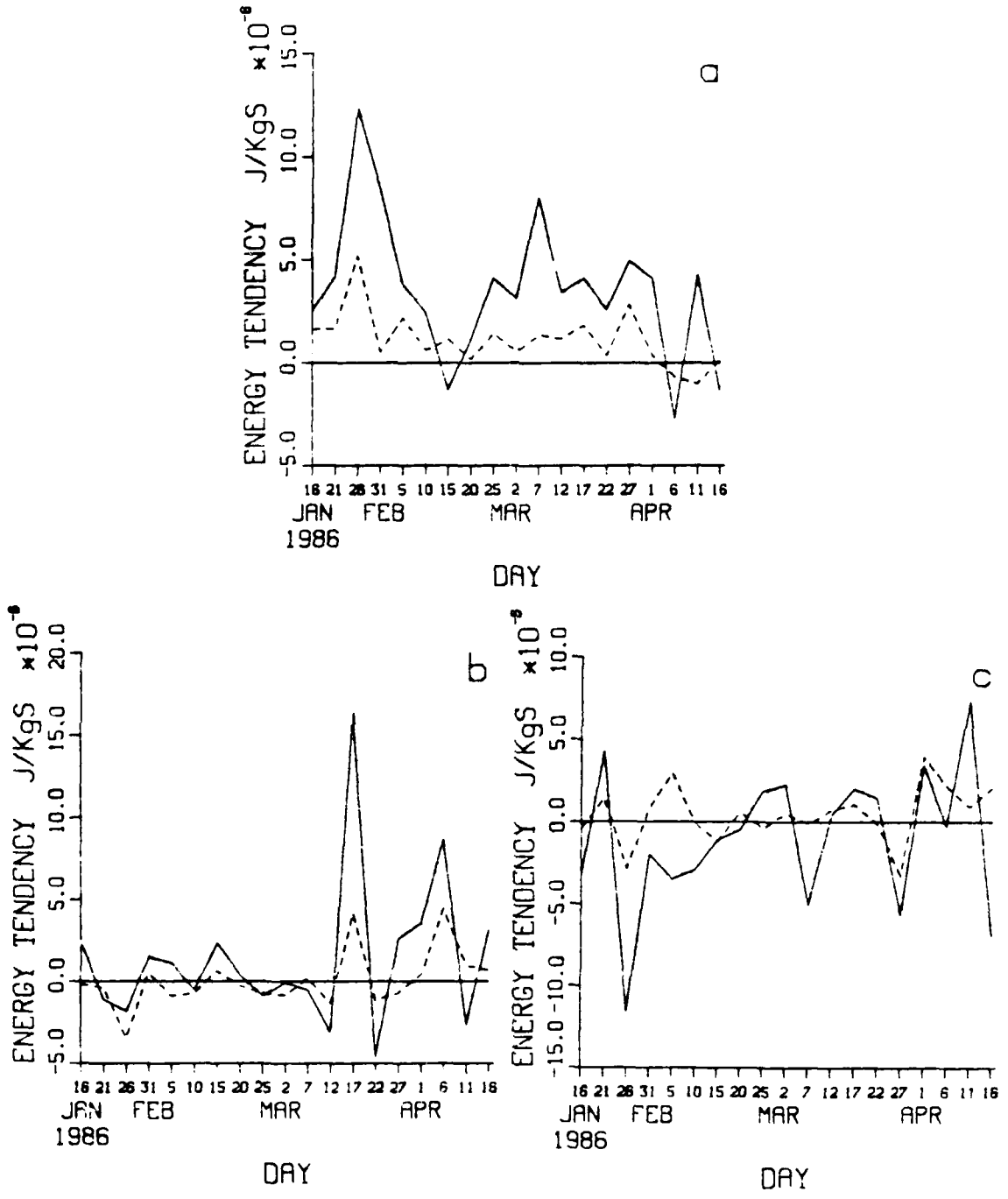

Figure 5.27. Energy tendency due to the total nonlinear term (solid) for the barotropic mode ($\ell = 1$) and the synoptic scale contribution to the energy tendency generated by the nonlinear term (dashed) for zonal wavenumbers m = 1-3 (a-c).

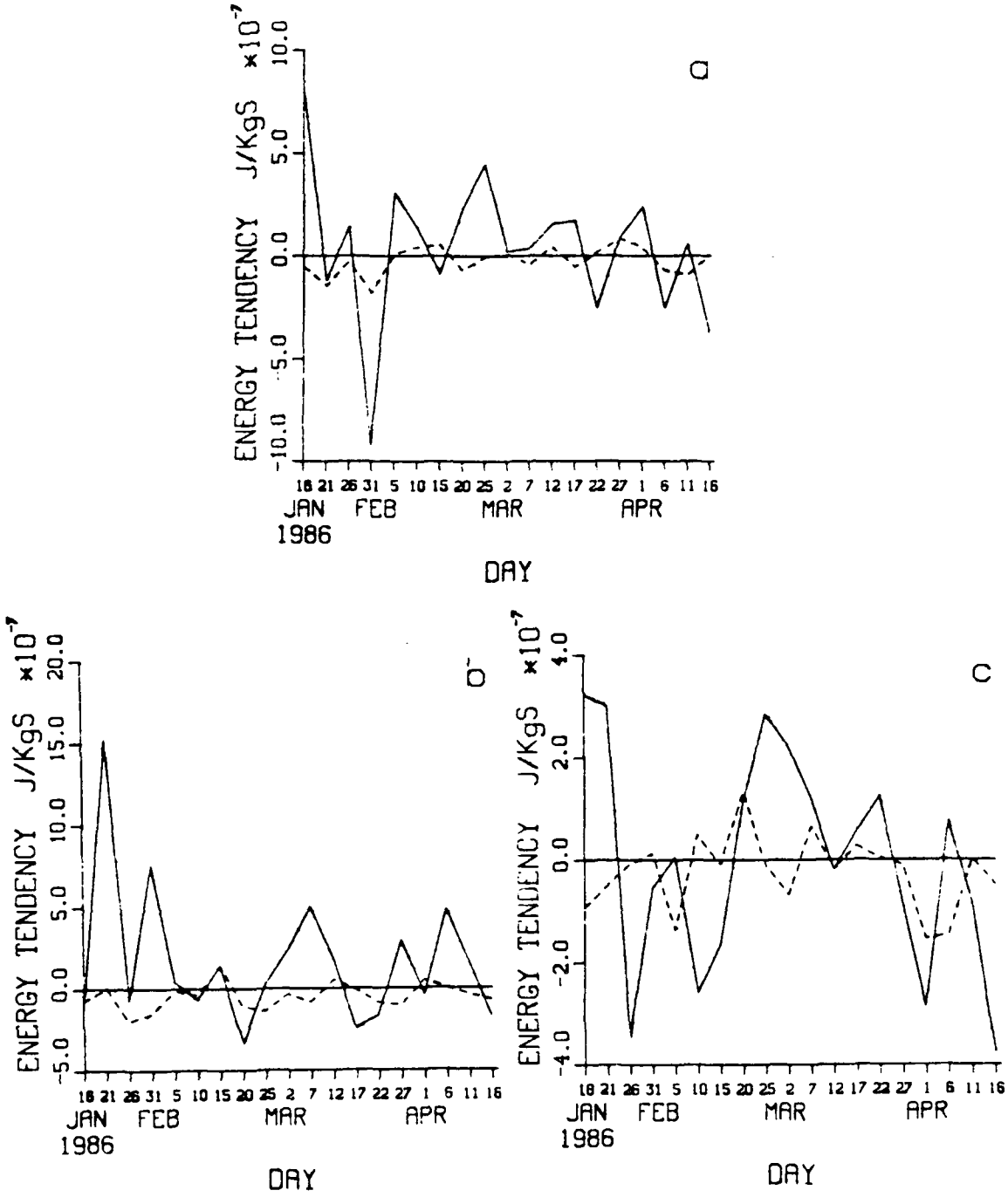

Figure 5.28. As in Figure 5.27, except for $\ell = 2$.

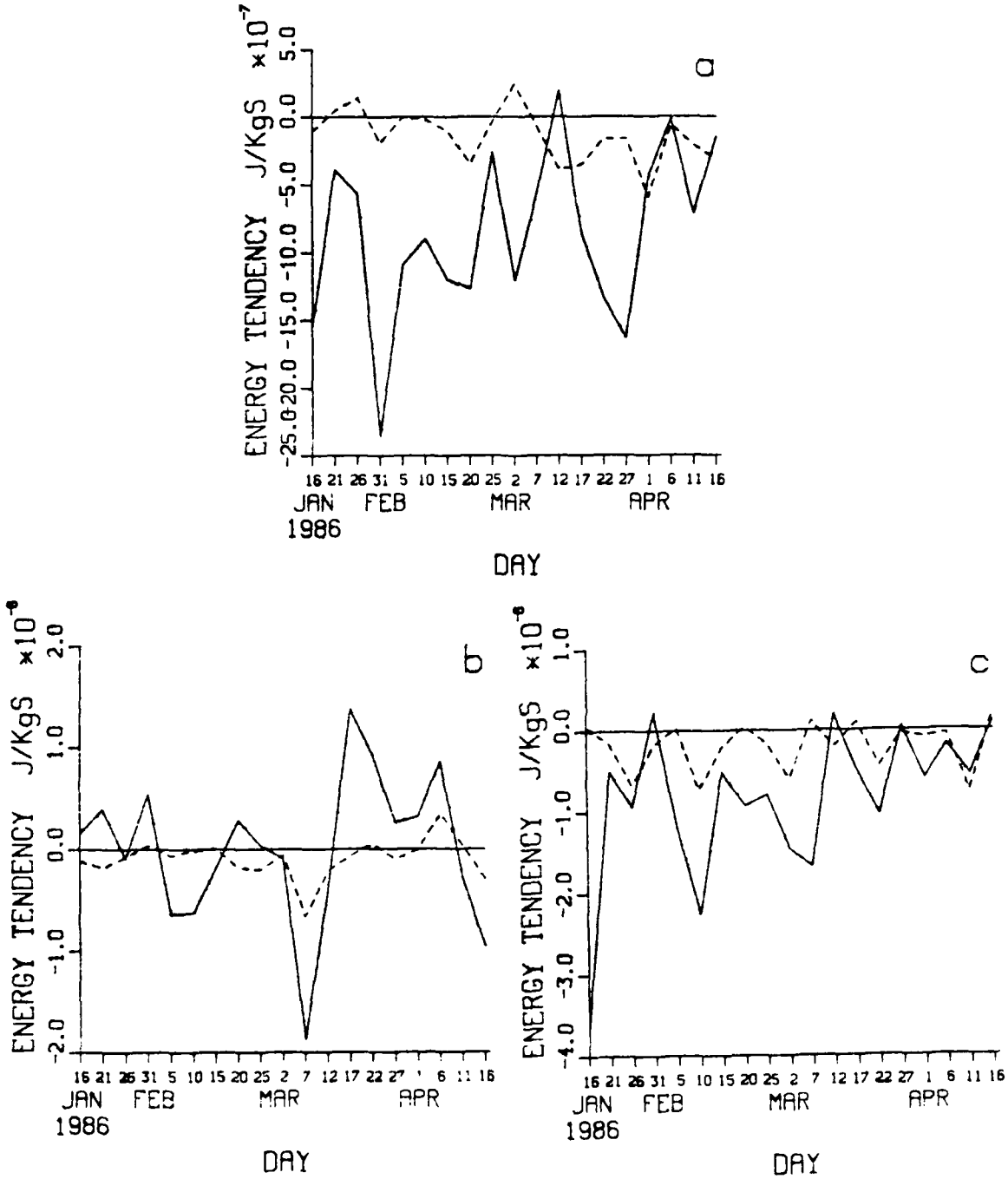

Figure 5.29. As in Figure 5.27, except for $\ell = 3$.

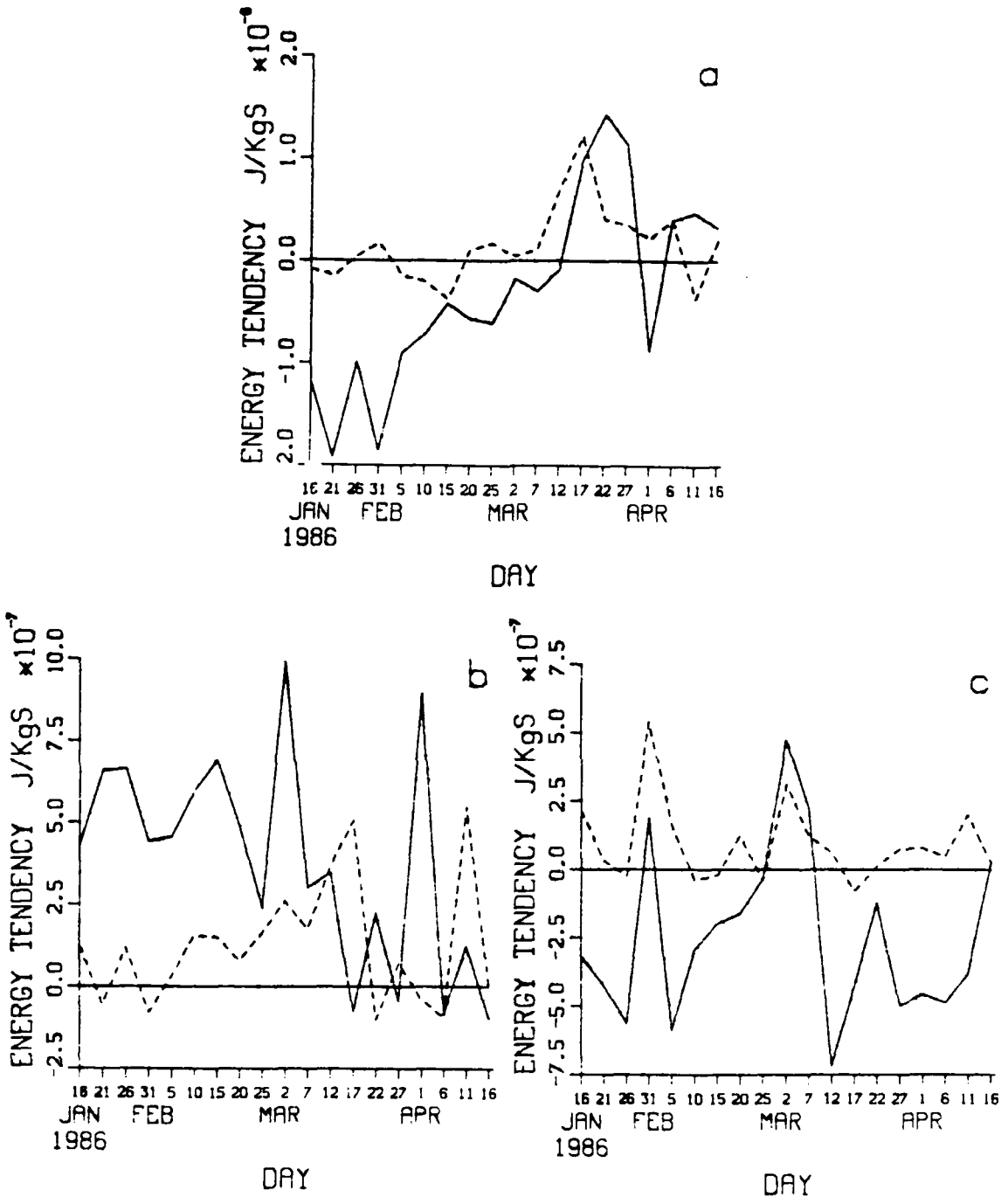

Figure 5.30. As in Figure 5.27, except for $\ell = 4$.

Table 7. Time averaged (over 85 days, taken between 16 January and 16 April 1986) synoptic-scale contribution to the energy tendency (J Kg^{-1} s^{-1}) generated by the total nonlinear term for an average of meridional modes n = 0-3.

Vertical mode index	Zonal Wavenumber		
	1	2	3
1	8.2×10^{-7}	5.7×10^{-7}	7.2×10^{-7}
2	-2.4×10^{-8}	-3.4×10^{-8}	-3.5×10^{-7}
3	-1.9×10^{-7}	-5.3×10^{-8}	-1.7×10^{-7}
4	9.7×10^{-8}	5.2×10^{-8}	4.9×10^{-9}

The analysis of the energy flows in this study between synoptic scales and planetary scales is unique in two ways: The analysis is done considering the **total** energy flow and it is specific to interactions between synoptic waves and planetary waves. Tanaka et al. (1986) examined kinetic energy flow for groups of modes, but they did not look at the total (kinetic and potential) energy flow and their emphasis was on zonal mean-eddy interaction. A important result of their study was that the zonal mean barotropic mode gained energy from the baroclinic modes of higher wavenumbers. Tanaka et al. indicated that the kinetic energy source for the higher wavenumber baroclinic modes came from the conversion of potential energy via baroclinic instability.

The results given in Table 7 show that the barotropic modes of all three zonal wavenumbers gain total energy from synoptic scales while the planetary-scale baroclinic modes ($\ell = 2,3$) were losing total energy to synoptic scales. These results are similar to the results of Tanaka et al. (1986) if one thinks of a local basic state having a projection on planetary scales. Here I use the term basic state to refer to the state obtained by zonally averaging over a restricted domain, such as the wavelength of one cyclone. The above is in contrast to a zonal basic state that implies averaging around an entire latitude circle. Because of the large scales of planetary waves, a local basic state may have a large projection on the planetary scales. Thus, the synoptic scale $\ell = 2$ and 3 vertical modes may be gaining potential energy from this basic state, converting this potential energy to kinetic energy via baroclinic instability and then

transfering this kinetic energy back to the barotropic ($\ell = 0$) component of basic state. In addition, the synoptic scale $\ell = 2$ and 3 vertical modes could at the same be transfering energy to the $\ell = 4$ planetary scale modes.

The hypothesized mechanism for the energy flow described above is also consistent with the results obtained from the analytic model presented in Chapter 4. For example, if the zonal wavenumber 6 mode for the first baroclinic mode ($\ell = 1$ in the notation of the simple analytic model, $\ell = 2$ for the NOGAPS analysis) were to interact with the zonal wavenumber 7 mode for the second baroclinic mode ($\ell = 2$ for the analytic model, and $\ell = 3$ for the NOGAPS model) then the zonal wavenumber 1 mode for the first baroclinic mode ($\ell = 1$ for the analytic model, ℓ for the NOGAPS model) and third baroclinic ($\ell = 3$ for the analytic model, $\ell = 4$ for the NOGAPS model) modes would be affected. Also, the first two baroclinic modes could interact with themselves to affect the barotropic mode.

Since the results presented in Table 7 are for the total energy flow it is not possible tell how much of the energy flow is kinetic energy and how much is potential energy. The results from the simple analytic model presented in Chapter IV, indicate that the majority (if not all) of the energy flow to the barotropic mode should be due to kinetic energy transfer while both kinetic and potential energy transfer are possible for the baroclinic modes. In the following section the relative importance of energy transfer through the momentum advection terms (kinetic energy transfer) to the energy transfer through the mass advection terms (potential energy transfer) will be examined.

D. SOME MECHANISMS OF SYNOPTIC-SCALE INTERACTIONS

It is clear from the analysis of the previous sections that synoptic scales can have a significant impact on the dynamics and energetics of planetary scales. What is not clear are the mechanisms by which the synoptic scales are interacting with the planetary scales. Are mass field interactions (e.g. temperature advection) the primary mechanism (Gall et al., 1979) or are momentum field interactions (e.g. momentum) advection more important? One of the reasons why the mechanisms of the interaction are not clear is that the adiabatic nonlinear term is a combination of of terms from the momentum equations and the thermodynamic energy equation. That is, the nonlinear term contains the effects of temperature advection as well as momentum advection. What is needed is a way to separate these effects. The method used to separate these effects is simple and direct. That part of the synoptic-scale contribution due to momentum field interactions is isolated in the following way:

- The data are filtered as described in the beginning of this Chapter.

- The nonlinear term for both the filtered and unfiltered data is computed by first computing the discrete time tendency of the coefficients via an adiabatic one-time step integration of the NOGAPS model, and then subtracting the linear term ($i\omega C$) from it. However, in this step the term representing the horizontal momentum advections is deleted.
- The energy tendency due to the nonlinear term with the momentum advections deleted is computed using (5.3) from both the unfiltered and filtered data.
- The energy tendency due to synoptic scales with and without the momentum advections is determined by subtracting the energy tendency computed from the filtered data set from the energy tendency computed from the unfiltered data for each case.
- The energy tendency due to synoptic scales that comes through the momentum advections is computed by subtracting the energy tendency due to synoptic scales computed without momentum advections from the synoptic-scale contribution to the energy tendency computed from integrations made with all of the advection terms included.

Care must be taken in using the above method. Since the synoptic scale contribution to the nonlinear term can often be a small difference between two large terms (the nonlinear terms computed from the filtered and unfiltered data) care must be taken to insure that the deletion of the momentum advection terms does not produce a large increase in time tendencies. A large increase in the time tendencies may mean that one would be trying to determine a value as a very small difference between two very large numbers. If this difference is smaller than the accuracy of the two values being subtracted, then the difference is not reliable. The error produced by the filtering process is such that only 3 to 4 significant digits are maintained after filtering. Thus if the original difference is small (an order of magnitude smaller than the original terms), and if the deletion of the momentum terms increases the time tendency by two orders of magnitude or more then the results would be questionable.

The other potential source of error in this method arises because the model equations are in a flux form so that deleting the term that represents the momentum advections also means deleting other terms (which enter via the continuity equation) which do not involve momentum advections. The continuous flux form of the momentum advection term in the sigma coordinate of the NOGAPS model is

$$\nabla \cdot (\pi \mathbf{V}\mathbf{V}) + \frac{\partial \pi \dot{\sigma} \mathbf{V}}{\partial \sigma}. \tag{5.4}$$

Where π is defined by (3.10). The discrete form of the first term in (5.4) is deleted from the NOGAPS model one-time step integrations as part of the analysis procedure which

AD-A192 328 INTERACTIONS BETWEEN SYNOPTIC AND PLANATERY SCALES OF MOTION(U) NAVAL POSTGRADUATE SCHOOL MONTEREY CA M D MCATEE DEC 87 2/2

UNCLASSIFIED F/G 4/2 NL

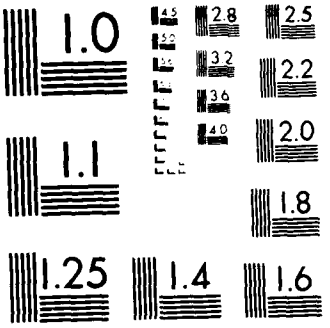

is designed to isolate interactions through the momentum advection term. The first term in (5.4) can be written

$$\pi(\mathbf{V}\cdot\nabla\mathbf{V}) + \pi\mathbf{V}\nabla\cdot\mathbf{V} + \mathbf{V}(\mathbf{V}\cdot\nabla\pi). \tag{5.5}$$

The variable π may be written as

$$\bar{\pi} + \pi' \tag{5.6}$$

where $\bar{\pi}$ is a constant over the globe and π' is a small deviation from this constant. In general, $\bar{\pi} >> \pi'$ except near high mountains. Thus the first term in (5.4) is approximated by

$$\bar{\pi}(\mathbf{V}\cdot\nabla\mathbf{V}). \tag{5.7}$$

The third term in (5.5) will in general be much smaller than (5.7) except near mountains. The second term in (5.4) and (5.5) will be small for the modes being considered because they represent interactions between the divergent and rotational parts of the motion (Errico, 1984).

Based on the above arguments concerning the smallness of the neglected terms, it can be seen that most of the nonlinear interactions that may occur through the flux form of the momentum advection term will be due to (5.7).

This method for determining the relative importantance of momentum and mass field interaction is most accurate wnen the synoptic-scale contribution to the total nonlinear term is large and when the deletions of the advection terms do not produce extremely large changes (at least two orders of magnitude) in the time tendencies of the modes. Deletion of the momentum advection terms does not produce extremely large changes to the time tendency of the modes. The above is not true when the temperature advection terms were deleted. Deletion of these terms produces large changes in the time tendencies of most of the baroclinic modes. Another point to consider when deleting nonlinear terms is that one must not delete terms that involve the mean state that the primitive equations are linearized about. For example, deletion of the vertical advection of temperature would delete the linear basic term

$$\dot{\sigma}\frac{\partial\bar{T}}{\partial\sigma}. \tag{5.8}$$

Such a deletion would mean that the frequencies that are determined as eigenvalues of the linearized equations, would no longer be valid. As result, the linear term $i\omega C$

would not be accurate. Since the linearization about a mean state of rest contains no horizontal advections, the deletions of the horizontal momentum advections will not alter the frequencies. Because deletion of the temperature advection produces large changes in the time tendency of the modes, the interactions that are due to mass field interactions are assumed to be the values computed with the momentum advection 'turned off'. These values do not represent just the horizontal temperature interactions since in sigma coordinates there are a number of nonlinear mass interaction terms e.g. the advection of surface pressure and the horizonal gradient of surface pressure. However, the temperature advection would be expected to comprise a substantial part of these nonlinear terms.

The synoptic-scale contribution to the energy tendency generated by the nonlinear term computed with all advections, and the difference between the synoptic scale contribution with all advection and that quantity computed without momentum advections are plotted in Figs. 5.31 - 5.34. The difference represents the portion of the synoptic scale contribution to the energy tendency that is due to the momentum advections. For the barotropic mode (Fig. 5.31), the synoptic scale contribution to the energy tendency generated by the nonlinear term is mainly due to momentum interactions. This is especially true when the synoptic scale contribution to the energy tendency is large. For example, compare the values of the total synoptic scale contribution to the energy tendency with that part due to the momentum advection terms on: 26 January, 17 and 27 March for zonal wavenumber one; 17 March and 6 April for zonal wavenumber two; and 26 January, 27 March and 1 April for zonal wavenumber three. Momentum advections are a slightly more important mechanism than mass field interactions for the second (Fig. 5.32) and third (Fig 5.33) vertical modes. However, the mass field interactions can be the larger contribution for some days (20 February for $\ell = 3$, $m = 1$; 26 January, 25 February, and 27 March for $\ell = 2$, $m = 2$; and 5 February for $\ell = 2$, $m = 3$). Mass field interactions are generally the dominant mechanism for the fourth (Fig. 5.34). This is especially true for days with a large energy tendency due to synoptic-scale interactions. However, there are also a a few days where momentum advections make a substantial contribution.

The results given in Table 7 show that the barotropic mode of all three zonal wavenumbers gains total energy from the synoptic scales. The results presented in Fig. (5.31) indicate that this total energy transfer is mainly due to momentum interactions. Thus, the energy being transfered from synoptic to planetary scales is kinetic energy.

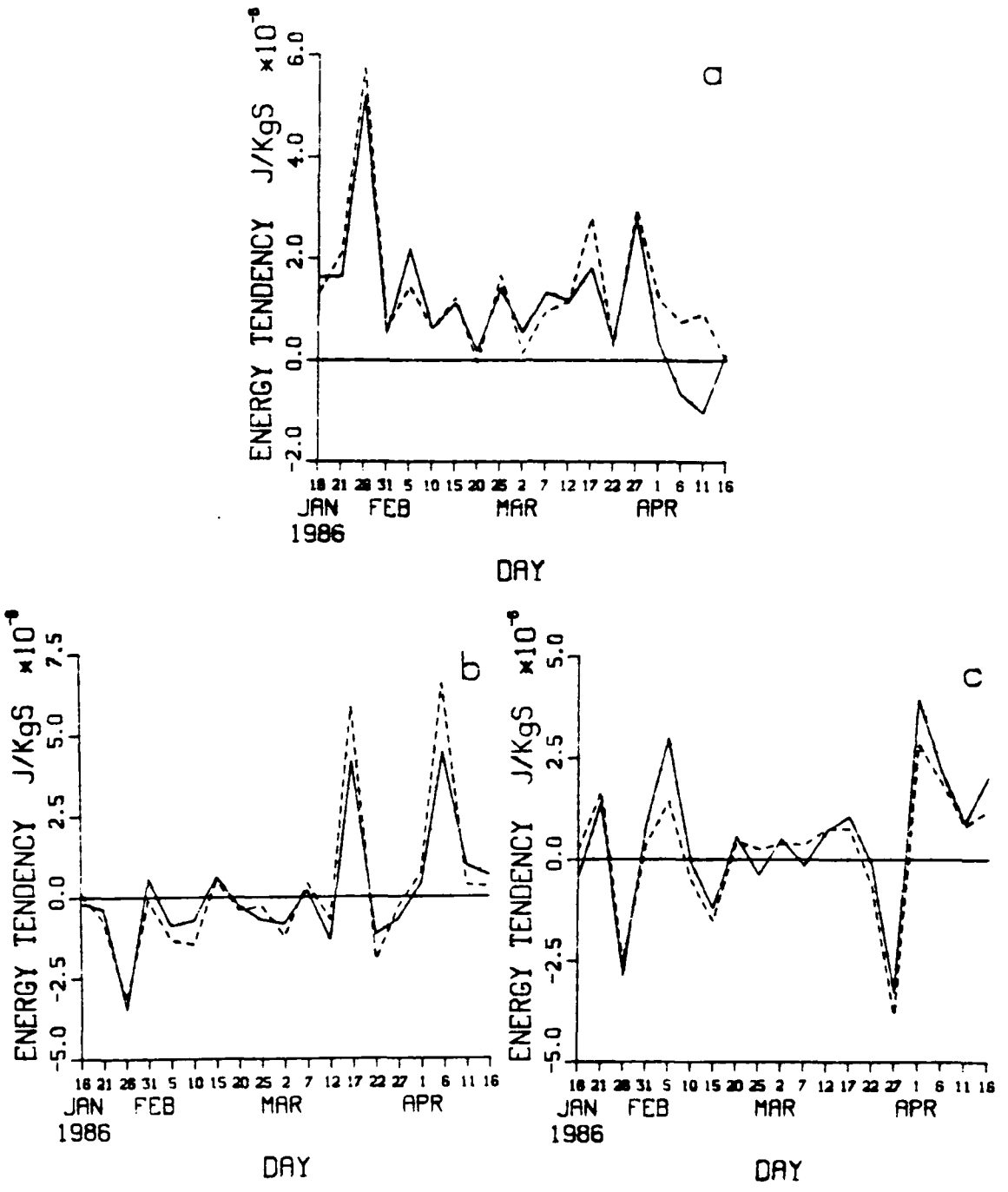

Figure 5.31. Synoptic scale contribution to the energy tendency generated by the nonlinear term for the barotropic mode ($\ell = 1$) with all advections (solid) and the contribution due to synoptic scale momentum advections (dashed) for zonal wavenumbers m = 1-3 (a-c).

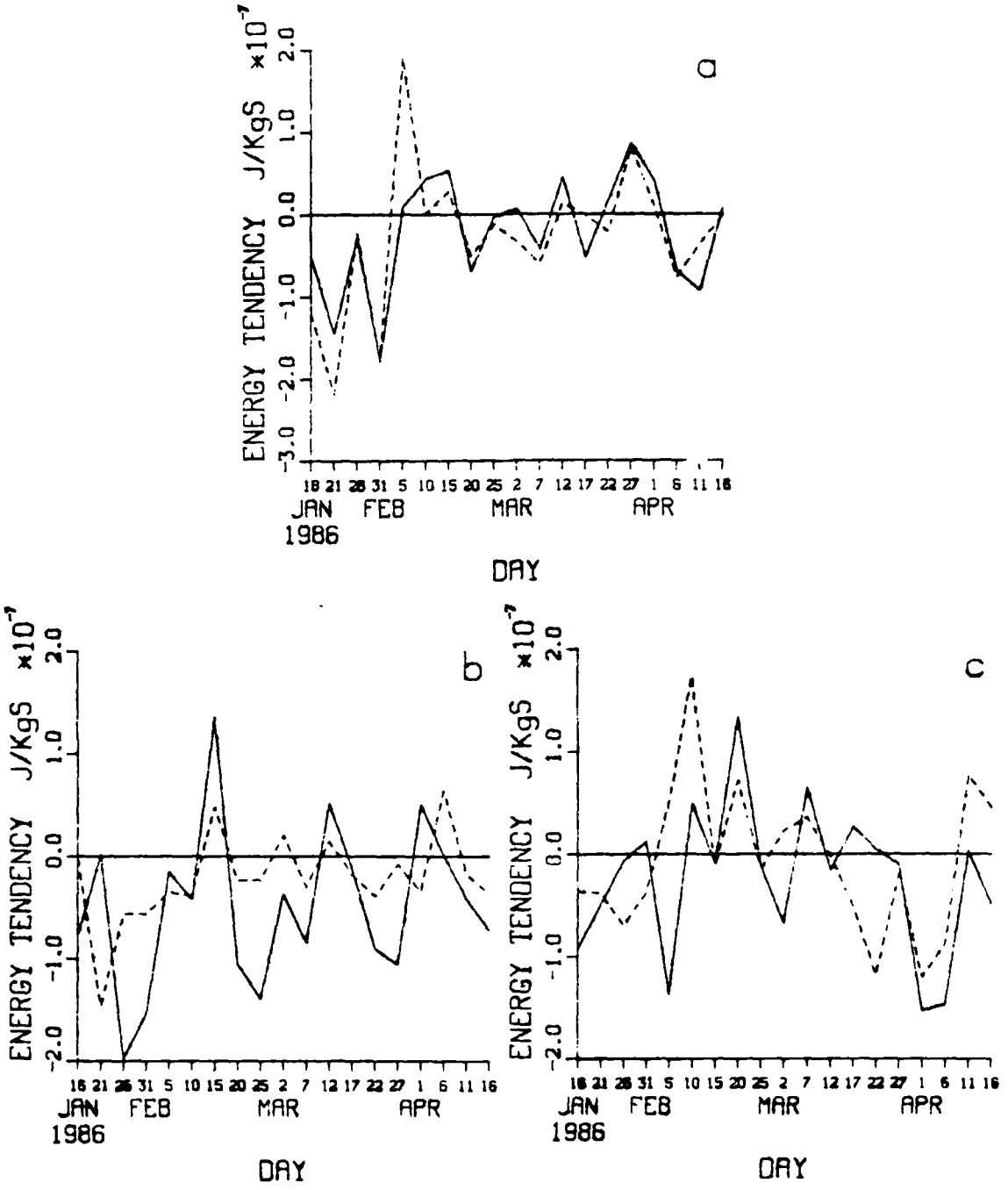

Figure 5.32. As in Figure 5.31, except for $\ell = 2$.

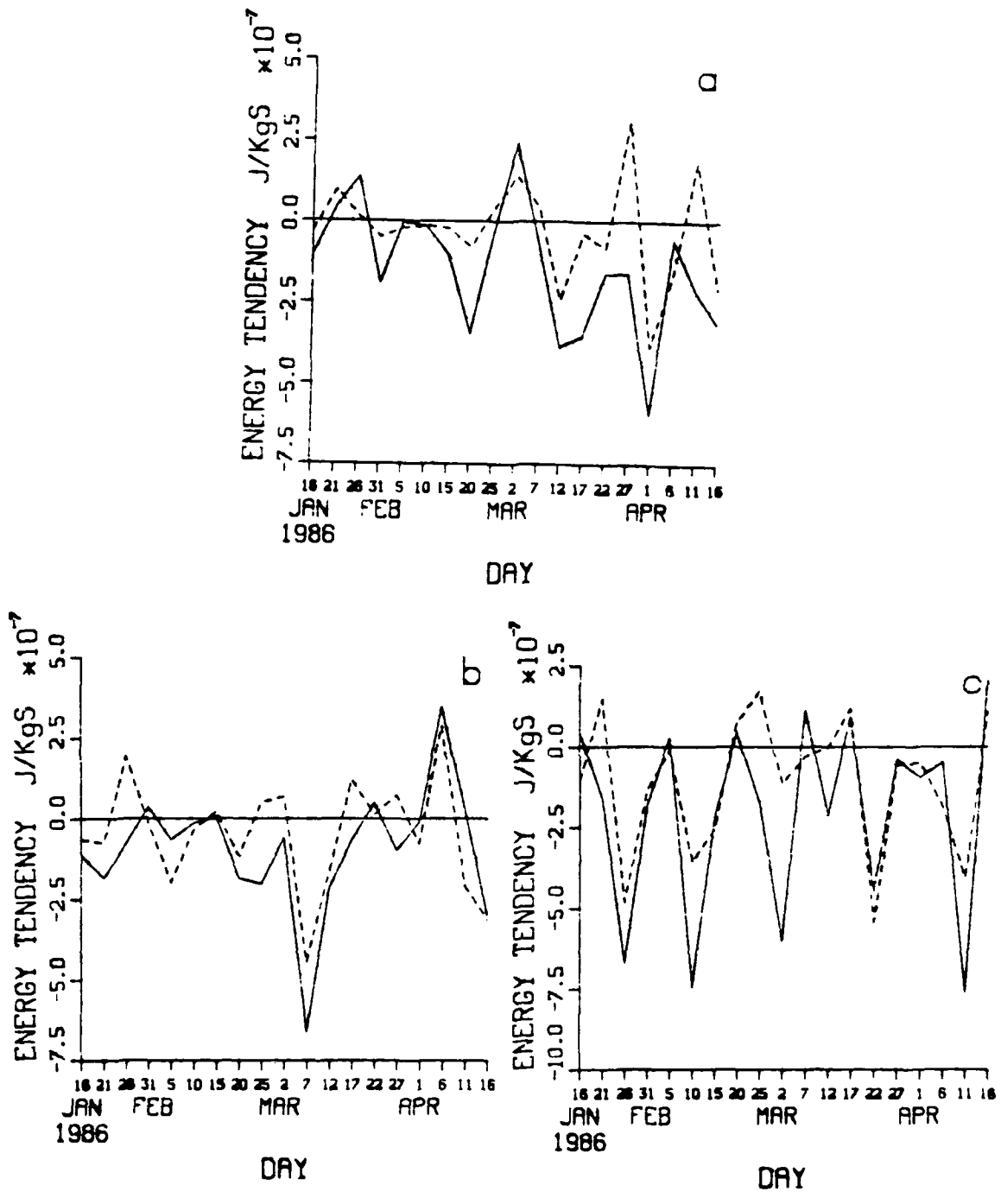

Figure 5.33. As in Figure 5.31, except for $\ell = 3$.

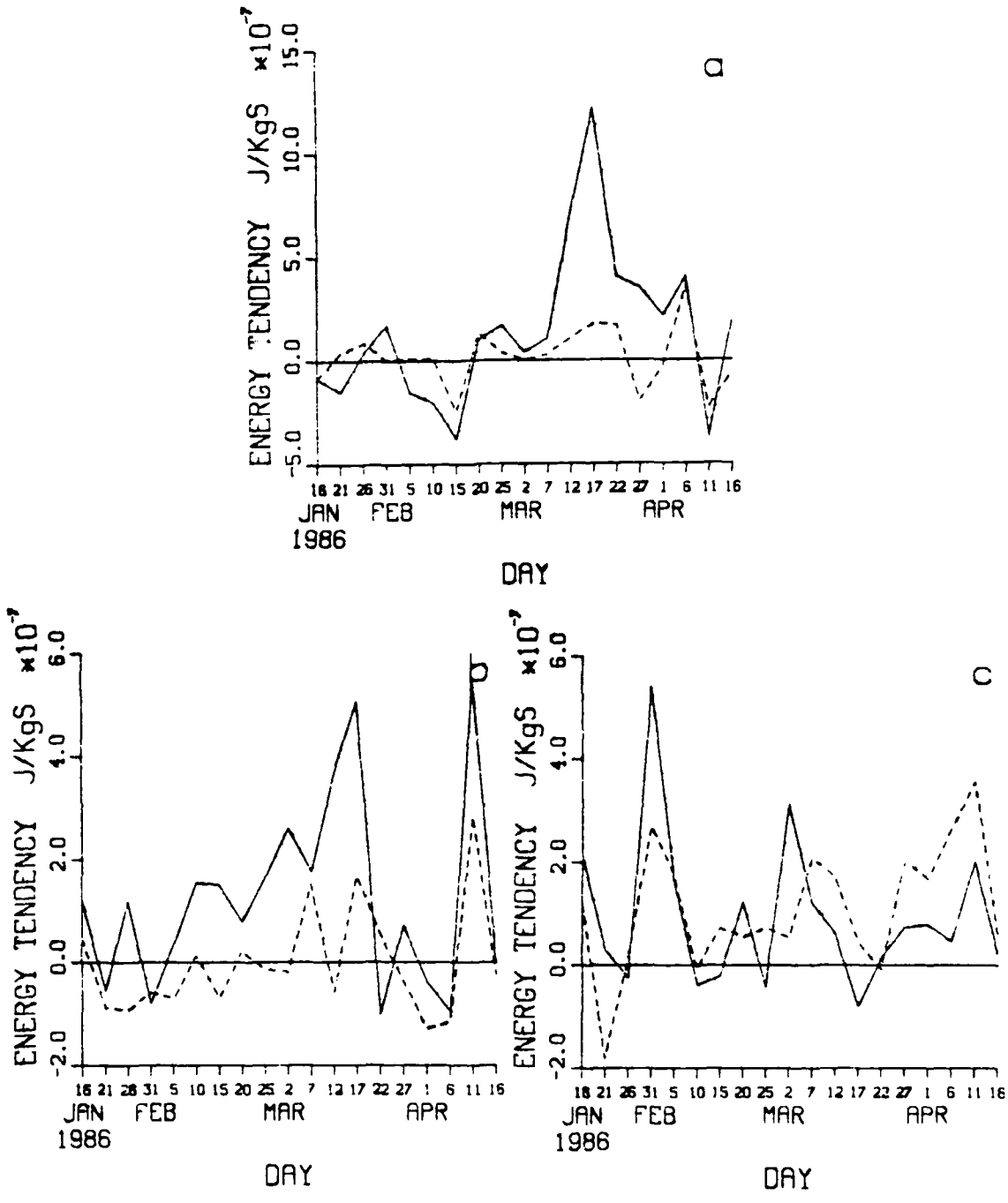

Figure 5.34. As in Figure 5.31, except for $\ell = 4$.

This result is consistent with the hypothesis presented in the previous section which is that the relation of the synoptic-scale waves to the planetary-scale waves can be likened to the relationship of an eddy to local mean flow. Assuming this hypothesis is correct, the transfer of kinetic energy from the synoptic-scale modes to the barotropic planetary-scale modes may be associated with the process of barotropic stability.

The results presented above for the barotropic mode are also consistent with those of the simple analytic model of Chapter IV. The results from this model indicate that mass field interactions would not be possible for the barotropic mode. This is not strictly the true for NOGAPS model, but it does appear from Fig. 5.31 that the momentum advections are also dominant in the NOGAPS barotropic mode.

The results presented in Table 7 indicate that on the average the synoptic scales are taking energy from the planetary-scale $\ell = 2$ and 3 modes while giving energy up to the planetary-scale $\ell = 4$ mode. From Figs 5.32-5.34 it is clear that the total energy transfer between these scales is due to both kinetic and potential energy transfer. The results from the simple analytic model indicated that both types of energy transfer are possible for baroclinic modes. Also the results for the $\ell = 2$-4 modes are not inconsistent with the idea that the relationship of the synoptic-scale modes to planetary-scale modes can be likened to the relationship of an eddy to a local mean flow. There are three possibilities for kinetic and potential energy flow between synoptic- and planetary-scale baroclinic modes:

- Synoptic-scale baroclinic modes can gain both kinetic and potential energy from planetary-scale baroclinic modes.
- Synoptic-scale waves can gain potential energy from planetary-scale baroclinic modes while losing kinetic energy to those same modes.
- Synoptic-scale modes can lose potential energy to planetary-scale modes while gaining kinetic energy from those same modes.

The final consequence of the above analogy, is that the type, sign and amount of energy transfer from synoptic-scale baroclinic waves to planetary-scale baroclinic waves would depend in a crucial way on the tilt of the synoptic scale waves' phase with respect to the vertical and horizontal wind shear of the planetary waves.

The potential energy flow from synoptic scales to the planetary scales of the $\ell = 4$ mode is similar to the flow proposed by Gall (1979). Gall proposed that the planetary scale waves were forced **mainly** by planetary scale variations in the meridional heat flux convergence of higher wavenumber modes i.e., the interaction between cyclone scales waves and the local basic state increased the amplitude of the planetary scale

temperature perturbation. This potential energy was then converted to kinetic energy due to a positive correlation between planetary scale upward motion and temperature. It is clear from the results presented in Fig. 5.34 that potential energy is being transfered to the $\ell = 4$ mode of the planetary scale waves. The above result is also consistent with the results obtained from the analytic model presented in Chapter IV. However, the results of this study also appear to conflict with the results of Gall et al. (1979) in that not all of the planetary scale modes (the $\ell = 1$ mode for example) are being forced mass field interactions. The apparent conflict between this study and that of Gall can be explained by the differences in the data rather than the mechanism. In Gall's experiment, synoptic-scale perturbations were allowed to grow from a zonal mean state. Gall argued that in developing waves/perturbations that wave/perturbation velocity (V') and the wave/perturbation vorticity (ζ') were uncorrelated while V' and the wave/perturbation temperature were correlated. In this study, the atmosphere data contained a variety of fully developed cyclones. For fully developed cyclones it cannot be said that $V'\zeta'$ are uncorrelated. In fact, general circulation theory would suggest that $V'\zeta'$ would be correlated. In a more recent study that was very similar to that done by Gall, Young and Villere (1985) showed that direct transfer of kinetic energy from intermediate scales to planetary scales was of equal importance to the transfer of potential energy. A possible reason for this conflict between these two similar studies is that the zonal mean state specified by Young and Villere was such that they obtained higher growth rates than Gall and their disturbances developed faster. I believe that the disturbances in the Young and Villere study developed to the stage where the correlation $V'\zeta'$ became significant. While it may be true for the simple state specified by Gall that the synopticscale forcing of planetary scale waves is mainly through the temperature advection term, this does not appear to be true for an atmosphere that contains fully developed cyclones. This is not to say that the mechanism proposed by Gall is invalid, as this mechanism may be active in the atmosphere given the proper distribution and variation of intensity of cyclones. However, the direct transfer of kinetic energy could be taking place that may or may not be in the same sense as the potential energy transfer.

In summary, the analysis of the results presented in this chapter have established the following:

- Synoptic-scale interactions can have a significant impact on the dynamics of planetary scale modes.

- For the barotropic mode ($\ell = 1$), the main balance is between the linear (Rossby wave) terms and adiabatic advection terms, so that the time derivative is smaller than either term. In this situation, the synoptic-scale interactions can have an important influence on the planetary scale waves even when they are not a large percentage of the total advection term.
- Synoptic-scale interactions tend to decrease the energy of the planetary $\ell = 2,3$ vertical modes while increasing the energy of the barotropic and $\ell = 4$ modes.
- The synoptic-scale interactions are mainly through the momentum terms for the barotropic mode and through both the momentum and mass advection terms for the baroclinic modes ($\ell = 2$-4 modes). The mass field interactions are generally dominate for the $\ell = 4$ modes.

There are some important implications of the above results to the forecastability of planetary-scale waves. One can easily see that if the strengths and or phases of synoptic-scale waves are not not forecast correctly then the interactions between synoptic and planetary scales will not be forecast correctly. This could immediately lead to a forecast error in the planetary scales. Showalter (1984), using a spectral forecast verification technique, noted a case where a poor synoptic-scale forecast by the NOGAPS model led to subsequent degradation in the planetary-scale forecasts of the model. The nonlinear linkage of synoptic and planetary scale of motion suggests that to forecast planetary scales more accurately, more accurate synoptic-scale forecast are required.

VI. SUMMARY AND CONCLUSIONS

The procedures used in this study are based on the normal mode analysis procedures developed by Errico (1984). NOGAPS analyses have been projected onto the normal modes and the different terms (**linear,nonlinear adiabatic and diabatic**) that affect a particular mode have been determined. The total energy for each mode and the energy tendencies due to the nonlinear term are determined. The effect of synoptic scales on the magnitude of the adiabatic nonlinear term (N_n), and the energy tendency due to N_n is also determined. By deleting the effect of the momentum advection terms, it is possible to determine the relative importance of interactions through the momentum or mass terms.

The importance of the nonlinear interactions in the dynamics of planetary waves has been demonstrated by computing the adiabatic nonlinear term for a two different data sets. The first data set is 19 days of 12UTC NOGAPS analyses taken every 5 days from 16 January 86 to 16 April 86. The second data set is a filtered version of the first data set. In this data set the data (u, v, T and $\ell n\ p_s$) are spectrally filtered by transforming the data to spectral space and then setting the coefficients of wave numbers 7-15 to zero. Reconstitution of the field then is a representation of the atmosphere without the influence of synoptic waves. The magnitude of the difference between the adiabatic nonlinear term computed from the original and the filtered data sets is taken as a measure of the dynamical importance of synoptic-scale interactions on planetary scale waves. The magnitude of this difference is on average about 20 -30% of the total nonlinear term, although it may be as much as 60-70% of the magnitude of the total nonlinear term in certain vertical modes for a given day.

The ratio of the synoptic scale contribution (N_{ns}) to the adibatic nonlinear term of a planetary-scale mode (N_n) is only one measure of the dynamical importance of synoptic scales. An additional measure (the ratio of the magnitude of N_{ns} to the magnitude of the time tendency $\Delta C/\Delta t$) is used to show that the ratio of the magnitudes of N_{ns} to $\Delta C/\Delta t$ may be large even though the ratio of the magnitude of N_{ns} to the magnitude of N_n is small. This is generally true of the first three vertical modes, although it was especially true for the barotropic mode. For this mode, the linear and nonlinear terms tend to balance such that the time tendency of this mode is

smaller than either of the two balancing terms. Even though small when compared to N_n, the contribution of synoptic scales may be important in determining the balance or nonbalance of the total nonlinear term with the linear term. In this case, N_{ns} might be very important in determining the time tendency of the barotropic mode.

Although the comparisons with the magnitude of N_{ns} to the magnitude N_n or to $\Delta C/\Delta t$ show that N_{ns} could play an important role in the dynamics of planetary scale modes, it does not show how planetary scale modes are affected by synoptic scale modes. To examine the mechanism through which the synoptic scales affect planetary scales, the energy equation for a given mode is derived and the energy tendencies generated by N_{ns} and N_n are examined. On the average, synoptic scales tend to give energy up to planetary scales for the barotropic $\ell = 1$ and baroclinic $\ell = 4$ vertical modes, while energy flows from planetary-scale waves to the $\ell = 2,3$ modes. The positive contribution of synoptic scales to the energy of the planetary scale $\ell = 1$ mode can be a large percentage of the energy tendency generated by N_n, which indicates that the synoptic scales play an important role in determining the time evolution of these modes.

To determine how energy is being transferred, the energy tendencies generated by N_n with the momentum advection term deleted from the equations are calculated. The deletion of this term eliminates most of the transfer of energy through the momentum term. By examining the difference between the energy tendency generated by N_{ns} with all the terms included and N_{ns} with no momentum advections, it is possible to determine how much of the energy tendency due to interaction with synoptic scales is due to the momentum advections. It is found that interactions through this term are, not unsurprisingly, responsible for almost all of the energy transfer from synoptic scales to the planetary scale barotropic modes. Interactions through this term are also important for the $\ell = 2,3$ modes, but do not seem to be quite as important as the interaction through the mass fields (temperature advections). The relative importance of interaction through the mass field increases as vertical mode number increases.

The results of this study confirm in part those of Gall et al. (1979). That is, synoptic scales do in fact play an important role in the dynamics of planetary scale waves and they can act to increase the energy of these waves. However, the results of this study also appear to conflict with the results of Gall et al. (1979). Gall proposed that the forcing of planetary scale waves by synoptic scale waves was mainly through

the planetary scale variations in the meridional heat flux convergence of synoptic waves, which produces a positive correlation between planetary wave upward motion and temperature. In this study, it is found that forcing through the momentum advections are also important (especially for the barotropic mode). The apparent conflict between this study can be explained by the differences in the data used rather than the mechanism.

There is no question that the synoptic scales have an impact on the dynamics of planetary scales. For example, if a major cyclonic development is missed in a forecast it could lead to a sizable error in the planetary waves because the nonlinear effects of cyclones would not be properly represented. This fact means that to more accurately forecast planetary scale waves one must improve the forecast of synoptic scales which will feed back and cause an increase in accuracy of the planetary scales. This has already been demonstrated to some degree because higher resolution models tend to give better planetary wave forecasts than lower resolution models even though the truncation error for the planetary waves should be negligible for both resolutions.

It remains for future studies to determine how well numerical models represent these interactions and how errors in forecasting these interactions affect the planetary scale forecasts. Future studies might should try to examine how periods of large synoptic-planetary interactions are affected by changes which occur on the time-scale of synoptic wave. The interactions in this study were examined only every five days so it was not possible to see how the interactions varied with the changing synoptic patterns.

Another possiblity for future study would be forecast verification using normal mode analysis. Using normal mode analysis, it may be possible to more fully examine the relationship between errors in determining the interactions between planetary and synoptic scales and any subsequent planetary-scale forecast error. Finally, other studies have indicated that nonlinear interactions may be important in maintaining blocking patterns. These studies did not use normal mode analysis. Much might be learned about the dynamics of these blocking patterns by examining the nonlinear interactions using normal mode analysis.

APPENDIX A
LINEARIZED HYDROSTATIC, THERMODYNAMIC AND CONTINUITY EQUATIONS

The vertical structure of the NOGAPS model follows the development given by Arakawa and Suarez (1983). The variables are staggered in σ so that all the variables (T, Φ, and V) except pressure and σ are carried at the mid-point of each layer. The vertical structure is illustrated in Fig. A.1

The finite difference form of the hydrostatic equation is:

$$\phi_k - \phi_{k+2} = C_p(P_{k+2} - P_k)\hat{\theta}_{k+1} \quad for \quad k = 1, 3, \ldots \kappa - 2 \tag{A.1}$$

and

$$\phi_K = \hat{\phi}_s + C_p(\hat{P}_s - P_k)\hat{\theta}_k \tag{A.2}$$

Where

$$P_k = \frac{1}{p_o^\kappa}\frac{1}{1+\kappa}\frac{\hat{p}_{k+1}^{1+\kappa} - \hat{p}_{k-1}^{1+\kappa}}{\hat{p}_{k+1} - \hat{p}_{k-1}} \tag{A.3}$$

$$P_K = \frac{1}{p_o^\kappa}\frac{1}{1+\kappa}\frac{\hat{p}_s^{1+\kappa} - \hat{p}_{k-1}^{1+\kappa}}{\hat{p}_s - \hat{p}_{k-1}} \tag{A.4}$$

and

$$\hat{\theta}_{k+1} = A_{k+1}\theta_k + B_{k+1}\theta_{k+2} \tag{A.5}$$

are the interpolation formulas used to produce energetically consistent equations where:

$$p_k = \sigma_k(p_s - p_t) + p_t \tag{A.6}$$

$$\hat{P}_k = \left(\frac{\hat{p}_k}{p_o}\right)^\kappa \tag{A.7}$$

$$A_{k+1} = \frac{\hat{P}_{k+1} - P_k}{P_{k+2} - P_k} \tag{A.8}$$

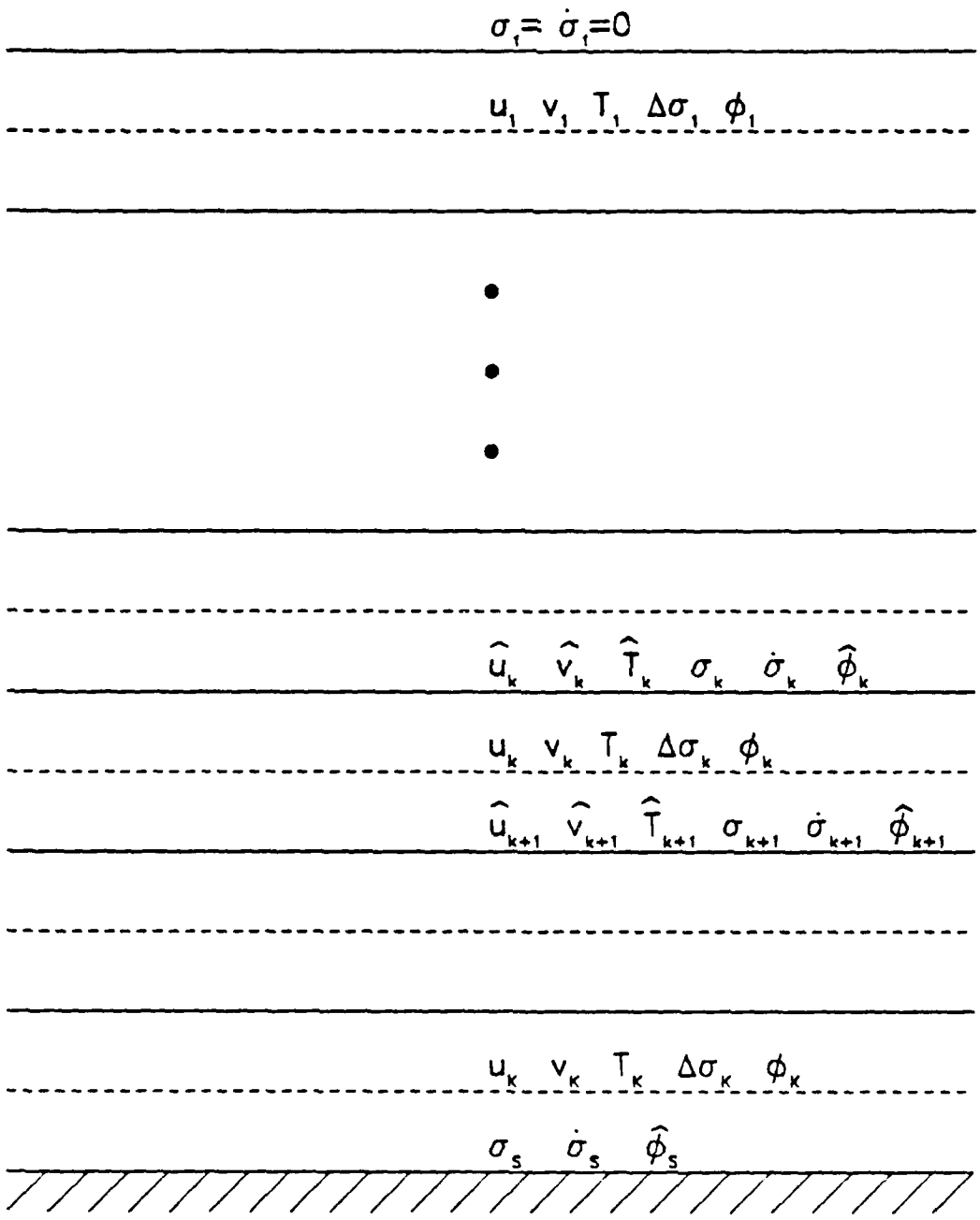

Figure A.1. Vertical grid structure for NOGAPS model.

$$B_{k+1} = \frac{P_{k+2} - \hat{P}_{k+1}}{P_{k+2} - P_k} \tag{A.9}$$

$$A_{K-1} = \frac{\frac{P_K P_{K-2}}{P_{K-1}} - P_{K-2}}{P_K - P_{K-2}} \tag{A.10}$$

$$B_{K-1} = \frac{P_K - \frac{P_K P_{K-2}}{P_{K-1}}}{P_K - P_{K-2}} \tag{A.11}$$

T is temperature, p is pressure and C_p is the specific heat at constant pressure. The geopotential at each level is computed using

$$\phi_K = \hat{\phi}_s + C_p(P_s - P_K)\theta_K \tag{A.12}$$

$$\begin{aligned}\phi_k = \hat{\phi}_s + &\sum'_{n=k}^{K} C_p(P_{n+2} - P_n)(A_{n+1}\theta_n) + \\ &\sum'_{n=k+2}^{K} C_p(P_n - P_{n-2})(B_{n-1}\theta_n)\end{aligned} \tag{A.13}$$

which are just integrated forms of (A.1) and (A.2). The primed sum indicates increments of 2. The above form of the hydrostatic equation can be written as:

$$\phi_k - \hat{\phi}_s = \sum'_{n=1}^{K} G_{kn} T_n \tag{A.14}$$

where

$$G_{kn} = \begin{cases} 0 & n < k \\ \dfrac{C_p(P_{n+2} - P_n)A_{n+1}}{P_n} & n = k \\ \dfrac{C_p(P_{n+2} - P_n)A_{n+1}}{P_n} + & \\ \dfrac{C_p(P_n - P_{n-2})B_{n-1}}{P_n} & n > k \end{cases} \tag{A.15}$$

or in matrix form as

$$\phi - \hat{\phi}_s = \mathbf{C}\mathbf{T} \tag{A.16}$$

The finite difference form of the thermodynamic equation (Eq. 299 in Arakawa and Lamb:1972) in orthogonal curvilinear coordinates is

$$\begin{aligned}&\delta_t[\pi T]^k_{ij} + [\delta_\epsilon(F\overline{T}^\epsilon) + \delta_\eta(G\overline{T}^\eta)]^k_{ij} + \frac{1}{\Delta\sigma}P^k_{ij}\delta_\sigma(\dot{S}\hat{\theta})^k_{ij} \\ &\quad = \frac{1}{C_p}[(\sigma\pi\alpha)\frac{\partial\Pi}{\partial t} + \overline{\frac{u\Delta\eta}{n}}^{\epsilon}\overline{(\sigma\pi\alpha)}^{\epsilon}\delta_\epsilon\pi + V\overline{\frac{\Delta\epsilon}{m}}^{\eta}\overline{(\sigma\pi\alpha)}^{\eta}\delta_\eta\pi + \Pi Q]^k_{ij}\end{aligned} \tag{A.17}$$

where

$$\Pi = \pi\frac{\Delta\epsilon\Delta\eta}{mn} \tag{A.18}$$

$$F = \pi u \frac{\Delta \eta}{n} \tag{A.19}$$

$$G = \pi v \frac{\Delta \varepsilon}{m} \tag{A.20}$$

$$\dot{S} = \Pi \dot{\sigma} \tag{A.21}$$

The overbar is a linear average in the direction of the variable indicated, and δ_χ is a difference taken in the direction of the subscript.

To linearized, first subtract

$$T_{ij}^k[\delta_t \Pi + \delta_e F + \delta_\eta G + \frac{\delta_\sigma(\dot{S})}{\Delta\sigma}]_{ij}^k = 0 \tag{A.22}$$

which gives

$$\Pi \delta_t T_{ij}^k + \frac{1}{\Delta\sigma} P_{ij}^k \delta_\sigma[\dot{S}\hat{\theta}]_{ij}^k - T\frac{\delta_\sigma[\dot{S}]_{ij}^k}{\Delta\sigma} - \frac{1}{C_p}(\pi\sigma\alpha)_{ij}^k \frac{\partial \Pi}{\partial t} = (Q_T)_{ij} \tag{A.23}$$

or

$$\delta_t T_{ij}^k + [\frac{\overline{T}_{k+1}}{P_{k+1}} P_k - \overline{T}_k]_+ \frac{\dot{\sigma}_{k+1}}{\Delta\sigma_k} - [\frac{\overline{T}_{k-1}}{P_{k-1}} P_k - \overline{T}_k]_- \frac{\dot{\sigma}_{k-1}}{\Delta\sigma_k} - \frac{(\sigma\pi\alpha)_k}{C_p} \frac{\partial \ln \pi}{\partial t} = (Q_T)_{ij} \tag{A.24}$$

where $\overline{T}_k$ is the rest-state temperature.

Substituting the linearized form of the continuity equation (Eqs. 166-167 in Arakawa and Lamb;1972)

$$\dot{\sigma}_{k+1} = -\sum_{n=1}^{k} (\nabla \cdot V)_n \Delta\sigma_n + \sigma_{k+1} \sum_{n=1}^{K} (\nabla \cdot V_n)\Delta\sigma_n + Q_+ \tag{A.25}$$

$$\dot{\sigma}_{k-1} = -\sum_{n=1}^{k-1} (\nabla \cdot V)_n \Delta\sigma_n + \sigma_{k-1} \sum_{n=1}^{K} (\nabla \cdot V_n)\Delta\sigma_n + Q_- \tag{A.26}$$

$$\delta_t \ln \pi = -\sum_{n=1}^{K} (\nabla \cdot V_n)\Delta\sigma_n + Q_p \tag{A.27}$$

and

$$(\overline{\sigma\pi\alpha})_k = C_p \frac{\overline{T}_k}{P_k}(\pi \frac{dP_k}{d\pi}) \tag{A.28}$$

gives

$$\delta_t T_{ij}^k + [\ ]_+ \frac{(\sigma_{k-1} - 1)\sum_{n=1}^{k-2} (\nabla \cdot V)_n \Delta\sigma_n + \sigma_{k+1} \sum_{n=k+2}^{K} (\nabla \cdot V_n)\Delta\sigma_n}{\Delta\sigma_k} \tag{A.29}$$

$$+[\,]_{-}\frac{(\sigma_{k-1}-1)\sum_{n=1}^{k-2}(\nabla\cdot V)_n\Delta\sigma_n+\sigma_{k-1}\sum_{n=k}^{K}(\nabla\cdot V_n)\Delta\sigma_n}{\Delta\sigma_k}$$

$$+\frac{\overline{T}_k}{P_k}(\pi\frac{dP_k}{d\pi})\sum_{n=1}^{K}(\nabla\cdot V_n)\Delta\sigma_n=(Q_T)_{ij}$$

In matrix form

$$\delta_t\mathbf{T}_{ij}+\tau(\nabla\cdot\mathbf{V})_{ij}=(\mathbf{Q}_T)_{ij} \tag{A.30}$$

where

$$\tau_{kn}=\begin{cases}\{[\,]_{+}\dfrac{(\sigma_{k+1}-1)}{\Delta\sigma_k}-[\,]_{-}\dfrac{(\sigma_{k-1})}{\Delta\sigma_k}+\dfrac{\overline{T}_k}{P_k}(\pi\dfrac{dP_k}{d\pi})\}\Delta\sigma_k & n<k\\ \{[\,]_{+}\dfrac{(\sigma_{k+1}-1)}{\Delta\sigma_k}-[\,]_{-}\dfrac{(\sigma_{k-1})}{\Delta\sigma_k}+\dfrac{\overline{T}_k}{P_k}(\pi\dfrac{dP_k}{d\pi})\}\Delta\sigma_k & n=k\\ \{[\,]_{+}\dfrac{(\sigma_{k+1})}{\Delta\sigma_k}-[\,]_{-}\dfrac{(\sigma_{k-1})}{\Delta\sigma_k}+\dfrac{\overline{T}_k}{P_k}(\pi\dfrac{dP_k}{d\pi})\}\Delta\sigma_k & n>k\end{cases} \tag{A.31}$$

The formula

$$\pi\frac{dP_k}{d\pi}=\frac{A_{k+1}[\sigma_{k+1}(P_{k+2}-P_k)]+B_{k-1}[\sigma_{k-1}(P_k-P_{k-2})]}{\Delta\sigma_k}\quad k<K \tag{A.32}$$

$$\hat{P}_s-P_k \qquad k=K$$

is that derived by Arakawa from the interpolation formulas (A.3) - (A.9). Note that the continuity equation may also be written in matrix form by defining

$$\Pi=\begin{bmatrix}\Delta\sigma_1\\ \Delta\sigma_2\\ \cdot\\ \cdot\\ \cdot\\ \Delta\sigma_K\end{bmatrix} \tag{A.33}$$

so that

$$\delta_t\ln\pi=-\Pi^T\delta+Q_p \tag{A.34}$$

APPENDIX B
NORMAL MODES OF THE QUASI-GEOSTROPHIC MODEL

It is convenient to use the following vertical coordinate

$$Z = -\ln(p/p_0), \tag{B.1}$$

where p_0 is a fixed standard sea-level pressure. The vertical coordinate Z is related to the actual height z, and the geopotential by the equation of state and the hydrostatic equation:

$$RT = p\alpha = pg\frac{\partial Z}{\partial p}\frac{\partial \phi}{\partial Z}. \tag{B.2}$$

This vertical coordinate is closely related to the more familiar pressure coordinate system and the vertical derivatives of the two system are related as follows:

$$\frac{\partial}{\partial p} = \frac{1}{p}\frac{\partial}{\partial Z}, \tag{B.3}$$

while the other partial derivatives are the same in both systems. The Z-velocity $\dot{Z}$ is related to ω through

$$\dot{Z} = \frac{\omega}{p}. \tag{B.4}$$

The basic equations of this model are:

$$\frac{\partial \phi}{\partial Z} = RT \tag{B.5}$$

$$\frac{\partial \mathbf{V}}{\partial t} + \mathbf{V}\cdot\nabla\mathbf{V} + \dot{Z}\frac{\partial \mathbf{V}}{\partial Z} + \nabla\phi + f\mathbf{k}\times\mathbf{V} = 0 \tag{B.6}$$

$$\frac{\partial T}{\partial t} + \mathbf{V}\cdot\nabla T + \dot{Z}\frac{\partial T}{\partial Z} + \dot{Z}RT = Q \tag{B.7}$$

$$\nabla\cdot\mathbf{V} + \frac{\partial \dot{Z}}{\partial Z} - \dot{Z} = 0. \tag{B.8}$$

We assume boundary conditions of $Z = 0$ at 0 and $Z = Z_T$, where Z_T is Z at the top of the atmosphere. An expression for Z may be obtained by rewriting B.8 as

$$\nabla \cdot \mathbf{V} + e^{z} \frac{\partial}{\partial Z}(e^{-z} \dot{Z}) = 0. \tag{B.9}$$

if we multiplly (B.9) by e^{-Z}, integrate from Z to Z_T and solve for Z we obtain

$$\dot{Z} = e^{z} \int_{z}^{z_T} e^{-z} \nabla \cdot \mathbf{V}\, dZ. \tag{B.10}$$

Assuming Boussinequess conditions i.e. e^{-Z} = constant then (B.10) can be written

$$\dot{Z} = \int_{z}^{z_T} \nabla \cdot \mathbf{V}\, dZ. \tag{B.11}$$

Next we linearize (B.5)-(B.8) about a hydrostatic and adiabatic mean state at rest by letting

$$\mathbf{V} = \mathbf{V}'(x, y, Z, t); \quad \phi = \bar{\phi}(Z) + \phi'(x, y, Z, t). \tag{B.12}$$

By combining the linearized versions of (B.10), (B.5), and (B.7) we obtain a single equation for mass which contains all of the vertical derivatives:

$$\frac{\partial^2 \phi'}{\partial t \partial Z} + \Gamma(z) \int_{z}^{z_T} \nabla \cdot \mathbf{V}\, dZ. \tag{B.13}$$

The term $\Gamma(Z)$ is the mean state static stability and is given by

$$\Gamma(Z) = \frac{\partial}{\partial Z}\left(\frac{\partial \bar{\phi}}{\partial Z} + \kappa \bar{\phi}\right) = \frac{H^2 g}{\bar{T}}\left(\frac{g}{C_p} + \frac{1}{H}\frac{\partial \bar{T}}{\partial Z}\right), \tag{B.14}$$

where

$$H = R\bar{T}g. \tag{B.15}$$

A vertical structure equation can now be determined from B.13 by first dividing by $\Gamma(Z)$ and then taking $\partial / \partial Z$ of (B.13) so that it can be written as

$$\frac{\partial}{\partial t}\left(\frac{\partial}{\partial Z}\left(\frac{1}{\Gamma}\frac{\partial \phi}{\partial Z}\right)\right) + \nabla \cdot \mathbf{V} = 0. \tag{B.16}$$

Next we can use the technique of separation of variables to determine the vertical structure equation. This is done by letting

$$\phi' = \Phi_n(x, y, t)\phi_n(Z) \tag{B.17}$$

$$\mathbf{V} = \mathbf{V}_n(x, y, t)\phi_n(Z) \tag{B.18}$$

and substituting these expressions into (B.16). The vertical structure equation obtained by the above procedure is.

$$\frac{\partial}{\partial Z}\left(\frac{1}{\Gamma}\frac{\partial \phi_n}{\partial A}\right) = -\lambda_n \phi_n . \tag{B.19}$$

The associated boundary conditions for this equation are

$$\frac{\partial \phi_n}{\partial Z} = 0. \tag{B.20}$$

The vertical modes of this model are just the eigenfunction of the boundary value problem given by (B.19) and (B.20). Assuming $\Gamma(Z)$ is constant then the vertical modes for this system are

$$\phi_n = A_n \cos\frac{n\pi Z}{Z_T} \qquad n = 0 - \infty \tag{B.21}$$

These function can be used to transform the basic equation into equations for each vertical mode.

LIST OF REFERENCES

Ahlquist, J. E., 1982: Normal-mode global Rossby waves: theory and observations. *J. Atmos. Sci.*, 39, 193-202.

Arakawa, A., and V. R. Lamb, 1977: Computational design of the basic dynamical processes of the UCLA general circulation model. *Methods in Computational Physics, Vol. 17*, Julius Chang, Ed., Academic Press, 174-264.

_____, and W. H. Schubert, 1974: Interaction of a cumulus cloud ensemble with the large scale environment, Part 1. *J. Atmos. Sci.*, 31, 674-701.

_____, and M. J. Suarez, 1983: Vertical differencing of the primitive equations in sigma coordinates. *Mon. Wea. Rev.*, 111, 34-45.

Barker, E. H., 1982: A Comparison of Two Initialization Methods in Data Assimilation. Ph.D Thesis, Naval Postgraduate School, 157 pp.

Barnes, S. L., 1964: A technique for maximizing details in numerical weather map analysis. *J. Appl. Meteor.*, 3, 396-409.

Baumhefner, D., and P. Downey, 1978: A comparison of six wintertime forecasts from several numerical weather prediction models. *Proc. 12th Stanstead Seminar*, McGill University Publications in Meteorology No. 121, 98 pp. (Department of Meteorology McGill University, 805 Sherbrooke St. W., Montreal P.Q., H3A 2K6 Canada.)

Bettge, T. W., and D. P. Baumhefner, 1984: Total and planetary-scale systematic errors in recent NMC operational model forecasts. *Mon. Wea. Rev.*, 112, 2317-2325.

Burger, A., 1958: Scale considerations of planetary motions of the atmosphere. *Tellus*, 10, 195-205.

Daley, R., J. Tribia, and D. Williamson, 1981: The excitation of large-scale free Rossby waves in numerical weather prediction. *Mon. Wea. Rev.*, 109, 1836-1861.

Dickenson R. E. and D. L. Williamson 1972: Free oscillations of a discrete stratified fluid with application to numerical weather prediction. *J. Atmos. Sci.*, 29, 623-640.

Errico,R. M., 1981: An analysis of interactions between geostrophic and ageostrophic modes in a simple model. *J. Atmos. Sci.*, 38, 544-553.

_____, 1984: The dynamical balance of a general circulation model. *Mon. Wea. Rev.*, 112, 2439-2454.

Gall, R., R. Blakeslee and R. C. J. Somerville, 1979: Cyclone-scale forcing of ultralong waves. *J. Atmos. Sci.*, 36, 1692-1698.

Haltiner, G. J. and R. T. Williams, 1980: *Numerical Prediction and Dynamic Meteorology*. John Wiley & Sons, 477pp.

Kao, S. K., and H. N. Lee, 1977: The nonlinear interactions and maintenance of the large-scale moving waves in the atmosphere. *J. Atmos. Sci.*, 34, 471-485.

Kasahara A., and K. Puri, 1981: Spectral representation of three-dimensional global data by expansion in normal mode functions. *Mon. Wea. Rev.*, 109, 37-51.

Ko, S. D., 1985: Vertical Modes and Energetics of Gravitational and Rotational Modes in a Multilevel Global Spectral Model. Ph.D Thesis, University of Michigan and National Center for *Atmospheric Research, 225 pp.*

Lambert, S., and P. Merilees, 1978: A study of planetary wave errors in a spectral numerical weather prediction model. *Atmos. Ocean*, 16, 197-211.

Leith, C. E., 1980: Nonlinear normal mode initialization and and quasi-geostrophic theory. *J. Atmos. Sci.*, 37, 958-968.

Lord, S. J., 1978: Development and observational verification of a cumulus cloud parameterization. Ph.D Thesis, University of California, Los Angeles, 359 pp. 37, 958-968.

Lorenz, E., 1960: Maximum simplification of the dynamic equations. *Tellus*, 12, 243-254.

_____, 1969: The predictability of a flow which possesses many scales of motion. *Tellus*, 21, 248-307.

Machenhauer, B., 1977: On the dynamics of gravity oscillations in a shallow water model, with application to normal mode initialization. *Contrib. Atmos. Phys.*, 50, 253-271.

Madden, R. A., 1978: Further evidence of traveling planetary waves. *J. Atmos. Sci.*, 35, 1605-1618.

_____, and P. A. Julian, 1972: Further evidence of global-scale 5-day pressure waves. *J. Atmos. Sci.*, 29, 1464-1469.

Morse, P. J., 1983: NOGAPS verification using spectral components. Masters Thesis, Naval Postgraduate School, 71 pp.

Randall, D. A., 1976: The interaction of the planetary boundary with large-scale circulations. Ph.D Thesis, University of California, Los Angeles, 308 pp.

Roads, J. O. and R. C. J. Somerville, 1982: Predictability of ultralong waves in global and hemispheric quasi-geostrophic barotropic models. *J. Atmos. Sci.*, 39, 745-755.

Rosmond, T. E., 1986: Personal communication.

Saltzman, B., 1957: Equations governing the energetics of the larger scales of atmospheric turbulence in the domain of wave number. *J. Meteor.*, 14, 513-523.

_____, B., 1959: On the maintenance of the large-scale quasi-permanent disturbances in the atmosphere. *Tellus*, 11, 425-431.

_____, and A. Fleisher, 1960: The exchange of kinetic energy between larger scales of atmospheric motion. *Tellus*, 12, 374-377.

_____, 1960: The modes of release of available potential energy in the atmosphere. *J. Geophys. Res.*, 65, 1215-1222.

_____, 1970: Large-scale atmospheric energetics in the wave-number domain. *Reviews Geophysics and Space Physics*, 8, 289-302.

Showalter, R. C., 1984: Spectral decomposition and verification of NOGAPS 500mb medium-range forecasts. Masters Thesis, Naval Postgraduate School, 92 pp.

Somerville, R., 1980: Tropical influences on the predictability of ultralong waves. *J. Atmos. Sci.*, 37, 1141-1156.

Tanaka, H., E. C. Kung and W. I. Baker, 1986: Energetics analysis of the observed and simulated general circulation using three-dimensional normal mode expansions. *Tellus*, 38A, 412-428.

Temperton C., 1977: Normal modes of a barotropic version of the E.C.M.W.F. gridpoint model. *European Centre for Medium Range Weather Forecasts Internal Report No. 12.*, 41 pp.

_____, and D. L. Williamson, 1981: Normal mode initialization for a multilevel grid-point model: linear aspects. *Mon. Wea. Rev.*, 109, 729-743.

Williamson, D. L., 1976: Normal mode initialization procedure applied to forecasts with the global shallow water equations. *Mon. Wea. Rev.*, 104, 195-206.

Young R. E., and G. L. Villere, 1985: Nonlinear forcing of planetary scale waves by amplifying unstable baroclinic eddies generated in the troposphere. *J. Atmos. Sci.*, 42, 1991-2006.

INITIAL DISTRIBUTION LIST

		No. Copies
1.	Defense Technical Information Center Cameron Station Alexandria, VA 22304-6145	2
2.	Library, Code 0142 Naval Postgraduate School Monterey, CA 93943-5002	2
3.	Chairman (Code 63Rd) Department of Meteorology Naval Postgraduate School Monterey, CA 93943-5000	1
4.	Prof. R. T. Williams (Code 63Wu) Department of Meteorology Naval Postgraduate School Monterey, CA 93943-5000	3
5.	Prof. M. Rennick (Code 63Re) Department of Meteorology Naval Postgraduate School Monterey, CA 93943-5000	1
6.	Prof. R. L. Elsberry (Code 63Es) Department of Meteorology Naval Postgraduate School Monterey, Ca. 93943-5000	1
7.	Prof. B. Neta (Code 53Nd) Department of Mathematics Naval Postgraduate School Monterey, Ca. 93943-5000	1
8.	Prof. R. W. Garwood (Code 68) Department of Oceanography Naval Postgraduate School Monterey, Ca. 93943-5000	1
9.	Commanding Officer Fleet Numerical Oceanography Center Monterey, CA 93943-5005	1
10.	Commanding Officer Naval Environmental Prediction Research Facility Monterey, CA 93940	1
11.	Lt Col John L. Hayes	1

Headquarters Air Weather Service DNX
Scott Air Force Base, IL 62225

12. Atmospheric Sciences Library — 1
National Oceanic and Atmospheric Administration
Silver Spring, MD 20910

13. Prof. C.-P Chang, (Code 63Cp) — 1
Department of Meteorology
Naval Postgraduate School
Monterey, CA 93943-5000

14. Dr. J. Holton — 1
Department of Atmoshperic Sciences
University of Washington
Seattle, WA 98105

15. Dr. B. J. Hoskins — 1
Department of Geophysics
University of Reading
Reading, United Kingdom

16. Dr. J. Young — 1
Department of Meteorology
University of Wisconsin
Madison, WI 53706

17. Dr. A. Kasahara — 1
National Center for Atmoshperic Research
P.O. Box 3000
Boulder, CO 80303

18. Dr. D. Williamson — 1
National Center for Atmoshperic Research
P.O. Box 3000
Boulder, CO 80303

19. Dr. R. Errico — 1
National Center for Atmoshperic Research
P.O. Box 3000
Boulder, CO 80303

20. Prof. C. H. Wash (Code 63Wx) — 1
Department of Meteorology
Naval Postgraduate School
Monterey, CA 93943-5000

21. Prof. C-S. Liou (Code 63Lq) — 1
Department of Meteorology
Naval Postgraduate School
Monterey, CA 93943-5000

22. Prof. M. Peng (Code 63) — 1
Department of Meteorology

Naval Postgraduate School
Monterey, CA 93943-5000

23. Dr. M. G. Wurtele — 1
Department of Meteorology
University of California
Los Angeles CA 90024

24. Dr. E. N. Lorenz — 1
Department of Meteorology
Massachusetts Institute of Technology
Cambridge, MA 02139

25. Dr. E. N. Lorenz — 1
Department of Meteorology
Massachusetts Institute of Technology
Cambridge, MA 02139

26. Meteorology Library (Code 63) — 1
Naval Postgraduate School
Monterey, CA 93943-5000

27. National Center for Atmoshperic Research — 1
P.O. Box 1470
Boulder, CO 80303

28. Director, Naval Research Laboratory — 1
ATTN: Technical Services Information Center
Washington, D.C. 20390

29. Office of Naval Research — 1
Department of the Navy
Washington, D.C. 20360

30. Dr. N. A. Phillips — 1
National Meteorological Center/NOAA
World Weather Building
Washington, D.C. 20233

31. Dr. J. D. Mahlman — 1
Geophysical Fluid Dynamics Laboratory
Princeton University
Princeton, NJ 08540

32. Capt Michael D McAtee — 5
705 Joseph Dr.
Papillion, NE 68128

33. Dr. T. Rosmond — 1
Naval Environmental Prediction Research Facility
Monterey, CA 93943

34. Dr. E. Barker — 1
Naval Environmental Prediction Research Facility
Monterey, CA 93943

35. Dr. M. J. P. Cullen
Meteorological Office
Bracknell, Berks,
United Kingdom — 1

36. Dr. A. Staniforth
Recherce en Prevsion Numerique
West Isle Office Tower, 5 ieme etage
2121 route Trans-Canada
Dorval, Quebec H9P1J3, Canada — 1

37. Lt Col J. Cipriano
AFIT/CIR
Wright Patterson AFB, OH 45433 — 1

38. AWS Technical Library
Scott AFB, IL 62225 — 1

39. Prof. [illegible]. Johnson
Department of Meteorology
University of Wisconsin
Madison, WI 53706 — 1

40. Prof. R. Gall
Institute of Atmospheric Physics
University of Arizona
Tucson, AZ 85721 — 1

END

DATE

FILMED

6-1988

DTIC